POLITECNICO DI MILANO

Facoltà di Ingegneria Industriale

Corso di Laurea Magistrale in Ingegneria Energetica Orientamento
Idrocarburi

A Numerical Upscaling Technique for Absolute Permeability and Single-Phase Flow

Based on the Finite-Difference Method

Relatore: Prof. Fabio INZOLI

Co-relatore: Prof. Luiz Adolfo HEGELE JUNIOR

Tesi di Laurea di:

Andrea FAILLA

Matricola 804958

Anno Accademico 2014 – 2015

Ringraziamenti

Milano, 28 Luglio 2015

Vorrei ringraziare alcune persone che hanno contribuito positivamente durante la mia esperienza universitaria e non solo.

Innanzitutto un grazie particolarmente sentito va a tutti gli amici che mi hanno sempre sostenuto ed aiutato nei momenti più difficili, specialmente Massimo con cui ho condiviso moltissimi anni della mia vita.

Un ringraziamento speciale alla mia ragazza Veronica con la quale ho trascorso anni fantastici e condiviso esperienze che non dimenticherò mai.

Nunca olvidaré mi experiencia en Chile. Por lo tanto unas gracias especiales para Ina Salaberry y Gustavo Pacheco.

Agradeço o Professor Luiz Adolfo Hegele Junior para a oportunidade que me deu e tambem porque encontrei em ele um amigo. Agradeço tambem a Professora Lindaura Maria Steffens para ter-me ajudado.

Un ringraziamento al Prof. Fabio Inzoli per essere stato il relatore di questo lavoro e per avermi indirizzato nei momenti in cui ne avevo bisogno.

Ringrazio infinitamente la mia famiglia, mia madre Antonella e mia sorella Valentina, per aver sempre creduto in me più di chiunque altro supportandomi con amore e dedizione.

Infine, un pensiero speciale a mio padre il quale sarebbe orgoglioso di me.

Andrea Failla

Sommario

Attualmente i geologi riescono a generare dei modelli di giacimenti altamente dettagliati, grazie alle più innovative tecnologie. Il gran numero di informazioni che riguarda la distribuzione di porosità, permeabilità assoluta e relative, saturazione, pressione e temperatura.La complessa struttura porosa che deriva da modelli dettagliati, rende la descrizione del flusso di fluido difficoltosa. In particolare, giacimenti altamente eterogenei sono particolarmente difficili da descrivere.Il numero di celle attive deve essere ridotto per mezzo di metodi di upscaling, per rendere il modello geologico e la simulazione del flusso di fluido più facilmente rappresentabili. In generale, le dimensioni di un modello raffinato viene ridotto di un fattore 100. Le tecniche di upscaling per permeabilità assoluta, così come le tecniche di media semplice, hanno spesso difficoltà nella rappresentazione del flusso in zone tortuose. Infatti, le condizioni al contorno giocano sempre un ruolo importante nello sviluppo di un metodo di upscaling. Le assunzioni riguardo le condizioni al contorno possono essere inappropriate, dipendendo dal grado di eterogeneità. Oltretutto, per tecniche di upscaling per permeabilità assoluta non esiste mai una soluzione analitica. Quindi solo metodi numerici dovrebbero essere usati per scalare qualunque modello geologico. In questo lavoro è stato sviluppato un metodo numerico di upscaling di permeabilità assoluta basato sul metodo delle differenze finite e in condizioni di flusso monofasico. Questo metodo è stato inizialmente testato su griglie particolari. Nel dettaglio, erano griglie simmetriche e stratificate, utilizzate principalmente per comparare i risultati ottenuti dal metodo stesso e quelli derivanti da formule teoriche. Quindi, il metodo qui proposto è stato applicato a due dataset forniti dalla SPE (Society of Petroleum Engineers) e alcuni campi di permeabilità generate da distribuzioni probabilistiche di permeabilità. Un gran numero di simulazioni sono state fatte per comparare I flussi di pozzo di entrambi i modelli. I risultati mostrano un incredibile miglioramento in termini di tempo di simulazione. Dipendendo dalla taglia del modello raffinato, il tempo è stato ridotto di diversi ordini di grandezza. Comunque i risultati relativi all'errore tra il flusso di pozzo possono considerarsi soddisfacenti, specialmente quando il pozzo di produzione è localizzato in una zona di alta permeabilità. È importante sottolineare che sono stati ottenuti anche alcuni pessimi risultati, ma solo quando il pozzo è stato posto in una zona di bassa permeabilità.

Parole chiave: Upscaling, Metodo delle Differenze-Finite, Permeabilità.

Abstract

Nowadays, geologists can generate highly detailed descriptions of reservoirs, thanks to the most sophisticated and state of the art technologies. The great amount of information regards porosity, absolute and relative permeability values, saturations, pressure and temperature distribution.

The complex porous structure that derives from detailed models makes it challenging to describe the fluid flow. In particular, highly heterogeneous reservoirs are very difficult to descript.

The number of active cells must be reduced by upscaling methods in order to get easier geological model representations and fluid flow simulations. In general fine model size is reduced of a factor of 100 down.

Conventional upscaling techniques of absolute permeabilty, such as average techniques, often have difficulties in the representation of tortuous flow paths. In fact, the boundary conditions always play an important role in whatever upscaling method development. The assumptions about the boundary conditions may be inappropriate, depending on the heterogeneity scale. Moreover, for upscaling techniques of absolute permeability an analytical solution never exists. It means that only numerical methods should be used to scale up whatever geological model.

However, a good upscaling method should have the goal of preserving the flow features caused by complex geological models. In this work a numerical upscaling technique for absolute permeability and single-phase flow based on the finite-difference method was developed. The new method has firstly been applied to artificial grids. In particular symmetric and stratified mesh were used in order to compare analytical results with the ones obtained from the new technique. Then, the method we propose was applied to two SPE's dataset (Society of Petroleum Engineers) and some permeability fields generated by numerical probability distribution. A large number of simulations wells were done, in order to compare well flows of both detailed and coarse models. The results show an incredible improvement in terms of simulation time. Depending on the fine model's size, it was reduced of several orders of magnitude. However, the results in terms of well flow comparison can be considered satisfactory, especially when the production well is located in a high permeability zone of the reservoir. Nevertheless, it is important to underline that some bad results were also obtained, but only when the well was placed in a low permeability area.

Keywords: Upscaling, Finite-Difference Method, Permeability.

Extended Summary

1. Introduction

Advanced technologies allow to make refined and detailed geological representation of reservoirs, which are computationally represented by discretized meshes. A great amount of active cells characterizes these digital models, unfortunately, under these conditions it is impossible to run fluid flow simulation. Oil and gas industry needs geological models that are usable in order to have forecasts about the amount of producible oil or gas. Upscaling techniques on rock properties are used for the reduction of the geological resolution, allowing production/injection flow simulations.

2. Fundamental Rock Properties

The second chapter is important in order to define and distinguish additive and non-additive properties. Porosity and absolute permeability are probably the most important rock properties in order to respectively understand the amount of oil in a reservoir and the percentage of it that is extractable. Porosity is defined as the ratio between the sum of the empty spaces volume and the total rock volume. However not all the empty spaces are connected and this aspect deserves to be taken into account, because oil can moves only through connected pores. It is possible to define the effective porosity as the ratio between the sum of all the empty connected spaces volume and the total empty volumes of the rock. Absolute permeability depends only on the rock type. Absolute permeability is the real permeability only when the fluid flow is single-phase. In fact, when a multi-phase flow is moving in the porous medium, the relative permeability for each phase must be defined.

$$kr_p = \frac{k_p(S_p)}{k_p(100\%)} \tag{I}$$

For the purposes of this work only absolute permeability will be taken into account.

3. Main Average Upscaling Techniques

The third chapter is a brief description of the main average upscaling methods that are commonly used in the oil & gas industry. They are largely used, even when they should not be, because of their simple implementation. Average techniques are analytical solutions, namely they are considered exact solutions. Unfortunately, these kind of techniques are applicable only for additive properties and rare cases of non-additive properties. In other words, the exact "equivalent value" is obtained only for simple cases. Most of the times, for non-additive properties, average techniques are not applicable and then numerical methods should be used in order to have approximated results. Porosity and absolute permeability are good examples respectively of additive and non-additive properties.

This section will be useful for the reader in order to understand how the analytical results were calculated and then compared in chapter 6, when particular permeability distributions were scaled up with the method. In detail, will be defined:

- Harmonic average
- Arithmetic average
- Power average

Harmonic and arithmetic average techniques are used for different cases. In fact, their application depends on the main permeability change direction. Whereas, it will be shown that the power average depends on a parameter, which will be indicated with p, which depends on the permeability distribution.

An important aspect, for the purposes of this work, is the possibility to combine harmonic and arithmetic averages in order to obtain two combined techniques, which are called: Harmonic-Arithmetic and Arithmetic-Harmonic. As well as for the singles harmonic and arithmetic average, the combined techniques must be applied depending on the main change permeability orientation.

4. Basic Equation for Single-Phase Flow

The fourth chapter is useful to understand what kind of equations were used. Darcy's Law is one of the basic equations of this work. It is an empirical equation for single-phase fluid flow but it is possible to extend it to multi-phase

flows simply introducing the relative permeability. Darcy's Law is characterized by practical limits. In fact, it based on simple assumptions as:

- Laminar flow
- No chemical and kinetic interactions between the fluid and the rock
- Newtonian and homogeneous fluids

Generalized fluid flow equations have been derived in order to give to the reader a complete guide about the method. All the assumptions and hypotheses have been specified. These equations are based on the mass conservation principle, starting from a generic control volume. The mass conservation equation, famously known as continuity equation, was derived in order to have a general expression of the mass balance for a whatever grid-block with or without the production/injection well. This expression was initially derived for a generic fluid flow, namely no assumptions have been made about the fluid nature. After that, the hypothesis of incompressible fluid flow and steady state were introduced.

5. Finite-Difference Approximation

Being useless the PDE form of the continuity equation, for this work, a discretization process was necessary in order to make them implementable on the software. The most famous discretization processes in oil industry are: the finite-difference method (FDM) and finite-element method (FEM). The production rate is function of time and space. So, it was necessary to discretize spatial and time partial derivatives contained in the continuity equation. Both of them were discretized using the Taylor series approximation. Second order spatial derivatives were approximated using in two steps the central difference approach. Unlike for time derivatives, because they are first order derivatives. In this case, it was used the backward difference because of stability problems that may occur using the forward difference.

6. Numerical Upscaling Method Proposed

The method that is proposed in this work is numerical. All the numerical upscaling methods that were developed in the history, even for us, the homogenization process plays a fundamental role. In other words a heterogeneous region of whatever property is homogenized using an equivalent

value in place of the original ones. The term "equivalent" regards the flux that is kept constant even when the original permeability values are replaced. This method can be considered non-local because the equivalent permeability is influenced by boundary conditions. However, the user has the freedom to use it as a local, because of some available options. Sealed-sides boundary conditions were used in order to force the fluid flows along a principal direction, under a constant gradient of pressure. The flux is forced to flow along a single direction, so it can be globally represented by three systems. Due to this kind of boundary conditions, each system is characterized by a different pressure distribution. In fact, the first step is the three pressure distributions computation. They are necessary in order to calculate the fluxes that are flowing through the three cross-sections. When the fluxes and the pressure distributions are known, they are used to calculate the equivalent permeability first trials. These values replace the original ones in each direction. They cause three new pressure distributions and three different values of fluxes. So, new equivalent permeability values are calculated using the original fluxes because they must be constant. The process starts over and it finishes when the difference between iterative permeability values (in alternative, it is possible to use the fluxes as iterative values) is small enough. The initial idea was modified in order to solve some problems, in particular: convergence and mutual influence among equivalent permeability values. In particular, the final form of the method has the purpose to reach the global homogenization. In other words, it tries to calculate a unique equivalent permeability for all the directions. These modifications have had success because some problems of convergence were solved.

7. Production Well Implementation

Production wells were implemented in the mesh in order to have a comparison between production rates of both systems, the original and the scaled up. It was used the single-layer model, based on the definition of equivalent radius given by Abou-Kassem and Aziz. It is possible to simulate a production well using two approaches: keeping the well flow constant or keeping the sandface pressure constant. In this work, the second option was used because the comparison must be between production rates. The single-layer model was used only for 2D models but it is common in reservoir engineering to neglect the vertical permeability. In other words, it is possible to treat the 3D well model as a 2D, paying attention to some modifications.

8. Results

The results will be shown for two-dimensional and three-dimensional models. The simulation time is a parameter that must be control in order to verify if the upscaling is sufficiently convenient. The results, in terms of computational time, have been satisfactory but it was predictable because of the scale increase. The most important and interesting results regard the difference between well flows. Most of the results, in two and three dimensions, can be considered good (25-50% of error between fluxes) or excellent (0-25% of error between fluxes); if the scale increase is not so marked. When the reservoir size reduction is more marked the model becomes too "approximated" and the well flow errors are no more acceptable. It is important to underline that all the simulations were done with a standard computer, so, it was impossible to simulate huge permeability fields. The results also highlight that most of the times the unsatisfactory well flow errors were obtained when the well-block permeability was too low. It also is an expected result, because it is more difficult to describe and to scale up the fluid flow when the region is characterized by low permeability and the pressure is influenced by the well. Another important aspect regards the heterogeneity. In fact, when the neighbouring blocks of the well block are characterized by highly different permeability values, the difference between flows is higher. Another consideration regards the self-similarity of the model, which is absent. In fact, the permeability probability distribution is not conserved when the original model is scaled. Moreover, after a certain number of scaling application, or in other words when the scaled model is scaled again and again, its permeability probability distribution turns in a Dirac's Delta distribution.

9. Conclusions and Future Directions

Despite the simple idea on which the method is based, it gave good results. The worst results are obviously correlated with particular aspects that also affect most of the actual upscaling techniques. Due to these "defects" it will be possible to improve this method, trying to develop a better version that is not sensible to high heterogeneous regions or low permeability well-blocks. Moreover, it is possible to extend it for multi-phase and compressible flows.

Riassunto esteso

1. Introduzione

Le tecnologie più avanzate consentono di rendere la rappresentazione di modelli geologici sempre più raffinata e dettagliata. Tali modelli sono rappresentati da maglie discretizzate. Una grande quantità di cellule attive caratterizza i modelli computazionali, purtroppo però non è possibile eseguire le simulazioni in tali condizioni. L'industria petrolifera ha la necessità di usare modelli geologici che siano adatti ai moderni software di simulazione e dunque avere delle stime circa la quantità di olio o gas producibile. Le tecniche di upscaling sono da sempre utilizzate per l'aumento in scala della maglia geologica, consentendo quindi rapide simulazioni di pozzi di produzione/iniezione .

2. Proprietà Fondamentali delle Rocce

Il secondo capitolo è importante per capire e distinguere le proprietà additive da quelle non-additive. La porosità e la permeabilità assoluta sono probabilmente le più importanti per comprendere rispettivamente quale sia il quantitativo di olio nel giacimento e quanto sia quello estraibile. La porosità è definita come il rapporto tra la somma del volume di tutti gli spazi vuoti e il volume totale della roccia. Non tutti gli spazi vuoti però sono connessi e questo aspetto merita di essere preso in considerazione in quanto l'olio non vi può fluire. Infatti, è possibile definire la porosità effettiva come il rapporto tra tutti gli spazi vuoti connessi e il volume totale di tutti gli spazi vuoti. La permeabilità assoluta dipende solo dal tipo di roccia. Comunque, è possibile definirla solo quando il flusso è mono-fasico. Quando un flusso multi-fasico è presente all'interno della roccia, si può definire la permeabilità relativa per ogni fase.

$$kr_p = \frac{k_p(S_p)}{k_p(100\%)} \tag{I}$$

Ai fini di questo lavoro sarà presa in considerazione solo la permeabilità assoluta.

3. Principali Tecniche di Upscaling

Il terzo capitolo è una breve descrizione delle principali tecniche di upscaling che sono comunemente usate nell'industria petrolifera. Sono largamente usate, anche quando dovrebbero essere utilizzati metodi numerici, a causa della loro semplice implementazione. Le tecniche che usano semplici medie danno soluzioni estate perchè derivano da una trattazione teorica. La prima importante distinzione deve essere fatta tra proprietà additive e non additive. Infatti, questo tipo di tecniche può essere usato per calcolare il valore equivalente di proprietà additive. Contrariamente con quanto accade per le proprietà non additive, che necessiterebbero di metodi numerici per essere "scalate". Porosità e permeabilità assoluta sono buoni esempi rispettivamente di proprietà additive e non additive. Questa sezione sarà presentata per comparare i risultati ottenuti dal metodo proposto in questo lavoro e i risultati analitici, quando sono state usate particolari distribuzioni di permeabilità. In questo capitolo saranno definite le seguenti medie:

- Media Armonica
- Media Aritmetica
- Media della Potenza

Medie armoniche ed aritmetiche sono usate in casi differenti. Infatti, la loro applicazione dipende dalla direzione principale lungo la quale la permeabilità cambia significativamente. La media della potenza dipende invece da un parametro, che sarà indicato con p, che a sua volta dipende dalla distribuzione di permeabilità. Un aspetto importante, per i fini di questo lavoro, è la possibilità di combinare le medie armoniche ed aritmetiche per ottenere due tecniche "combinate", che sono chiamate: Armonica-Aritmetica e Aritmetica-Armonica. Così come per le singole medie armoniche ed aritmetiche, anche queste tecniche combinate devono essere applicate in funzione della direzione principale lungo la quale cambia la permeabilità.

4. Equazioni Basiche per Flusso di Fluido

Il quarto capitolo sarà utile per capire quali equazioni sono state usate. La legge di Darcy è una delle equazioni di base di questo lavoro. Essa è una equazione empirica per flussi mono-fasici ma può essere estesa a flussi multi-fase semplicemente introducendo la permeabilità relativa. La legge di Darcy è caratterizata da limiti pratici. Infatti, essa è basata su semplici assunzioni come:

- Flusso laminare
- Nessuna interazione chimica o cinetica tra il fluido e la roccia
- Fluidi omogenei e Newtoniani

Le equazioni di flusso generalizzate che sono state derivate saranno utili al lettore per avere una guida completa del metodo. Tutte le assunzioni e le ipotesi saranno specificate. Queste equazioni sono basate sul principio di conservazione della massa, partendo da un volume di controllo. L'equazione di conservazione della massa, meglio conosciuta come equazione di continuità, è stata derivata per avere una espressione generale del bilancio di massa per una qualsiasi cella con o senza la presenza del pozzo. Questa espressione è stata inizialmente derivata per un flusso generico, ossia nessuna ipotesi è stata fatta riguardo la natura del fluido. Dopodichè, l'ipotesi di fluido incomprimibile e stato stazionario sono state introdotte.

5. Approssimazione con Differeze-Finite

L'equazione di continuità scritta sotto forma di equazione alle derivate parziali è inutile per i nostri fini, è stato necessario un processo di discretizzazione per renderle implementabili. I processi di discretizzazione più utilizzati in ambito petrolifero sono il metodo alle differenze finite (FDM) e il metodo degli elementi finiti (FEM) ed è stato usato il primo. Il flusso di olio prodotto è funzione dello spazio e del tempo. Quindi è stato necessario discretizzare le equazioni alle derivate parziali nello spazio e nel tempo contenute l'equazione di continuità. Entrambe sono state discretizzate usando l'approssimazione in serie di Taylor. Le derivate spaziali del secondo ordine sono state approssimate usando due volte l'approccio alle differenze centrate. Contrariamente alle derivate temporali, che, essendo del primo ordine sono state approssimate usando l'approccio delle differenze all'indietro.

6. Metodo Numerico di Upscaling Proposto

Il metodo qui proposto è di tipo numerico. Così come per tutti i metodi numerici di upscaling che sono stati sviluppati fin'ora, il processo di omogenizazzione gioca un ruolo fondamentale. In altre parole una regione eterogenea in permeabilità è omogenizzata usando un valore equivalente di tale proprietà. Il termine "equivalente" si riferisce alla conservazione del flusso che passa attraverso una sezione trasversale, anche quando i valori di permeabilità

originali vengono sostituiti. Questo metodo può essere considerato un metodo non locale perchè la permeabilità equivalente è influenzata dalle condizioni al contorno; ma allo stesso tempo si da la libertà all'usuario di usarlo come se fosse locale. Le condizioni al contorno utilizzate in questo lavoro forzano il fluido a fluire lungo una direzione, sotto un gradiente di pressione costante arbitrariamente scelto. Il flusso però è forzato ad andare lungo una sola direzione e quindi per rappresentarlo globalmente sono necessari tre sistemi. Dovuto a questo tipo di condizioni al contorno, ogni sistema è caratterizzato da una differente distribuzione di pressione. Infatti il primo passo è il calcolo delle tre distribuzioni di pressione. Esse sono necessarie per calcolare i flussi che stanno fluendo attraverso le tre sezioni trasversali. Quando i flussi e le distribuzioni di pressione sono conosciute, sarà possibile usarle per calcolare i valori di primo tentativo delle permeabilità equivalenti. Questi valori prenderanno il posto dei valori di permeabilità originali lungo ogni direzione. Dovuto a ciò, si avranno tre nuove distribuzioni di pressione che dovranno essere calcolate. Le nuove pressioni daranno come risultato tre nuovi flussi, che saranno diversi dagli originali. Così i nuovi valori di permeabilità equivalente saranno calcolati usando i valori di flusso originali e non quelli iterativi perché il flusso sia costante. Il processo dunque ricomincia e terminerà quando la differenza fra i valori iterativi di permeabilità sarà sufficientemente piccola. L'idea iniziale è stata modificata per risolvere alcuni problemi, in particolare: convergenza e la mutua influenza tra i valori di permeabilità equivalente. In particolare, la forma finale di questo metodo ha come obiettivo la completa omogenizzazione del dominio e quindi tenta di calcolare un unico valore di permeabilità equivalente per tutte le direzioni. Queste modifiche hanno avuto successo perchè hanno risolto gran parte dei problemi di convergenza.

7. Implementazione del Pozzo di Produzione

Il pozzo di produzione è stato implementato al fine di avere una comparazione tra flussi di produzione per entrambi i sistemi (quello originale e quello scalato). È stato usato il modello a singolo strato, basato sulla definizione di raggio equivalente data da Abou-Kassem e Aziz. È possibile simulare un pozzo di produzione usando due approcci: mantenendo il flusso costante o mantenendo la pressione di fondo pozzo costante. Ovviamente è stato scelto il secondo approccio perchè altrimenti la comparazione non avrebbe avuto senso. Il modello a singolo strato è stato usato per il caso di 2D e il 3D usando però i

giusti accorgimenti, ossia trascurando la permeabilità verticale (pratica di uso comune in ingegneria di giacimento).

8. Risultati

I risultati saranno mostrati per i modelli 2D e 3D. Il tempo di simulazione è un parametro importante che deve essere tenuto sotto controllo per verificare se l'upscaling ha avuto l'effetto desirato. I risultati in termini di tempo computazionale sono soddisfacenti anche se ciò era prevedibile, dovuto alla riduzione di risoluzione del modello. I risultati più importanti e interessanti riguardano la differenza tra i flussi. Molti dei risultati, in due e tre dimensioni, possono essere considerati buoni (25-50% di errore tra flussi) o eccellenti (0-25% di errore tra flussi); se l' aumento in scala non è troppo marcato. Quando l' aumento di scala è più marcato il modello diventa eccessivamente approssimato e gli errori non sono più accettabili. È importante sottolineare che tutte le simulazioni sono state fatte con un computer standard pertanto è stato impossibile simulare grandi campi di permeabilità. I risultati sottolineano anche che il più delle volte gli errori insoddisfacenti si sono verificati quando il pozzo si trova in una zona di bassa permeabilità. Anche questo è un risultato aspettato, perchè è più difficile descrivere e scalare il flusso di fluido quando la permeabilità è bassa e quando la pressione è influenzata dalla presenza del pozzo. Un altro aspetto importante riguarda il livello di eterogeneità. Infatti, quando i blocchi vicini al pozzo sono caratterizzati da valori di permeabilità altamente differenti, la differenza tra flussi aumenta. Un altro aspetto riguardante il metodo è la sua auto-consistenza, che non è rispettata. Infatti si è visto che applicando l'upscaling sul modello originale la distribuzione di probabilità cambiava. Inoltre applicando il processo di upscaling più volte la distribuzione di probabilità cambiava fino a diventare una distribuzione tipo Delta di Dirac.

9. Conclusioni e Suggerimenti Futuri

A dispetto del fatto che l'idea sulla quale si basa il metodo sia semplice, I risultati ottenuti sono stati buoni. I peggiori risultati sono stati riscontrati per casi particolari che normalmente causano problemi ai processi di upscaling. Dovuto alla presenza di questi difetti sarà possibile migliorare il metodo, tentando di sviluppare una versione migliore che non sia sensibile alle regioni eterogenee o

di bassa permeabilità. Oltretutto è possibile estendere il metodo per fluidi multi-fase e compressibili.

Contents

Nomenclature

V_{es} = empty rock volume, [m^3]

V_{tot} = total rock volume, [m^3]

φ = rock porosity

φ_e = effective rock porosity

φ^0 = reference effective rock porosity

c_φ = porosity compressibility, [kPa^{-1}]

p = pressure, [kPa]

p^0 = reference pressure, [kPa]

S_p = phase saturation

k = permeability, [mD]

kr_p = relative permeability of the phase p

$\mathbf{u}(x)$ = filtration velocity, [m^3/(day m^2)]

∇p = gradient of pressure, [kPa]

$\mathbf{k}$ = local permeability tensor

β_c = unit conversion factor for the transmissibility coefficient, 86.4 x 10^{-6}

ρ = density, [kg/m^3]

ρ_0 = oil density, [kg/m^3]

ρ_g = gas density, [kg/m^3]

g = gravity acceleration, 9.81 [m/s^2]

μ = fluid viscosity, [Pa·s]

A = cross-sectional area, [m^2]

q_0 = oil flow rate, [m^3/day]

q_g = gas flow rate, [m^3/day]

μ_o = oil viscosity, [Pa·s]

μ_g = oil viscosity, [Pa·s]

$\Delta \mathrm{x}$ = difference along x direction, [m]

$\Delta \mathrm{y}$ = difference along y direction, [m]

$\Delta \mathrm{z}$ = difference along z direction, [m]

m_i = mass in, in the control volume, [kg]

m_0 = mass out, in the control volume, [kg]

m_s = mass source/sink, in the control volume, [kg]

m_a = mass accumulation, in the control volume, [kg]

w = mass flow rate, [kg/day]

Δt = time difference, [day]

q_m = mass production rate, [kg/day]

w_x = mass flow rate in x direction, [kg/day]

w_y = mass flow rate in y direction, [kg/day]

w_z = mass flow rate in z direction, [kg/day]

$\dot{m}_x$ = mass flux vector in x direction, [kg/(day m^2)]

$\dot{m}_y$ = mass flux vector in y direction, [kg/(day m^2)]

$\dot{m}_z$ = mass flux vector in z direction, [kg/(day m^2)]

a_c = volume conversion factor, 5.614583 (for metric unit)

u_x = superficial velocity in x direction, [m^3/(day m^2)]

u_y = superficial velocity in y direction, [m^3/(day m^2)]

u_z = superficial velocity in z direction, [m^3/(day m^2)]

A_x = cross-sectional area normal to x direction [m^2]

A_y = cross-sectional area normal to y direction [m^2]

A_z = cross-sectional area normal to z direction [m^2]

V_b = block volume, [m^3]

B = fluid volume factor, [m^3/ m^3]

ρ_{sc} = density at standard conditions, [kg/m^3]

ρ_{rc} = density at reservoir conditions, [kg/m^3]

q_{sc} = production rate at standard conditions, [std m^3/day]

$\boldsymbol{A}$ = coefficient matrix

k_h = horizontal permeability, [mD]

r_w = well radius, [m]

H = depth of the well, [m]

p_{wf} = sandface pressure, [kPa]

r_e = external radius, [m]

p_e = external pressure, [kPa]

r_{eq} = equivalent radius, [m]

f = fraction of well flow coming from the well-block

$r_{i,j}$ = distance between the block i and the well j, [m]

T_i = interface transmissibility

a_j = distance from the well to its image j, [m]

γ_{wb} = multiphase hydrostatic wellbore pressure gradient, [kPa/m]

γ_c = gravity conversion factor, 10^{-3} (for metric unit)

List of Figures

List of Tables

List of Acronyms

FDM	Finite-Difference Method
FEM	Finite-Element Method
SPE	Society of Petroleum Engineers
PDE	Partial Differential Equation
EOS	Equation Of State
FVF	Fluid Volume Factor

1 Introduction

Reservoir simulations are based on conventional and unconventional techniques but both should need a large number of data in order to better describe reservoir properties. [1]

Through advanced instruments, methods and measurements, it is possible to reach a really good knowledge about hydrocarbons deposits and to make accurate three-dimensional geological models. Nowadays, geological models may consist of 10 million active grid blocks, depending on the deposit's size. [2]

Fluid flow simulations in complicated geological model would be impossible to run. Asking a software to elaborate such a great amount of information requires long time and it results, most of the times, in exceeding the practical limits. [3]

Actually, reservoir engineers use coarse models from realistic geological ones and apply on them upscaling techniques. Scaled models are made up of a significantly lower number of active grid cells; in this way it is possible to run fluid flow simulations with a reasonable time consumption. [3]

Scaling up a fine geological model is always a fundamental and critical step in reservoir simulation processes. Basically, it is a process which determines the effective property value of a heterogeneous model and it is represented by a correspondent homogeneous model. [4] In other words, it is essentially an averaging procedure where the static and dynamic characteristics of the fine scale model are approximated by those of the coarse one. Figure (1.1) shows an example of averaging procedure on porosity, it was used the harmonic average:
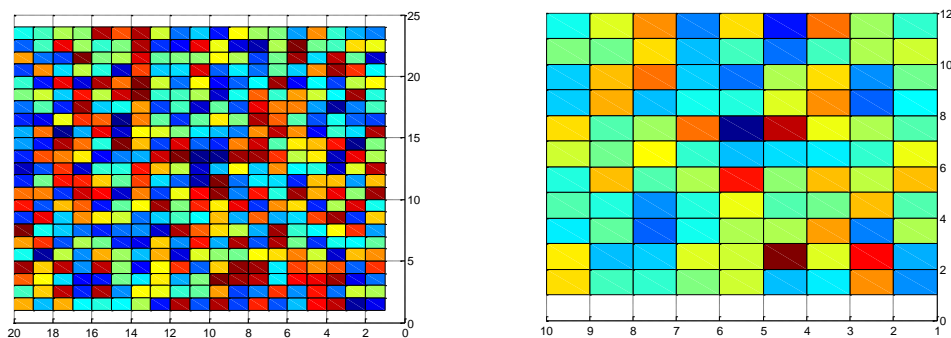
Figure 1.1: Example of upscaling on a porosity field. The fine model (on the left) and the scaled up (on the right) using the harmonic average technique.

This explains why upscaling techniques are nowadays so important and they cannot be avoided.

Obviously, change in scale processes are not painless. In fact, replacing a more detailed model with an approximated one, implies the loss several information. The direct consequence is a lower quality prediction of flow rates and pressure distributions. [5]

For additive properties it is easy to achieve a really good approximation of the original fine grid. [6] Volumetric (or additive) properties, such as porosity and saturation, don't need particular scaling technique. [7] Their "upscaled" representation is given by simple averaging methods, in other words they are obtained applying analytical solutions. [7] However, when dealing with non-additive properties, it is not always possible to approximate effective values by simply using weighted arithmetic average techniques. [8] In fact, in this case, it is necessary to take into account different aspects and the problem gets complicated. A good example is the calculation of absolute permeability [8].

This work is composed of an introductive part, made up of a brief introduction about fundamental rock properties such as porosity and permeability, two important examples of, respectively, additive and non-additive properties.

The second part is about the main average techniques of upscaling for absolute permeability. This part is useful to better understand what kind of tools will be used in this work and why. The third part is the introduction of all the physics concepts, laws, hypothesis and equations on which this work is based. It is advisable for the reader to pay attention to chapters 4, 5 and 7. In particular, chapter 4 illustrates the fluid flow equations on which this numerical method is based. In order to make them useful for the purposes of this work, it was necessary to discretize them through a common discretization process, which is shown in chapter 5. So, chapter 6 is the "heart" of this work. In fact, it will explained how the numerical technique was implemented. All the steps that have contributed to its final form will be shown in chronological order, trying to be as detailed as possible. In chapter 7 will be shown how a production well was implemented in both fine and coarse model. The last part of this work is about the results analysis and conclusions, including advices for future improvements about this method.

2 Fundamental Rock Properties

Hydrocarbons are always situated in deposits. Economically exploitable deposits are composed of two parts: the reservoir and the trap, but only the reservoir has the characteristic of being porous and permeable. [9] Figure (2.1) illustrates how is composed a hydrocarbon deposit. The trap is the upper limit and it is made of a distribution of rocks which holds hydrocarbons inside the reservoir, till it is drilled or broken because of natural movements [9].
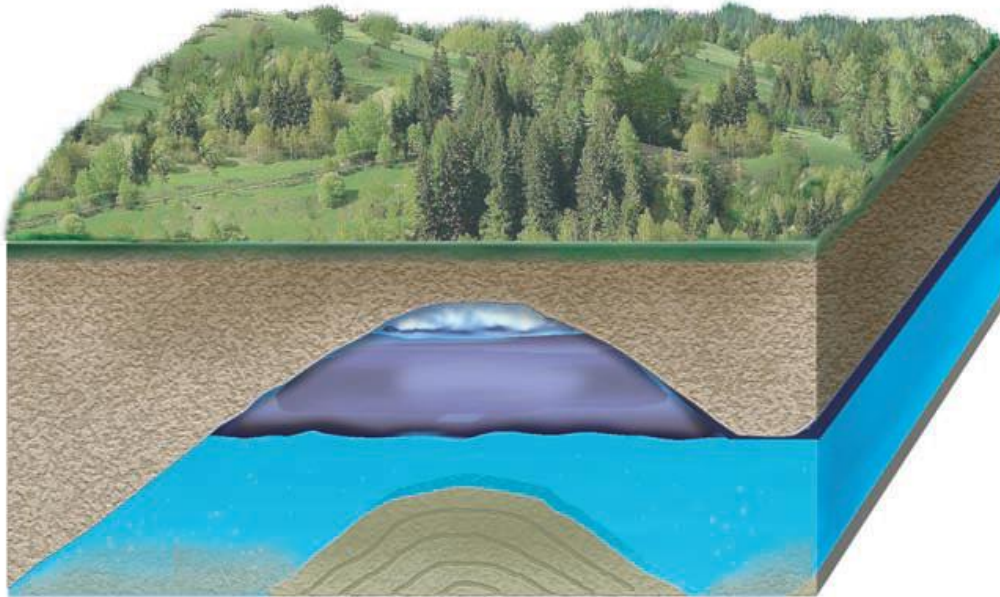
Figure 2.1: A typical hydrocarbons deposit representation. *[9]*

Reservoirs are really complicated systems, characterized by a set of physical parameters, such as porosity, permeability, pressure, temperature, density and the phases which characterize each fluid present in the porous medium. Phases can be gaseous, liquid or solid [9].

For the purpose of this work the most important parameters are porosity and permeability. They are independent of the fluid content, provided that the rock and fluid are nonreactive. In this paragraph porosity and permeability of rocks

will be introduced, together with two fundamentals concepts, namely additive and non-additive properties.

2.1 Porosity and Effective Porosity

Porosity is determined by all the pores, empty spaces and fractures of the rock. It is quantified simply by using a volumetric percentage of empty volumes (V_{es}) over total volume of the rock (V_{tot}) [10]:

$$\varphi = \frac{V_{es}}{V_{tot}} \tag{2.1}$$

Because of its definition porosity is an additive and dimensionless property of the rock. A distinction between total porosity and effective porosity needs to be done. The former, which is defined above, takes into account every single empty space.

Unfortunately, not all the empty spaces are interconnected, therefore hydrocarbons can't flow through them. Others empty spaces are surrounded by connate water which doesn't allow hydrocarbons movements. So, effective porosity is defined as the total volume where fluids can flowing (V_{ees}) over the total volume of the rock [10].

$$\varphi_e = \frac{V_{ees}}{V_{tot}} \tag{2.2}$$

From now on, every time porosity will be mentioned, it will refer to effective porosity. In this sense, porosity is considered a measure of the reservoir capacity for storing fluids.

Porosity varies with depth and horizontal distance and it depends on the nature of the rock. It is influenced by the sedimentation environment as in the space (horizontal variations) as in time (vertical variations). [11]

Because of the rock compressibility, porosity also depends on the pressure, which is usually assumed to be constant. However an expression of porosity in function of pore pressure is given by [11]:

$$\varphi = \varphi^0 \left[1 + c_\varphi(p - p^0)\right] \tag{2.3}$$

Where p^0 and φ^0 are the reference values, in particular p^0 is the reference pressure when the porosity is φ^0. The reference pressure can be the atmospheric

_____

pressure or the initial reservoir pressure at the time $t=0$. Moreover, c_φ it is the porosity compressibility. [11]

The relation written above expresses the proportionality between porosity and pressure. Apparently it looks a nonsense, but the pressure that is in equation (2.3) regards the pore pressure. So, because of the rock compressibility, when the internal pore pressure increases, the pore expands. [11]

Porosity is evaluated in laboratory, using some rock samples and a porosimeter or others methods, such as neutron-log and formations density, which are subsoil methods. [10]

However, a generic rock property often vary in space, sometimes from a point to another one or from a region to another region. If the property never changes in space, then the rock is defined as homogeneous for that specific property. In the most real cases this situation is never verified, in other words almost all the rocks are heterogeneous. [10]

In particular, reservoir rocks were born because of a long geological process. Nevertheless, sometimes is possible to approximate a heterogeneous region with a homogeneous one, if the variation of the property in space is not statistically important. [11] This kind of approximation helps reservoir engineers to solve problems otherwise intractable [11].

2.2   Absolute and Relative Permeability

Absolute permeability is the most important property for this work, because in single-phase flow it is the most important property to scale up. [12] Absolute permeability allows fluids to flow through the rock, without a physical change of it. [9] If porosity is an interesting parameter for understanding the potential amount of hydrocarbons in a reservoir, permeability is fundamental to understand the potential amount of extractable oil. [11]

It is important to distinguish between absolute permeability and relative permeability. The former is independent of the fluid's nature and it depends on the rock. [9] It is possible to talk about absolute permeability when the fluid flow is single-phase, otherwise it is necessary to specify the relative permeability. Darcy's law is based on the assumption of single-phase flow but, in a real situation, all the three phases are present and each one obstacles the movements of the others. [8] This fact it is taken into account by relative permeability that characterize each phase.

It is defined as the effective permeability (expressed in Darcy) for a given saturation of the phase (S_p), over the permeability for a phase saturation of 100% [10].

$$kr_p = \frac{k_p(S_p)}{k_p(100\%)} \tag{2.4}$$

Fluid saturation is simply expressed by the volume of rock filled (V_f) by a single phase over the total empty volume (V_t). [8]

$$S_p = \frac{V_f}{V_t} \tag{2.5}$$

Saturation is a dimensionless magnitude, as it is shown on equation (2.5) and it can varies within 0 and 1.
So, relative permeability values, which are dimensionless, are strictly correlated to fluid saturations. For example, when the oil saturation is higher than water saturation, its relative permeability is higher than water relative permeability. *[10]* An example is shown in figure (2.2):
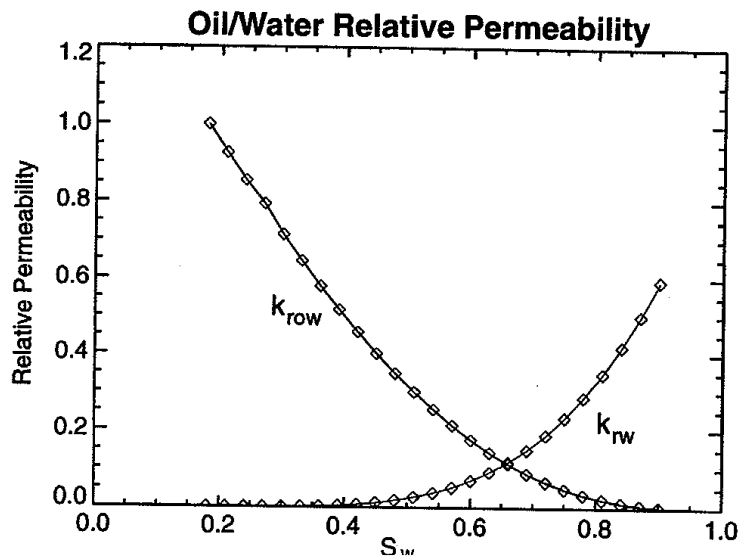
Figure 2.2: Example of Relative permeability values in function of Water Saturation. [13]

Statistically, to high porosity values correspond high permeability values, in fact a theoretical relationship exists between these two properties. However, for many reasons, points with similar or equal porosity may show significant

_____

differences in permeability [10]. In many practical problems, local absolute permeability, it can be represented by three values: k_x, k_y and k_z. [9]

Permeability is not an additive property, unlike porosity. It depends on several factors that are not necessary correlated [10]. This consideration is really important for this work, because it means that simple averaging methods are not always a good approximation of effective (or equivalent) permeability.

3 Main Average Upscaling Techniques

Many upscaling techniques for permeability were, and will be developed using different approaches. From simple statistical averages to advanced numerical methods, the upscaling's history is still in evolution and it is connected with the necessity of higher quality predictions.

Each upscaling technique is based on homogenization process. This kind of process is essential for the calculation of equivalent permeability. In this chapter will be illustrated different processes for homogenization.

First of all, a distinction should be made among three fundamental concepts concern absolute permeability: equivalent, effective and block permeability. They have different meanings, depending on boundary conditions and heterogeneity level:

- **Equivalent permeability (K_{eq}-tensor).**

The term equivalent indicates a constant permeability tensor that has to represent a heterogeneous medium [14]. Two different approaches are usable in order to calculate the equivalent permeability tensor. The former consists in keeping the flow at the boundaries constant, namely it has to be the same when it flows through the heterogeneous and the homogenized medium. The latter is based on the energy dissipation by the viscous forces in both mediums. Even if these two approaches look different, they are equivalent in case of periodic boundary conditions. However, the perfect equivalence between the real and the fictitious model is impossible to reach [14].

- **Effective permeability (K_{ef}-tensor).**

Effective permeability is the term used for porous mediums that are statistically homogeneous on large scale. In other words, the scale over which the averaged permeability is defined must be larger than the heterogeneity scale within the porous medium [15]. It is an intrinsic property because it does not depends on the macroscopic boundary conditions. Effective permeability has been studied by two different methods, namely stochastic and homogeneous-equation approach [14].

In the first case the permeability field is represented by a random function. Whereas, in the second case the porous medium is supposed to be spatially periodic [14].

Most of the times, reservoirs cannot be considered homogeneous on large scale and, therefore, the basic conditions to calculate effective permeability are not satisfied [14].

- **Homogenized permeability (or block – permeability, K_b).**

Homogenized permeability is the equivalent permeability of a finite-volume block [14]. The concept of statistical homogeneity is not used, unlike the previous definitions. In facts, the block – permeability can be calculated if the block volume is small enough [14]. So, irrespectively of the block being strongly or weakly heterogeneous, the homogenized permeability can be calculated as: [14]

$$\frac{1}{V} \int_V \mathbf{u}(x)dV = -\mathbf{K}_b \left(\frac{1}{V} \int_V \nabla p \, dV \right)$$

(3.1)

Where V is the volume of the block (expressed in cm^3) and $\mathbf{u}$ is the filtration velocity (by the Darcy's law, expressed in m/s) and ∇p is the gradient of pressure (expressed in kPa). Block – permeability is not unique because it depends on the boundary conditions and then it is not an intrinsic property of the porous medium [14].

It is important to understand what the difference among them is because from now on the equivalent grid-block permeability will be the protagonist of this work but, for simplicity, it will be called equivalent permeability.

Upscaling methods can be divided into three principal groups: heuristic, deterministic and stochastic. Deterministic methods imply that the geological model is perfectly known. Different is for stochastic methods, for which, in a first stage, an approximated model has to be considered as a starting point and only then probabilistic techniques are applied on it [14].

Heuristic methods propose formulas to compute equivalent permeability, based on empirical rules [14].

Analytical solutions are obtained from theoretical approaches and they are considered exact solutions. Whereas, numerical solution are often based on approximated approaches, such as discretization of space and time. Due to that, they represent just approximated solutions. However, most of the real cases are

_____

so complicated that it is impossible to apply analytical formulas, that's why numerical methods are more important nowadays [14].

In particular, when absolute permeability must be scaled up, there is no applicable analytical solution.

Upscaling methods can be further classified in local and no-local approaches.

The formers do not consider the influence of boundary conditions, namely pressure and blocks around the core. As a consequence, the block – permeability is an intrinsic property. It is known from the electrical conductance analogy that arithmetic and harmonic average can be used for mono-dimensional cases [16]. So, local methods are considered a sort of natural extension of the mono-dimensional results and the block-permeability is a function of the core permeability values. Non-local techniques depend on the boundary conditions that influence the flow within the block [16].

The method developed in this work has a dual nature: the user can choose the number of surrounding blocks that must be considered. From now on the number of surrounding blocks will be synthetically called "rings". The rings around the core, which is the domain subjected to homogenization, are useful to avoid an excessive influence due to the boundary conditions.

Concluding, heuristic methods will be briefly explained in the next paragraph because they are part of this work. In particular, some mathematical tools, such as harmonic and arithmetic averages have been used. Moreover, when the method was tested using particular permeability distributions, they played a fundamental role in order to give the exact solutions of the problem.

3.1   Heuristic Methods

3.1.1   Combined Averaging Methods and Directional Averages

The concept behind these techniques is quite simple: achieving an intermediate value between two theoretical bounds. Averaging techniques are local techniques. Equivalent grid-block permeability, in this case, is an intrinsic property because the boundary conditions do not affect the final result [14].

So, it is possible define the equivalent permeability, k_ϱ, as:

- **Arithmetic average.**

  For a dataset $k_1, \ldots, k_n$, it is defined as: [12]

$$k_\varrho = \frac{\sum_{i=1}^{n} k_i}{n} \tag{3.2}$$

- **Harmonic average.**

For a dataset $k_1, \ldots, k_n$, it is defined as: [12]

$$k_\varrho = \frac{n}{\sum_{i=1}^{n} \frac{1}{k_i}} \tag{3.3}$$

These methods are considered as the fastest and intuitively techniques for upscaling. However, those methods could be disadvantageous when a particular rock formation, such as shale rock, is characterized by a permeability value close to zero. In other words, when a non-flow barrier is present in the system. [12]

To this limitation, it has to be added that these methods can only solve 1-D problems in order to determine the effective permeability. So, for how fast and easy they are, it is difficult to apply them on real cases. Most of the reservoir can be considered as vertically homogeneous. It is due to the geological process for which the reservoir was created. Therefore, the main changes of permeability occur horizontally. Averaging methods can be combined together to calculate, for some particular cases, effective permeability. However, they deserve to be described because they will be useful later. Effective permeability can be calculated if permeability is described by a random numeric distribution or if it has a periodic behaviour as a function of space. Depending on the flow direction, effective permeability can be obtained using arithmetic, harmonic or geometric average. For example, for 1-D flow, global effective permeability for a group of cells connected in series, as figure (3.1) shows, can be determined exactly through the harmonic average [16].
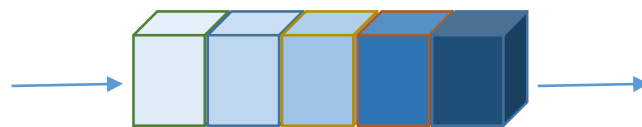
Figure 3.1: Example of cells connected in series

In other words, when the flow is parallel to the main permeability changes, it is possible to use the harmonic average. While, for a plane made up of a single layer of cells crossed by flow perpendicular to the main permeability changes, as figure (3.2) shows, effective permeability can be obtained by using the arithmetic average technique.
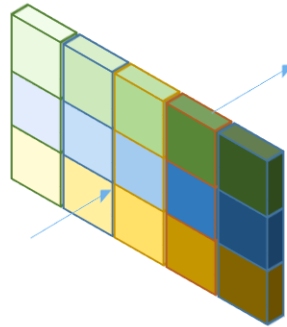
Figure 3.2: Example of cells connected in parallel

Due to that, the arithmetic average (as described in equation (3.4)) is considered the upper bound of the effective permeability. On the other hand, the harmonic average is considered to be the lower bound of the effective permeability. [12]
Whereas, geometric average is used when there is no apparent preference for vertical or horizontal flow. [16]
Harmonic and arithmetic techniques can be combined together in order to obtain the so called combined averaging homogenization methods of permeability. Arithmetic-Harmonic and Harmonic-Arithmetic method are also called directional mean methods. [17]
The order of application is important and it depends on the main permeability changes direction.

- **Harmonic -Arithmetic.**

    If the permeability main change is parallel to the flow, the harmonic average is applied first, as it is shown in figure (3.3) step 1.

In this way the homogenized columns are connected in parallel, namely the permeability main change is now perpendicular to the flow. So, the arithmetic average is now applicable among homogenized columns, as it is illustrate in figure (3.3) in step 2, obtaining the final, scaled up porous medium. [18]
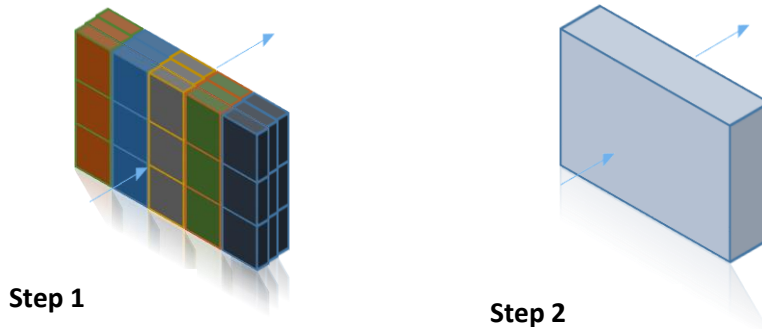
Step 1

Step 2

Figure 3.3: Example of Harmonic-Arithmetic technique applied. Step 1 graphically represents the harmonic average applied. Step 2 is the final step, when the arithmetic average is apllied.

- **Arithmetic-Harmonic.**

When the fluid flow is perpendicular to the permeability main change direction, then the arithmetic average is used first, giving homogenized plans as it is shown in step 1 of figure (3.4). Now, the permeability main change direction is parallel to the flow and the harmonic average has to be used to calculate the effective permeability of the entire block. The step 2 gives a homogenized domain, illustrate in figure (3.4). [18]
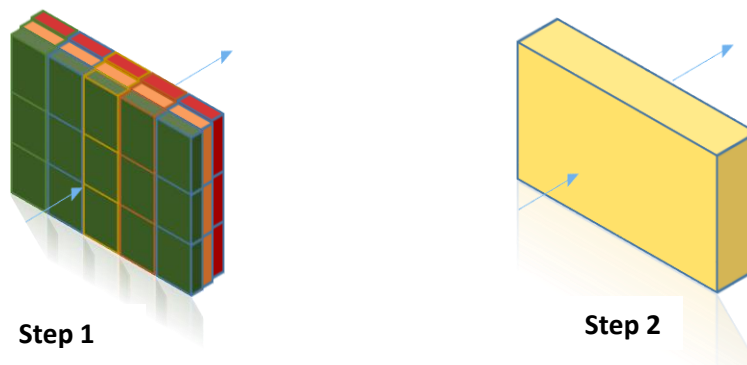
Step 1

Step 2

Figure 3.4: Example of Arithmetic-Harmonic technique applied. Step 1 graphically represents the Arithmetic average applied. Step 2 is the final step, when the Harmonic average is apllied.

_____

Sometimes it is possible to substitute the arithmetic or the harmonic average with the geometric one, depending on the permeability main changes direction.

- **Power average.**

It is defined as: [12]

$$k_e = \sqrt[p]{\frac{\sum_i^n k_i^p}{n}}$$

(3.4)

It is simply the generalization of all the exponential methods that have been already shown. The power average requires the knowledge of *p*, which is called power factor. It should be in the range of between -1 and 1. The possible cases are resumed below: [12]

- If p = -1, the power average is equivalent to the harmonic average

- When p is approximately 0.57 it is the best approximation for horizontal flow in shale-sand environments.

- When p = 1, it coincides with the arithmetic average

- For p = 0.12, it is the best characterization of vertical flows.

To conclude this section can be interesting to introduce one of the most used numerical approach. Most of the numerical methods require to solve the flow equation at the fine scale for portions of reservoir. This kind of approach requires computational time. The diagonal tensor is based on periodic boundary conditions and nowadays is one of the most approach used. [12]
Darcy's Law equation is solved in order to guarantee the mass conservation, or in other words, a constant flow at the borders. Boundary conditions and pressure drop are applied in order to determine the effective properties, such as figure (3.5) shows: [12]

$$\frac{\partial p}{\partial y} = 0$$

$$p_1 = 1 \longrightarrow \qquad \longrightarrow p_2 = 0$$

$$\frac{\partial p}{\partial y} = 0$$
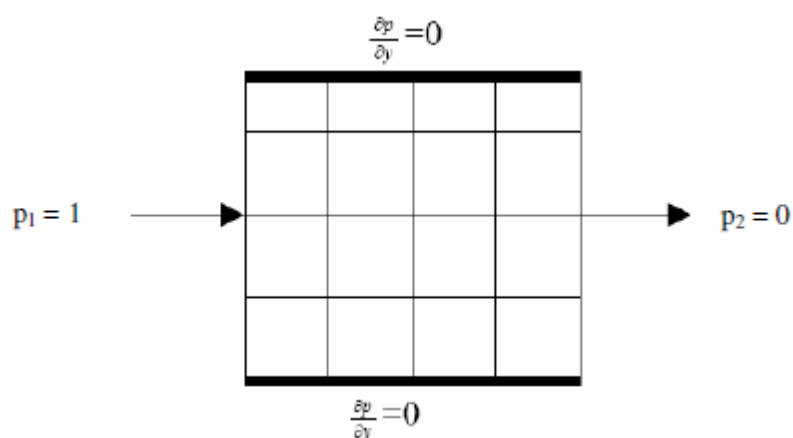
**Figure 3.5: Example of sealed-sides boundary condition applied on a
fine scale model subjected to a constant pressure drop.** *[12]*

Most of the times numerical methods are iterative. The one that is proposed in
this work follows this kind of approach, but it will be better explained in the
next chapters. However, it is possible to anticipate that the sealed-sides
boundary conditions and the pressure drop as it is shown in figure (3.5), were
used in this work.

4 Basic Equations for Single-Phase Flow

This work is based on simple equations that describe single-phase fluid flows inside a porous medium. All the mathematical equations derive from physical processes and considerations that concern reservoirs. Because of that, they will be initially expressed in form of Partial-Differential Equations (PDEs) that include the dynamic relationships among the fluid flow, mechanical and physical properties of the porous medium and, obviously, flow conditions of the system.

4.1 Darcy's Law

The purpose of this paragraph is to introduce clearly the Darcy's Law for single-phase flow in three-dimension. The most famous law used in reservoir simulation is Darcy's law, obviously for fluid flowing in a porous medium.

Darcy's law is an empirical relationship between fluid flow rate and pressure gradient (or hydraulic gradient). Its mathematical expression is [13]:

$$q = -\beta_c \frac{\mathbf{k}}{\mu} * \left(\overrightarrow{\nabla P} - \rho g \right) * A \tag{4.1}$$

Where β_c it is the unit conversion factor for the transmissibility coefficient (its value is 86.4 x 10^{-6}, to convert magnitudes of the metric system), $\mathbf{k}$ is the absolute rock permeability tensor, μ is the fluid viscosity (expressed in centipoise or in Pa·s), $\overrightarrow{\nabla P}$ is the gradient of pressure, $\rho \cdot g$ is the gravitational term (ρ is expressed in kg/m^3 and g in m/s^2) and A is the cross-sectional area (expressed in m^2). [13]

Equation (4.1) is the basis for any understanding and prediction of flow. Permeability appears in Darcy's law as local permeability tensor, mathematically represented by $\mathbf{k}$, as shown here [15]:

$$\mathbf{k} = \begin{bmatrix} k_{xx} & k_{xy} & k_{xz} \\ k_{yx} & k_{yy} & k_{yz} \\ k_{zx} & k_{zy} & k_{zz} \end{bmatrix} \tag{4.2}$$

Fluid viscosity (μ) is the internal resistance of the fluid, namely the resistance that each particle runs up against others particles when they are sliding. The hydraulic potential, in a reservoir, is the difference between the gradient of pressure and the gravity term. The gravity term works against the gradient of pressure, this explains why they are opposite. The unit conversion factor (β_c) is a coefficient that takes into account the transmissibility, which is a geometric factor (it is going to be explained better later) [19].

However, reservoir engineers should pay attention to some intrinsic assumptions that characterize Darcy's law. This empirical equation can be used for homogeneous fluid, single-phase and Newtonian fluids, such as oil or water. Moreover, if chemical reactions occur between the fluid and the porous medium, Darcy's law is no more valid. It is important that the nature of both rock and fluid, never changes. The absence of electro-kinetic and slippage effect is another important condition that has to be satisfied. [20] Moreover, as it has been already mentioned in the previous paragraphs, absolute permeability tensor is an intrinsic property of the porous medium so, it doesn't depends on pressure, temperature or the fluid flow.

One of the most important intrinsic assumption of Darcy's Law, is the laminar-flow condition. The flow speed inside a rock is typically 10 m/day. In fact, the Reynold's number of a fluid that is moving in a porous medium results within a range of $1 - 10$. [21] It means that viscous over inertial forces are preponderant and that's why laminar flow is an excellent approximation.

$$Re = \frac{\rho v D}{\mu} \tag{4.3}$$

Where ρ is again the fluid density, D is the pore diameter (expressed in m), μ is the fluid viscosity and v is the fluid velocity (expressed in m/s).

The form of Darcy's law that is used in order to formulate fluid flow equations assumes that the coordinate system and the principal axes of the permeability tensor are aligned. The resulting diagonalized permeability tensor simplifies the fluid flow equations and they can be easily solved. [22]

$$\mathbf{k} = \begin{bmatrix} k_{xx} & 0 & 0 \\ 0 & k_{yy} & 0 \\ 0 & 0 & k_{zz} \end{bmatrix} \tag{4.4}$$

_____

For a two dimensional system the permeability tensor can be written as:

$$\mathbf{k} = \begin{bmatrix} k_{xx} & 0 & 0 \\ 0 & k_{yy} & 0 \\ 0 & 0 & 0 \end{bmatrix} \tag{4.5}$$

It should be noticed and highlighted how the absolute permeability tensor is defined for each grid-block. It is really important to underline this concept, because if the cells are isotropic, it can be said that: [21]

$$k_{xx} = k_{yy} = k_{zz} \tag{4.6}$$

Which is a further simplification of the analysis, but it is supposed to be true just for the fine model because it is commonly discretized to have homogeneous cells.

Another important aspect of Darcy's law concerns the assumption of single-phase flow. Luckily it is possible to extend it for multiphase flows by simply considering the relative permeability (a magnitude that has been already introduced in chapter 2). For example, a two-phase flow of oil and gas can be represented by [5]:

$$q_0 = -\frac{kk_{ro}}{\mu_o} * \left(\overrightarrow{\nabla P} - \rho_0 \vec{g}\right) * A \tag{4.7}$$

$$q_g = -\frac{kk_{rg}}{\mu_g} * \left(\overrightarrow{\nabla P} - \rho_g \vec{g}\right) * A \tag{4.8}$$

Where *o* and *g* indicate the oil and gas phases. In these two equations, relative permeability for the oil and gas phases replaced absolute permeability.

4.2 Derivation of Generalized Flow Equations in Rectangular Coordinates

The method has been developed using rectangular coordinates. It means that the reservoir has to be an ensemble of parallelepipeds (or squares). However, in this paragraph basic principles will be shown, such as the respect of mass conservation. The continuity equation, which is a mathematical expression of material balance for a given control volume, [23] it is one of the most important equation for the purpose of this work. The mass conservation must be always

respected. To derive its expression a rectangular prism is used as control volume. The prism has dimensions Δx, Δy and Δz (expressed in m).

Each flux is perpendicular to the surface it is flowing through. The prism's center is located in (x, y, z) and consequently all the faces have coordinates: x - $\Delta x/2$, y - $\Delta y/2$, z - $\Delta z/2$, x + $\Delta x/2$, y + $\Delta y/2$ and z + $\Delta z/2$.

Fluxes and fluid's density, in each direction, are evaluated on the prism's surface borders. For example, the following notation will be used to indicate the flux rate and the fluid's density evaluated in x - $\Delta x/2$: $q_{x - \Delta x/2}$, $\rho_{x - \Delta x/2}$. Likewise for the other boundary surfaces of the control volume as shown in figure (4.1). [19]
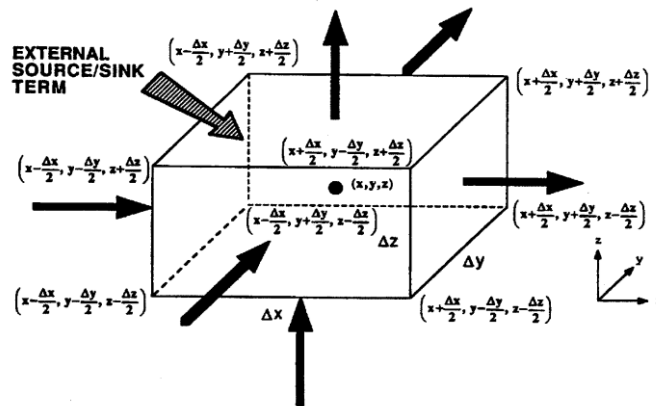
Figure 4.1: Example of control Volume, Basic Reservoir Simulation, Ertekin, King and Abou - Kassem. *[19]*

The mass balance for the given control volume in Figure (4.1) can be expressed in the following form [19]:

$$(m_i - m_0) + m_s = m_a \qquad (4.9)$$

Where, *mi* is the amount of mass that is entering in the control volume through the surfaces, m_o is the mass which is flowing out, m_s is the source/sink term and m_a is the mass accumulation. All of them are expressed in kg. The mathematical expression for the mass flow rate is given by [19]:

$$w = q * \rho \qquad (4.10)$$

Where, q is the flow rate (expressed in m^3/day) and ρ is the fluid density. So, w is expressed in kg/day. The equation (4.10) is useful to write the explicit form of the mass balance as follows: [19]

_____

$$[(w)_{\text{x-}\Delta\text{x/2}}\Delta t + (w)_{\text{y-}\Delta\text{y/2}}\Delta t + (w)_{\text{z-}\Delta\text{z/2}}\Delta t]$$

$$- [(w)_{\text{x+}\Delta\text{x/2}}\Delta t + (w)_{\text{y+}\Delta\text{y/2}}\Delta t + (w)_{\text{z+}\Delta\text{z/2}}\Delta t]$$

$$+ q_m \Delta t = (\varphi\, \Delta x \Delta y \Delta z\, \rho)_{\text{t+}\Delta\text{t}} - (\varphi\, \Delta x \Delta y \Delta z\, \rho)_t \qquad (4.11)$$

Where, Δt is the difference of time (expressed in days), q_m is the mass production rate (also expressed in kg/day).

So, the mass flow rate along each direction can be also expressed as: [19]

$$w_x = \dot{m}_x \Delta y \Delta z = m_x A_x \qquad (4.12)$$

$$w_y = \dot{m}_y \Delta x \Delta z = m_y A_y \qquad (4.13)$$

$$w_z = \dot{m}_z \Delta y \Delta x = m_z A_z \qquad (4.14)$$

The mass fluxes in equations (4.12), (4.13) and (4.14) can be expressed in terms of fluid density and volumetric velocity, u_i, (or Darcy velocity, expressed in m3/(day m^{-2})) as: [19]

$$\dot{m}_x = a_c \rho u_x \qquad (4.15)$$

$$\dot{m}_y = a_c \rho u_y \qquad (4.16)$$

$$\dot{m}_z = a_c \rho u_z \qquad (4.17)$$

Where, a_c is called volume conversion factor. It is a dimensionless number used to adjust the volume in reservoir conditions, which value is 5.614583. [19] So, replacing these expressions in equation (4.12) results in the following expression: [19]

$$[(a_c \rho u_x A_x)_{\text{x-}\Delta\text{x/2}}\Delta t + (a_c \rho u_y A_y)_{\text{y-}\Delta\text{y/2}}\Delta t + (a_c \rho u_z A_z)_{\text{z-}\Delta\text{z/2}}\Delta t]$$

$$- [(a_c \rho u_x A_x)_{\text{x+}\Delta\text{x/2}}\Delta t + (a_c \rho u_y A_y)_{\text{y+}\Delta\text{y/2}}\Delta t$$

$$+ (a_c \rho u_z A_z)_{\text{z+}\Delta\text{z/2}}\Delta t] + q_m \Delta t \qquad (4.18)$$

$$= (\varphi \Delta x \Delta y \Delta z \rho)_{\text{t+}\Delta\text{t}} - (\varphi \Delta x \Delta y \Delta z \rho)_t$$

By calculating the ration between equation (4.18) and the control volume (which is given by $\Delta y \Delta x \Delta z$), it becomes [19]:

$$-\frac{[(\rho u_x)_{x+\Delta x/2} - (\rho u_x)_{x-\Delta x/2}]}{\Delta x} - \frac{[(\rho u_y)_{y+\Delta y/2} - (\rho u_y)_{y-\Delta y/2}]}{\Delta y}$$

$$-\frac{[(\rho u_z)_{z+\Delta z/2} - (\rho u_z)_{z-\Delta z/2}]}{\Delta z} + \frac{q_m}{a_c V_b} \qquad (4.19)$$

$$= \frac{1}{a_c}\frac{(\varphi\rho)_{t+\Delta t} - (\varphi\rho)_t}{\Delta t}$$

Simply approaching $\Delta t, \Delta x, \Delta y, \Delta z$ to zero and multiplying for the volume of the element, it becomes [19]:

$$-\frac{\partial(a_c \rho u_x A_x)\Delta x}{\partial x} - \frac{\partial(a_c \rho u_y A_y)\Delta y}{\partial y} - \frac{\partial(a_c \rho u_z A_z)\Delta z}{\partial z} + \frac{q_m}{a_c} = \frac{V_b}{a_c}\frac{\partial(\varphi\rho)}{\partial t} \qquad (4.20)$$

Equation (4.20) is a common way for reservoir engineers to write the continuity equation, also called mass-conservation equation in three dimensions. Other two fundamentals laws must be included in equation (4.20), namely the Equations of State (also called EOS) and the Darcy's Law.

The EOS is a relationship among the fluid's density, the pressure and the temperature. A simple way to connect them is through the fluid formation volume factor (which acronym is FVF) B, which is a dimensionless number [19]:

$$B = \frac{\rho_{sc}}{\rho_{rc}} \qquad (4.21)$$

Equation (4.21) simply expresses the ratio between the fluid's density at standard condition and the fluid's density at reservoir condition. FVF can be defined for each phase that is present in the reservoir, namely water, gas and oil. FVF of water, which is almost an uncompressible fluid, is around 1. FVF of oil is usually less than 1 because at reservoir conditions the oil contains dissolved gas. While, FVF of gases is obviously much larger than 1.

_____

The velocities that appear in equations (4.15), (4.16) and (4.17) can be expressed by the Darcy's Law [19]:

$$u_x = -\beta_c \frac{k_x}{\mu} \frac{\partial p}{\partial x} \tag{4.22}$$

$$u_z = -\beta_c \frac{k_z}{\mu} \frac{\partial p}{\partial z} \tag{4.23}$$

$$u_y = -\beta_c \frac{k_y}{\mu} \frac{\partial p}{\partial y} \tag{4.24}$$

The source/sink term can be expressed in terms of volumetric rate at standard conditions rather than mass rate, then [19]:

$$q_m = a_c q_{sc} \rho_{sc} \tag{4.25}$$

Where q_{sc} is the production rate at standard conditions (expressed in std m³/day) and ρ_{sc} is the fluid density at standard conditions (expressed in kg/m³). [19] Equations (4.21), (4.22), (4.23), (4.24) and (4.25) can be substituted now in equation (4.21), so [19]:

$$\frac{\partial}{\partial x}\left(\beta_c \frac{A_x k_x}{\mu B} \frac{\partial p}{\partial x}\right)\Delta x + \frac{\partial}{\partial y}\left(\beta_c \frac{A_y k_y}{\mu B} \frac{\partial p}{\partial y}\right)\Delta y + \frac{\partial}{\partial z}\left(\beta_c \frac{A_z k_z}{\mu B} \frac{\partial p}{\partial z}\right)\Delta z$$
$$+ q_{sc} = \frac{V_b}{a_c}\frac{\partial}{\partial t}\left(\frac{\varphi}{B}\right) \tag{4.26}$$

Equation (4.26) is the most general form of the continuity equation for single-phase newtonian flows. It should be noticed that no assumption has been made about the fluid compressibility, it could be incompressible, slightly compressible or compressible. However, what is here assumed is that the gravity term (or

gravitacional forces) are supposed to be neglectable if they are compared with the pressure gradient [19].

4.3 Incompressible Fluid Flow Equation

The method was implemented for incompressible fluids. Due to the fact that the implementation in Matlab was not so easy, some simplification about fluid's nature were done. It's important to highlight that every single simplification or hypothesis constitutes a limit of this work. In fact, fluid's density is function of pressure and temperature. [19] So, being the pressure distribution for both fine and scaled up model considerably different, the fluid's density values may be really different too.

However, this method has been created not only for oil or gas reservoirs but for any upscaling application on porous medium, including acquifers.

For uncompressible fluids, FVF can be considered equal to 1. In according to these hypotheses equation (4.27) can be rewritten as [19]:

$$\frac{\partial}{\partial x}\left(\beta_c A_x k_x \frac{\partial p}{\partial x}\right)\Delta x + \frac{\partial}{\partial y}\left(\beta_c A_y k_y \frac{\partial p}{\partial y}\right)\Delta y + \frac{\partial}{\partial z}\left(\beta_c A_z k_z \frac{\partial p}{\partial z}\right)\Delta z + \mu q_{sc} = 0 \qquad (4.27)$$

The solution of equation (4.28) is independent of time due to the assumption of incompressibility of the fluid. It leads to no accumulation or depletion terms. It means that it can be treated as a steady state flow. Rock porosity is also considered constant, because the reservoir is supposed to be incompressible as well as the fluid [19].

If in the control volume, namely the grid-block, there are not production/injection wells the sink/source term is zero and equation (4.28) becomes [19]:

$$\frac{\partial}{\partial x}\left(A_x k_x \frac{\partial p}{\partial x}\right)\Delta x + \frac{\partial}{\partial y}\left(A_y k_y \frac{\partial p}{\partial y}\right)\Delta y + \frac{\partial}{\partial z}\left(A_z k_z \frac{\partial p}{\partial z}\right)\Delta z = 0 \qquad (4.28)$$

Equation (4.29) is also called Laplace equation.

_____

The partial derivative equations that were derived till now are fundamentals for each reservoir simulation software or technique. Moreover, it is important to understand what kind of hypothesis are used in this work in order of a better interpretation of the final results. The assumptions were made till now ca be resumed here: [19]

- Incompressible fluid
- Single-phase flow
- Constant porous medium's (reservoir) geometry
- No chemical or electrical interactions between fluid and rock or in the fluid itself

Numerical methods, such as the one that is proposed in this work, are based on approximated equations.

So, from now on the partial derivative form has to be abbandoned.The fluid flow equations must be discretized and the finite-difference method is a common way to do that.

5 Finite – Difference Approximation.

The PDE's equations derived in the previous chapter contain continuous derivatives of second order in space and first order in time. Due to their non-linear nature, it's impossible to solve them using any analytical approach [24]. Discretization processes help reservoir engineers for overcoming this obstacle. In fact, almost all the most famous numerical method, for upscaling and not, used in the oil industry are based on discretized equations.
In the next paragraph will be introduced the first important step: the discretization in space of reservoirs using the finite-difference method.

5.1   Construction of the Grids

It's important to understand what kind of reservoir representation was used in this work. The most common numerical methods used in oil industry are based on the finite-difference method [24]. The proposed method in this work is not an exception.
The purpose of a mesh system is to assign to each cell their own values of rock properties, pressure and temperature. In this way, a useful graphic resume can be used to have a clear idea about heterogeneity, pressure distribution, porosity etc. For example, a good representation of the permeability distribution is necessary to understand where the production or injection wells must be collocated.
The spatial derivatives are approximated by a finite-difference grid, which is superimposed over the reservoir. The discretized equations are obtained by the Taylor series, which are truncated. [24]
Depending on the reservoir type and the availability of data, engineers can choose between two different techniques for discretization: block-centred and point-distributed technique. [25]
Block-centred technique imposes grid-blocks with known dimensions over the reservoir. For rectangular or square geometries, namely Cartesian coordinates, the grid-points are defined as the grid-blocks centre. [25]
Whereas, a point-distributed system is exactly the opposite, grid-points are imposed over the reservoir and then the block boundaries are designed halfway

between two adjacent centre points. The difference between these two techniques is represented in figure (5.1). [25]
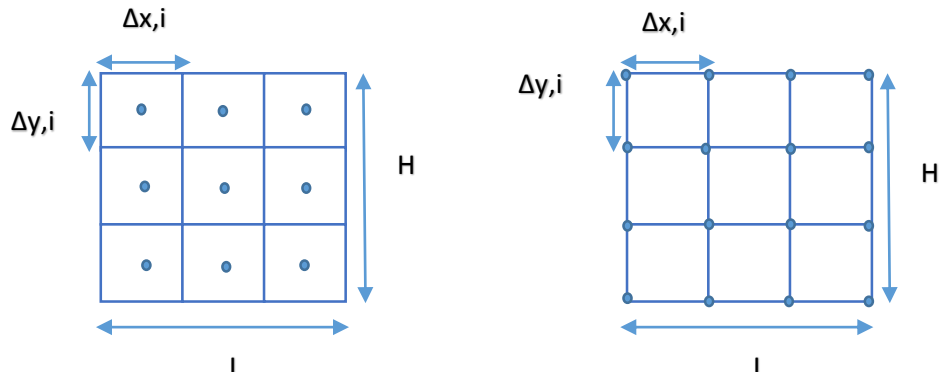
Figure 5.1: Examples of block-centered grid (on the left) and point-distributed grid (on the right). *[25]*

The block-centred configuration is the most used in oil industry because the block volume is always clearly defined. All the permeability grids were used in this work, for simulations and tests, were designed using block-centred technique. However, Matlab (the numerical software used for this work) can generate point-distributed grids (using the function "surf").

So, from now on all the permeability fields will be graphically shown are represented by a point-distributed configuration. It does not mean that the results were affected, it is only a graphical specification.

The block-centred design is also useful when no-flow conditions are imposed on the grid, such as it was done in this work. This explain why block-centred was chosen here. [24]

Grid-blocks can have whatever geometry. Nevertheless, the most used geometry for three-dimensional representation is the prismatic. In order to provide a good approximation of permeability, porosity or pressure average values, the block may not have the same dimensions. The smaller the spatial steps are (Δy, Δx and Δz), the better the approximation.

_____

Moreover, Δx_i, Δy_i and Δz_i are not necessarily equal for all the blocks but, for sure, they have to satisfy the following relationships [24]:

$$\sum_i^n \Delta x, i = L \tag{5.1}$$

$$\sum_i^n \Delta y, i = H \tag{5.2}$$

$$\sum_i^n \Delta z, i = D \tag{5.3}$$

Where *L*, *H* and *D* are the three reservoir dimensions. It means that the grid-blocks have to span the entire reservoir. SPE's (Society of Petroleum Engineers) datasets don't specify what kind of discretization have been used, therefore it was assumed to be a block-centred model. Whereas, permeability fields generated by probability distributions can be considered block-centred matrices. Pressure, porosity and permeability are defined in the grid – block's centre, which is indicated with x_i in figure (5.2).
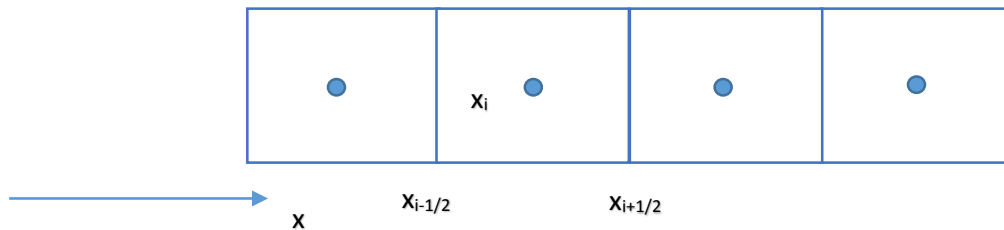
Figure 5.2: Example of grid notation. *[24]*

It means that each point held within the block's volume has the same permeability, porosity and pressure of the centre. The boundaries in x were indicated with $x_{i+1/2}$ and $x_{i-1/2}$, likewise in y and z.

For prismatic or cubic geometry are valid the following notations:

- $x = (x_{i+1/2} + x_{i-1/2})/2$
- $\Delta x_i = x_{i+1/2} - x_{i-1/2}$
- $y = (y_{i+1/2} + y_{i-1/2})/2$
- $\Delta y_i = y_{i+1/2} - y_{i-1/2}$
- $z = (z_{i+1/2} + z_{i-1/2})/2$
- $\Delta z_i = z_{i+1/2} - z_{i-1/2}$

5.2 Spatial Derivatives Approximation

Fluid flows in such a porous medium is a very complex phenomena. If analytic solutions give continuous solutions in time and space, numerical approaches are useful in order to obtain approximated solutions at discrete points in time and space. [24]

Darcy's law and mass conservation equations were shown in the previous chapters in the form of PDEs. Beyond the pure mathematical sense, is possible to implement them in a software through a discretization process.

Expanded Taylor series are useful mathematical tools for the purposes of discretization process. Equation (4.29) contains second order spatial derivatives. The first step is to discretize the partial derivatives outside the brackets using the central-difference approximation for first order derivatives [24]:

$$\frac{\partial}{\partial x}\left(\beta_c \frac{A_x k_x}{\mu B}\frac{\partial p}{\partial x}\right)_i \approx \frac{1}{\Delta x_i}\left[\left(\beta_c \frac{A_x k_x}{\mu B}\frac{\partial p}{\partial x}\right)_{i+1/2} - \left(\beta_c \frac{A_x k_x}{\mu B}\frac{\partial p}{\partial x}\right)_{i-1/2}\right] \quad (5.4)$$

$$\frac{\partial}{\partial y}\left(\beta_c \frac{A_y k_y}{\mu B}\frac{\partial p}{\partial y}\right)_j \approx \frac{1}{\Delta y_j}\left[\left(\beta_c \frac{A_y k_y}{\mu B}\frac{\partial p}{\partial y}\right)_{j+1/2} - \left(\beta_c \frac{A_y k_y}{\mu B}\frac{\partial p}{\partial y}\right)_{j-1/2}\right] \quad (5.5)$$

$$\frac{\partial}{\partial z}\left(\beta_c \frac{A_z k_z}{\mu B}\frac{\partial p}{\partial z}\right)_k \approx \frac{1}{\Delta z_k}\left[\left(\beta_c \frac{A_z k_z}{\mu B}\frac{\partial p}{\partial z}\right)_{k+1/2} - \left(\beta_c \frac{A_z k_z}{\mu B}\frac{\partial p}{\partial z}\right)_{k-1/2}\right] \quad (5.6)$$

_____

Substituting the equations (5.4), (5.5) and (5.6) in equation (4.29), it becomes:

$$\frac{1}{\Delta x_i}\left[\left(\beta_c\frac{A_x k_x}{\mu B}\frac{\partial p}{\partial x}\right)_{i+1/2}-\left(\beta_c\frac{A_x k_x}{\mu B}\frac{\partial p}{\partial x}\right)_{i-1/2}\right]\Delta x_i$$

$$+\frac{1}{\Delta y_i}\left[\left(\beta_c\frac{A_y k_y}{\mu B}\frac{\partial p}{\partial y}\right)_{j+1/2}-\left(\beta_c\frac{A_y k_y}{\mu B}\frac{\partial p}{\partial y}\right)_{j-1/2}\right]\Delta y_i$$

$$+\frac{1}{\Delta z_i}\left[\left(\beta_c\frac{A_z k_z}{\mu B}\frac{\partial p}{\partial z}\right)_{k+1/2}-\left(\beta_c\frac{A_z k_z}{\mu B}\frac{\partial p}{\partial z}\right)_{k-1/2}\right]\Delta z_i \qquad (5.7)$$

$$+q_{lsci}=\left(\frac{V_b\,\varphi\,c_l}{a_c\,B^0_{\,l}}\frac{\partial p}{\partial t}\right)_i$$

Where q_{lsci} is the production rate of phase l at standard conditions for the grid-block i. Now, using again the central-difference approach for the first derivatives of pressure inside the brackets [24]:

$$\left(\frac{\partial p}{\partial x}\right)_{i+\frac{1}{2}}=\frac{p_{i+1}-p_i}{x_{i+1}-x_i}=\frac{p_{i+1}-p_i}{\Delta x_{i+1/2}} \qquad (5.8)$$

$$\left(\frac{\partial p}{\partial x}\right)_{i-\frac{1}{2}}=\frac{p_i-p_{i-1}}{x_i-x_{i-1}}=\frac{p_i-p_{i-1}}{\Delta x_{i-1/2}} \qquad (5.9)$$

Likewise for partial derivatives of pressure in y and z. Equations (5.8), (5.9) and all the correspondent expressions in y and z can be substituted in equation (5.7) [24]:

$$\frac{1}{\Delta x_i}\left[\left(\beta_c\frac{A_x k_x}{\mu B\Delta x_{i+1/2}}\right)_{i+1/2}(p_{i+1}-p_i)-\left(\beta_c\frac{A_x k_x}{\mu B\Delta x_{i-1/2}}\right)_{i-1/2}(p_i-p_{i-1})\right]\Delta x_i +$$

$$\frac{1}{\Delta y_i}\left[\left(\beta_c\frac{A_y k_y}{\mu B\Delta y_{j+1/2}}\right)_{j+1/2}(p_{j+1}-p_j)-\left(\beta_c\frac{A_y k_y}{\mu B\Delta y_{j-1/2}}\right)_{j-1/2}(p_j-p_{j-1})\right]\Delta y_i +$$

$$(5.10)$$

$$\frac{1}{\Delta z_i}\left[\left(\beta_c\frac{A_z k_z}{\mu B\Delta z_{k+1/2}}\right)_{k+1/2}(p_{k+1}-p_k)-\left(\beta_c\frac{A_k k_k}{\mu B\Delta x_{k-1/2}}\right)_{k-1/2}(p_k-p_{k-1})\right]\Delta z_i +$$

$$q_{lsci}=\left(\frac{V_b\,\emptyset\,c_l}{a_c\,B^0_{\,l}}\frac{\partial(p)}{\partial t}\right)_{i,j,k}$$

Equation (5.10) is valid for a single-phase fluid flow, which is indicated with l. For the purposes of this work the phase will be just oil or water. Equation (5.10) can be written in a more compact way by simply introducing the transmissibility coefficient. Transmissibility is mathematically expressed as [3]:

$$T_l{}_{\text{x i-1/2}} = \left(\beta_c \frac{A_x k_{\text{x,i-1/2}}}{\mu B \Delta x_{\text{i-1/2}}} \right)_{\text{i-}1/2} \tag{5.11}$$

$$T_l{}_{\text{x i+1/2}} = \left(\beta_c \frac{A_x k_{\text{x,i+1/2}}}{\mu B \Delta x_{\text{i+1/2}}} \right)_{\text{i+}1/2} \tag{5.12}$$

It is a property which depends on the porous medium, the direction (subscript by *x*), the position (subscript by *i+1/2, i-1/2*) and the phase (subscript by *l*). Due to the fact that block – centered grids were used in this work, the transmissibility coefficient must be evaluated on the block's boundaries. It means that permeability will be given by the harmonic mean among two cells connected in series [24]:

$$k_{x_{\text{i+1/2}}} = \frac{n}{\sum_{i=1}^{n} \frac{1}{k}_i} \tag{5.13}$$

Transmissibility is physically considered an index of fluid's transmission through a surface in common between two control volumes. The larger the permeability and contact surface, the larger the permeability. Moreover, it is inversely proportional to the fluid viscosity B_l and Δx.

5.3 Time Derivatives Approximation

The discretization for time derivatives is very similar to the one illustrated in the previous paragraph, with an exception. Due to the fact that time derivatives have a different order it is not convenient to approximate them by using the central-difference approximation because of stability problems and difficulties in applying initial conditions. So, backward or forward – difference approximation are more appropriate. [24]
Reservoir engineers use backward – difference in order to have an implicit formulation of the set of equations. Whereas, the forward – difference approximation is used for explicit formulations but they may cause stability

_____

problems. So, applying the definition of backward - difference for first order time derivative [24]:

$$\frac{\partial p}{\partial t} \approx \frac{p(t^{n+1}) - p(t^n)}{\Delta t} \tag{5.14}$$

Or using a more comfortable and compact notation:

$$p^n = p(t^n) \tag{5.15}$$

$$p^{n+1} = p(t^{n+1}) \tag{5.16}$$

Equation (5.10) can be written as:

$$\frac{1}{\Delta x_i}\left[\left(\beta_c \frac{A_x k_x}{\mu B \Delta x_{i+1/2}}\right)_{i+1/2}(p^{n+1}_{i+1} - p^{n+1}_i) - \left(\beta_c \frac{A_x k_x}{\mu B \Delta x_{i-1/2}}\right)_{i-1/2}(p^{n+1}_i - p^{n+1}_{i-1})\right]\Delta x_i +$$

$$\frac{1}{\Delta y_i}\left[\left(\beta_c \frac{A_y k_y}{\mu B \Delta y_{j+1/2}}\right)_{j+1/2}(p^{n+1}_{j+1} - p^{n+1}_j) - \left(\beta_c \frac{A_y k_y}{\mu B \Delta y_{j-1/2}}\right)_{j-1/2}(p^{n+1}_j - p^{n+1}_{j-1})\right]\Delta y_i +$$

$$\frac{1}{\Delta z_i}\left[\left(\beta_c \frac{A_z k_z}{\mu B \Delta z_{k+1/2}}\right)_{k+1/2}(p^{n+1}_{k+1} - p^{n+1}_k) - \left(\beta_c \frac{A_k k_k}{\mu B \Delta x_{k-1/2}}\right)_{k-1/2}(p^{n+1}_k - p^{n+1}_{k-1})\right]\Delta z_i +$$

$$q_{lsci} = \left(\frac{V_b \varphi c_t}{\Delta t\, a_c B}\right)_{i,j,k}(p^{n+1}_i - p^n_i)$$

$$\tag{5.17}$$

The term on the left side of equation (5.17) is the amount of fluid that flows at time *n+1*, from a block to another one [24]. Whereas, the term on the right side is the fluid accumulation, or depletion, for the block *i*. So, the final form of the discretized continuity equations is reached and shown in equation (5.17). The next chapter will illustrate how the method was chronologically implemented.

6 Description of the Numerical Upscaling Method

What was illustrated till now should be useful for the reader for better understanding what mathematical tools and approximations were used to develop the method in this work. Now, it's time to introduce how this technique has been ideated. It is obviously based on the flux rate conservation, in other words it looks for the equivalent permeability values that keeps the flux rates constant.

The reduction of computational time is the most important objectives of any upscaling method, in order to avoid significant errors in terms of produced oil forecasts.

The chapter can be divided into two main parts. The former is about the homogenization process, which can be considered the heart of this work. What will be shown here, it is the method's chronological evolution and the convergence problems that were encountered. Convergence of numerical methods is always connected with their stability.

So, the second part of this chapter is about the tests that were done in order to verify if the outcome had physical sense or not. Starting from simple bi-dimensional domains under steady-state conditions, the first tests gave really good and, maybe, unexpected results in terms of flux rates conservation. After becoming more confident about the method, the next step was the implementation of a single production well, removing the steady-state hypothesis. This process will be explained better in chapter 7. Due to the fact that it is new, it could be a good idea to show its path for two main reasons: in this way is possible to fully understand it and, to give ideas to whom is interested for future improvements or adjustments.

So, its evolution from the beginning to its final form is going to be explained accurately in this chapter.

6.1 Pressure Distribution Calculation

The first problem that has to be solved is how to find the pressure distribution, which is necessary to calculate the flux rates. Most of the hypotheses about the fluid flow were already explained in the chapter 4 and 5. It is important to underline and remember that every single cell, which belongs to the fine grid, will be considered homogeneous and isotropic. In this work was used the sealed-sides boundary condition [2]. In other words, at the fluid is allowed to flow along a single direction, that from now on it will be called "main direction". The sealed-sides conditions are similar to the ones encountered in laboratory when a
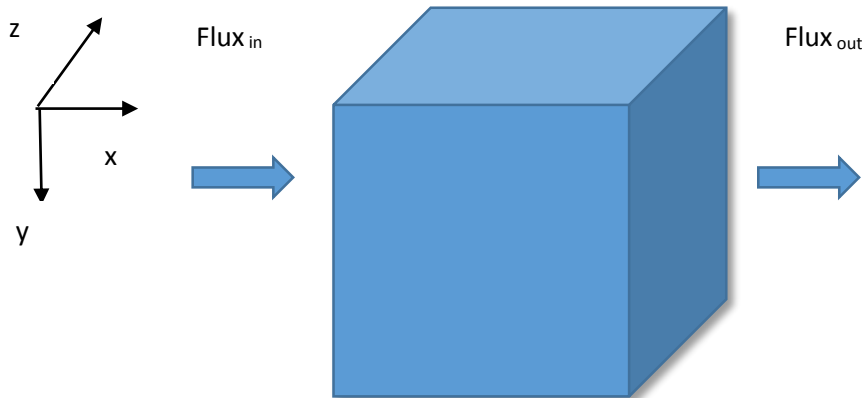
Figure 6.1: Example of porous medium through by a fluid along x-axis.

sample is tested with a permeameter. The fluid can flow through a porous medium if a pressure gradient is applied on it, this is the second boundary condition. The pressure gradient can be whatever value, because the purpose of this work is to develop a method that is not affected by the pressure. Figure (6.1) shows an example of cubic porous medium, which is subjected to a pressure gradient and the fluid is flowing parallel to x-axis.

The porous medium is figure (6.1) has to be imagined as internally sub-divided in smaller cells. The adiabatic boundary conditions are applied on the surfaces that are perpendicular to y and z-axes. The flow along x must be constant for any cross-section and it doesn't vary with time if the steady-state condition is satisfied. Then, it is possible to express again the mass conservation as:

$$Flux_{in} = Flux_{out} = Flux_{mid} \qquad (6.1)$$

_____

Simplifying equation (5.17) for a mono-dimensional, uncompressible and steady state flow and applying it on the system represented in figure (6.2) it is possible to make a set of equations:
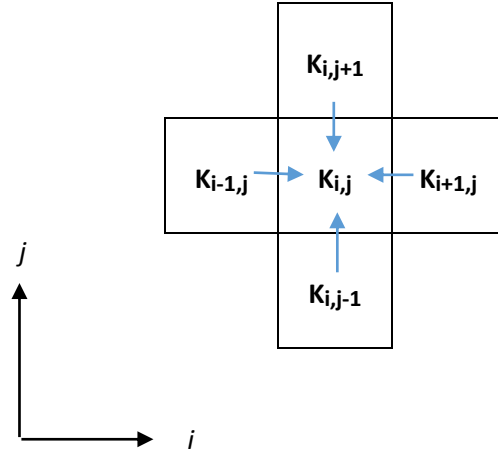
Figure 6.2: Graphical representation of internal blocks in two dimensions. They are useful in order to describe the mass conservation equations.

Figure (6.2) represents blocks in two dimensions because it is easier to represent but it is easy to visualize the correspondent 3D situation.

The sum of all the fluxes has to be zero because there is not mass accumulation or depletion:

$$\sum_{n=1}^{4} q_n = 0 \qquad (6.2)$$

Or explicitly becomes:

$$q_1 = \beta_c \frac{A_1}{\mu B \Delta x} * 2 * \frac{k_{i,j+1} \, k_{i,j}}{k_{i,j+1} + k_{i,j}} * (P_{i,j+1} - P_{i,j}) \qquad (6.3)$$

$$q_2 = \beta_c \frac{A_2}{\mu B \Delta x} * 2 * \frac{k_{i,j-1} \, k_{i,j}}{k_{i,j-1} + k_{i,j}} * (P_{i,j-1} - P_{i,j}) \qquad (6.4)$$

$$q_3 = \beta_c \frac{A_3}{\mu B \Delta y} * 2 * \frac{k_{i-1,j} \, k_{i,j}}{k_{i-1,j} + k_{i,j}} * (P_{i-1,j} - P_{i,j}) \qquad (6.5)$$

$$q_4 = \beta_c \frac{A_4}{\mu B \Delta y} * 2 * \frac{k_{i+1,j} k_{i,j}}{k_{i+1,j} + k_{i,j}} * (P_{i+1,j} - P_{i,j}) \tag{6.6}$$

Whereas, for a block that is situated on one of the external surfaces, for example at the entrance as it is shown in figure (6.3):
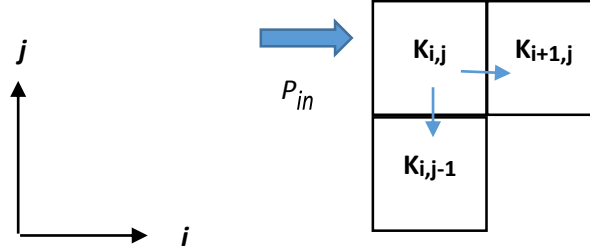
Figure 6.3: Example of mass balance for an external block at the entrance.

The fluid flow equations can be written as:

$$q_1 = \frac{A_1}{\frac{\mu \Delta x}{2}} * k_{i,j} * (P_{in} - P_{i,j}) \tag{6.7}$$

$$q_2 = \frac{A_2}{\mu \Delta x} * 2 * \frac{k_{i,j-1} k_{i,j}}{k_{i,j-1} + k_{i,j}} * (P_{i,j-1} - P_{i,j}) \tag{6.8}$$

$$q_3 = \frac{A_3}{\mu \Delta y} * 2 * \frac{k_{i+1,j} k_{i,j}}{k_{i+1,j} + k_{i,j}} * (P_{i+1,j} - P_{i,j}) \tag{6.9}$$

From now on, equation (6.7), (6.8) and (6.9) will be used to continue this example. Now, it is possible to add them, remembering that the sum must be zero:

$$-\frac{A_1}{\frac{\mu \Delta x}{2}} * k_{i,j} * (P_{in} - P_{i,j}) + \frac{A_2}{\mu \Delta x} * 2 * \frac{k_{i,j-1} k_{i,j}}{k_{i,j-1} + k_{i,j}} * (P_{i,j-1} - P_{i,j}) + \frac{A_3}{\mu \Delta y} * 2$$

$$* \frac{k_{i+1,j} k_{i,j}}{k_{i+1,j} + k_{i,j}} * (P_{i+1,j} - P_{i,j}) = 0 \tag{6.10}$$

_____

Then, it is possible to isolate the known term from equation (6.10), which contains the pressure at the entrance, and to move it to the right side of the equation:

$$\frac{A_1}{\frac{\mu\Delta x}{2}} * k_{i,j} * (P_{i,j}) + \frac{A_2}{\mu\Delta x} * 2 * \frac{k_{i,j\text{-}1} k_{i,j}}{k_{i,j\text{-}1} + k_{i,j}} * (P_{i,j\text{-}1} - P_{i,j}) +$$

(6.11)

$$\frac{A_3}{\mu\Delta y} * 2 * \frac{k_{i+1,j} k_{i,j}}{k_{i+1,j} + k_{i,j}} * (P_{i+1,j} - P_{i,j}) = \frac{A_1}{\frac{\mu\Delta x}{2}} * k_{i,j} * (P_{in})$$

So, if the same procedure is applied on all the blocks of the grid, it is possible to make a linear system, whose unknown terms are the pressure on the blocks.
Any software for numerical simulations can easily solve linear systems. It is necessary to express the system as a matrix equation:

$$A\, p = b$$

(6.12)

The coefficient matrix, which is indicated with A, contains the transmissibility factors, namely what is multiplying the pressure difference. The vector b is the known terms vector, which contains the solutions of all the mass balance equations, such as equation (6.11). The vector p is the unknown terms vector, which contains all the pressure values, excluding the pressure at the entrance and the exit that are known (boundary conditions). Therefore, we are dealing with a set of n equations with n unknowns. The coefficient matrix will be a square matrix made of n x n elements. It has to be epta – diagonal, if the mass balance is applied on three-dimensional blocks, or penta – diagonal for two-dimensional problems, exactly as figure (6.4) shows:
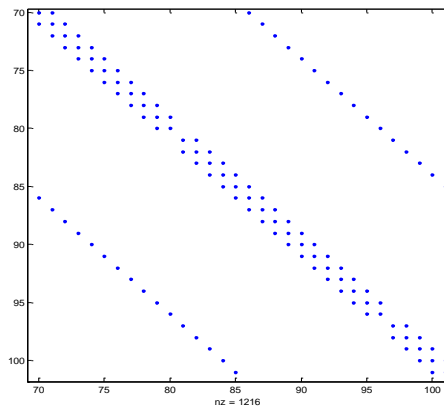
Figure 6.4: Example of coefficient matrix for problems in two dimensions.

The vector of pressure is given by:

$$p = A \backslash b \qquad (6.13)$$

Equation (6.13) is the matrix division of A and b, which is equivalent to invert A and multiply it by b.

Fig (6.1) shows the fluid flows parallel to x-axis but the same approach can be used when the fluid is flowing parallel to y or z-axis. In other words, using the boundary conditions that were used in this paragraph, it is possible to calculate three (or two, in case of two-dimensional problem) different pressure distributions.

In the next paragraph will be explained how three different pressure distributions are used, introducing the homogenization process of this work.

6.2 First form of the Homogenization Process

The process that precedes the upscaling is called homogenization. It consists in homogenizing a heterogeneous region with an equivalent homogeneous one. Due to the fact that it is a numerical process, a practical example can be useful to illustrate every single step and lead to its full comprehension.

In paragraph 6.1 it was shown how the pressure distribution is calculated using two kinds of boundary conditions. So, the way to homogenize the entire sample follows the same approach. In other words, the problem will be discomposed in a number of sub-problems that depends on the number of dimensions

_____

considered. For example, two-dimensional problems will be divided into two sub-problems, each one concerning the fluid flowing along the "main direction". As a consequence of this approach, each flow will be useful in order to calculate the equivalent permeability that is associated to the flow main direction. Despite that, every single permeability value influences the pressure distribution. For better understanding this concept it is sufficient to read carefully the previous paragraph.

The following example will be developed in two dimensions because of its easier representation, but all the general concepts are absolutely valid for more complex cases in three dimensions. The grid shown in figure (6.5) is a representation of a heterogeneous medium.

Each active cell is supposed to be homogeneous and isotropic.

$$k_{i,x} = k_{i,y}$$ (6.14)

These hypotheses don't affect the general validity of this method, rather they are useful to simplify the problem, making it easier for the reader.

The cells on the corners cannot be taken into account because of the finite-difference method. In fact, the contact surface between them and the "core", namely the central cells, of the grid is zero.
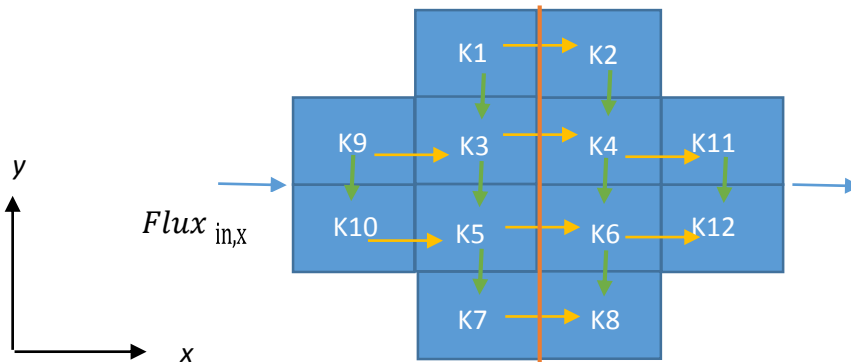
Figure 6.5: Portion of a porous medium in two dimensions

The fluid flows through the orange cross-section and it can be written as the sum of smaller fluxes, which are indicated with yellow arrows:

$$Flux_{\text{in,x}} = q_{1,2} + q_{3,4} + q_{5,6} + q_{7,8}$$ (6.15)

While the sum of all the vertical flows is zero because of the sealed-sides conditions. From now on, to give the general form of the equations, the

directions will be explicited as subscripts. The permeability values along x and y influence the distribution of pressure because they constitute the coefficient matrix (see equation (6.13)). Each flow can be defined as:

$$q_{1,2} = \left(\beta_c \frac{A_{12} k_{12,x}}{\mu B_l \Delta x} \right) (P_1 - P_2) \tag{6.16}$$

$$q_{3,4} = \left(\beta_c \frac{A_{34} k_{34,x}}{\mu B_l \Delta x} \right) (P_3 - P_4) \tag{6.17}$$

$$q_{5,6} = \left(\beta_c \frac{A_{56} k_{56,x}}{\mu B_l \Delta x} \right) (P_5 - P_6) \tag{6.18}$$

$$q_{7,8} = \left(\beta_c \frac{A_{78} k_{78,x}}{\mu B_l \Delta x} \right) (P_7 - P_8) \tag{6.19}$$

It is important to underline that, at the moment, to the fluid is allowed to flow parallel to the x-axis (see figure (6.5)). In equations from (6.16) to (6.19) Δx is the distance between the centers of two adjacent blocks, which is measured parallel to the x-axis. The contact area A_{ij} is defined as the common area between two adjacent blocks i and j; $k_{ij,x}$ is the harmonic mean among the permeability values along the x-axis, and $(P_i - P_j)$ is the pressure difference between two adjacent blocks.

The homogenization process can be applied on the four cells placed in the center (made up of blocks number 3, 4, 5 and 6) which are originally characterized by $k_{3x}, k_{4x}, k_{5x}, k_{6x}$.
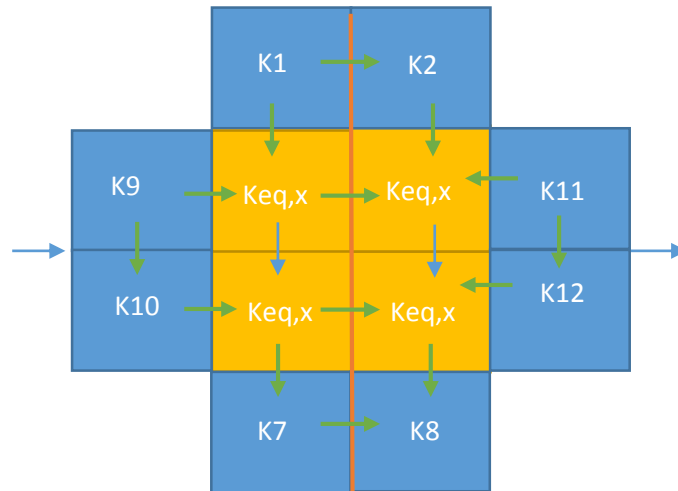
Figure 6.6: Homogenized porous medium on the central region, along x.

_____

The purpose is to replace the original core permeability value along the x-axis, with a single value, which ensures that the flow along the *x-axis* is kept constant. In other words:

$$Flux_{in,x} = q_{1,2} + q_{eq,3,4} + q_{eq,5,6} + q_{7,8} \qquad (6.20)$$

It is important to note that the flow must be constant through the orange cross-section and not through the core cross-section (the core is made up of the yellow cells). It means that the cells around the core influence the equivalent permeability calculation but, at the same time, they are useful to reduce the influence due to the boundary conditions. From now on, the cell layer, or layers, around the core will be called "ring".

However, $q_{eq,i,j}$ is the equivalent flow, namely the flow calculated using the Darcy's Law when the equivalent permeability replaces the original permeability values. Its mathematical expression is given by:

$$q_{eq,3,4} = \left(\beta_c \frac{A_{34}k_{eq,x}}{\mu B_l \Delta x}\right)(P_3 - P_4) \qquad (6.21)$$

$$q_{eq,5,6} = \left(\beta_c \frac{A_{56}k_{eq,x}}{\mu B_l \Delta x}\right)(P_5 - P_6) \qquad (6.22)$$

The same approach must be applied on the grid. This time, the sealed-sides boundary conditions are applied on the sides that are perpendicular to x-axis and the flow is allowed to move parallel to the y-axis; as the figure (6.7) shows:
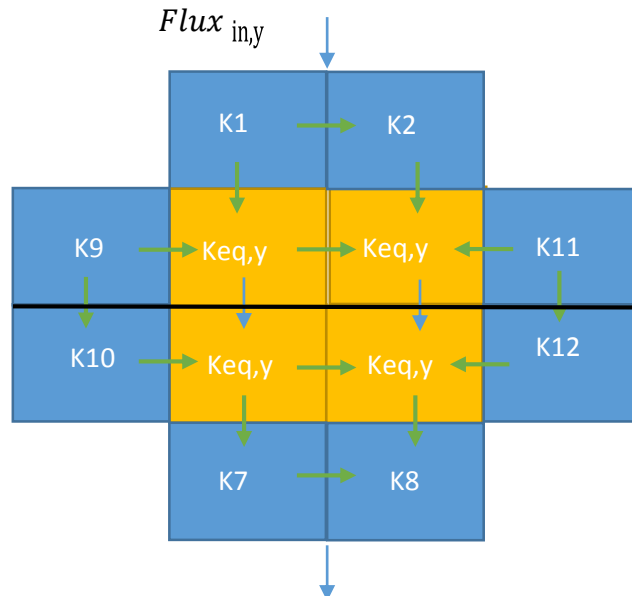
Figure 6.7: Homogenized porous medium along y-direction.

The original core permeability values along the y-axis are substituted by a single equivalent value, which is called here $k_{eq,y}$. Even in this case the flow must be constant throughout the black cross-section, when $k_{eq,y}$ is placed in the core.

$$Flux_{in,y} = q_{eq,3,5} + q_{eq,4,6} + q_{9,10} + q_{11,12} \qquad (6.23)$$

The mathematical expression of $q_{eq,i,j}$ is given by:

$$q_{eq,3,5} = \left(\beta_c \frac{A_{35} k_{eq,y}}{\mu B_l \Delta y} \right) (P_3 - P_5) \qquad (6.24)$$

$$q_{eq,4,6} = \left(\beta_c \frac{A_{46} k_{eq,y}}{\mu B_l \Delta y} \right) (P_4 - P_6) \qquad (6.25)$$

The distance between two adjacent blocks is Δy. All the comments were done for equations (6.21) and (6.22) are valid for the last two equations here.

The coefficient matrix of both systems varies due to the introduction of equivalent permeability. As a consequence also the pressure distributions vary.

Due to that, the set of flow equations that is used to calculate the pressure distribution is non-linear. The fluid flow equations clearly show clearly the non – linearity. In fact, despite a new incognita is introduced, the number of flow equations doesn't vary. So, the system must be linearized in order to be solved. Linearization can be done in many ways and one of them is the implementation of an iterative process.

Numerical methods based on iterative cycles may present some convergence and stability problems. Unfortunately there was not enough time to do a rigorous analysis of the method's stability.

However, achieving the convergence can depend on the first trial values that have to be chosen or calculated.

Due to the fact that the pressure distribution and the equivalent permeability vary proportionally, for each system, it could theoretically be possible to choose indifferently an initial best guess.

In practice, it could be risky to start the iterative process choosing a single pressure value as a first try. It makes more sense to choose, or to calculate, a first try of equivalent permeability. Choosing a permeability initial best guess in a real case is unconvenient, because of the great number of cells. So, luckily it is possible to calculate the first try of equivalent permeability values by simply using the original pressure distribution and equation (6.20) and (6.23):

_____

$$k^0_{eq,x} = \frac{Flux_{in,x} - q^0_{1,2} - q^0_{7,8}}{\left(\beta_c \frac{A_{34}}{\mu B \Delta x}\right)(P^0_3 - P^0_4) + \left(\beta_c \frac{A_{56}}{\mu B \Delta x}\right)(P^0_5 - P^0_6)} \qquad (6.26)$$

$$k^0_{eq,y} = \frac{Flux_{in,y} - q^0_{9,10} - q^0_{11,12}}{\left(\beta_c \frac{A_{35}}{\mu B \Delta y}\right)(P^0_3 - P^0_5) + \left(\beta_c \frac{A_{46}}{\mu B \Delta y}\right)(P^0_4 - P^0_6)} \qquad (6.27)$$

The original pressure of block i is indicated with P^0_i. They represent the pressures at iteration number zero, likewise for the equivalent permeability values, $k^0_{eq,x}$ and $k^0_{eq,y}$, which will replace the original permeability values in both cores.

The coefficient matrices have again only known terms, it means that both systems gained again their linearity. The first iteration creates two pressure vectors, which may be called p_x^1 and p_y^1:

$$p_x^{1} = A_x^{0} \backslash b_x \qquad (6.28)$$

$$p_y^{1} = A_y^{0} \backslash b_y \qquad (6.29)$$

Using the pressure distributions of equations (6.28) and (6.29) it is possible to calculate the equivalent permeabilities of the first iteration:

$$k^1_{eq,x} = \frac{Flux_{mid} - q^1_{1,2} - q^1_{7,8}}{\left(\beta_c \frac{A_{34}}{\mu B \Delta x}\right)(P^1_3 - P^1_4) + \left(\beta_c \frac{A_{56}}{\mu B \Delta x}\right)(P^1_5 - P^1_6)} \qquad (6.30)$$

$$k^1_{eq,y} = \frac{Flux_{in,y} - q^1_{9,10} - q^1_{11,12}}{\left(\beta_c \frac{A_{35}}{\mu B \Delta y}\right)(P^1_3 - P^1_5) + \left(\beta_c \frac{A_{46}}{\mu B \Delta y}\right)(P^1_4 - P^1_6)} \qquad (6.31)$$

An error between iterative permeability values of 10^{-9} is considered to be acceptable, which means an also really small difference between the flows.

$$\frac{k^n_{eq,x}}{k^{n-1}_{eq,x}} - 1 < 10^{-9} \quad \& \quad \frac{k^n_{eq,y}}{k^{n-1}_{eq,y}} - 1 < 10^{-9} \qquad (6.32)$$

The iterative process stops if the condition represented by equation (6.32) is satisfied, otherwise it starts over till convergence is reached.

The reader will certainly have noticed that the homogenization process, in this example, needed to work with different representations. It is due to the sealed-sides boundary conditions. The final results, then, will be represented in as many grids, namely two for the example that was shown here.

In other words, the superposition principle is applied on this work and the total amount of fluid that is flowing is given by the sum of every single flow along a "main direction".

In three dimensions basically the same happens and then, in general, the "equivalent" matrices are three, as figure (6.8) shows:
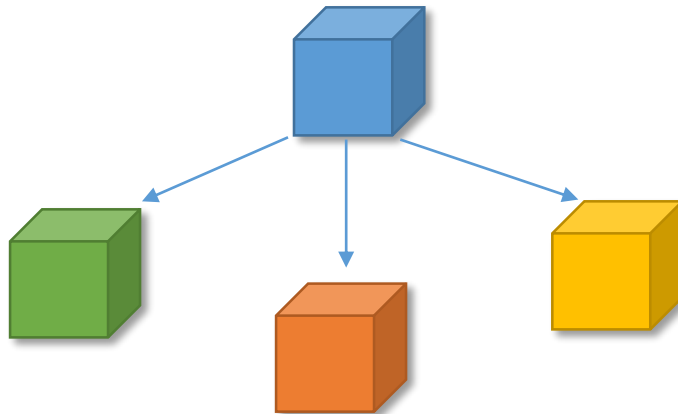
Figure 6.8: Here an illustration of how represents homogenized permeability grids.

Figure (6.8) schematizes the problem: starting from a fine model, which contains just homogeneous and isotropic elements, the final results consists in three different matrices. Each one contains only equivalent permeability values along a single direction.

It is important to note that the term "homogenization" is improperly used. In fact, the core in the previous example, was globally characterized by heterogeneity even if each single cell was homogeneous. After homogenization the core is still heterogeneous because it is characterized by three different permeability values. Moreover, each single cell has lost its homogeneity because they are characterized by three different permeability values as well. So, the term "homogenization" is in truth associated to the permeability along a single direction. Again, it is due to the boundary condition's nature.

However, this method was implemented in Matlab and convergence problems were encountered during the production simulations. Certainly they are correlated to the homogenization process because the scale is decreasing. However, the way to calculate the equivalent permeability values, till now, looks too artificial.

In a real situation the fluid is moving in all directions, it means that each permeability also influences the fluid movement along other directions. Nevertheless, the method considers separately two flows, each one along its own way. Both equivalent permeability calculations are independent from one another and there is no interaction between them. So, the method was modified, trying to implement a better iterative process, which considers mutual influence among equivalent permeability values, in order to make more realistic the fluid flow simulation.

6.2.1 Improved Homogenization Process

The sealed-sides condition implies that the flow is directly influenced by the equivalent permeability along the main direction. The process that was explained on the previous paragraph has an evident lack. The distribution of pressure of both matrices is affected by its own equivalent permeability and the original permeability values. This aspect can be improved. Figure (6.9) helps in better understanding how:
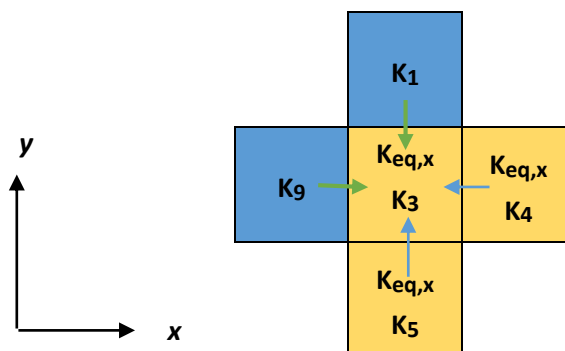
Figure 6.9: Example of mass balance useful to fine the pressure distribution during the homogenization process.

In figure (6.9) it is shown a part of the core of figure (6.6), because the reader has to keep their attention on the mass balance. It is important to underline that

k_3, k_4 and k_5 are shown to highlight that a part of the system is still affected by them. In fact, by applying the mass balance for the central-block (number 3) in order to calculate the pressure distribution it is found that:

$$q_1 = \beta_c \frac{A_1}{\mu B \Delta y} * 2 * \frac{k_1 k_3}{k_1 + k_3} * (P_1 - P_3) \tag{6.33}$$

$$q_2 = \beta_c \frac{A_2}{\mu B \Delta x} * 2 * \frac{k_9 k_{eq,x}}{k_9 + k_{eq,x}} * (P_9 - P_3) \tag{6.34}$$

$$q_3 = \beta_c \frac{A_3}{\mu B \Delta y} * 2 * \frac{k_5 k_3}{k_5 + k_3} * (P_5 - P_3) \tag{6.35}$$

$$q_4 = \beta_c \frac{A_4}{\mu B \Delta x} * 2 * \frac{k_{eq,x} k_{eq,x}}{k_{eq,x} + k_{eq,x}} * (P_4 - P_3) \tag{6.36}$$

It is evident that $k_{eq,y}$ is not affecting the calculation of pressure distribution for the system that regards the flow moving along x-axis. In other words, in equation (6.34) and (6.36) it should make sense to replace k_3 and k_5 with $k_{eq,y}$.

The same considerations are absolutely valid for the second system, namely for the flow which is moving along the y-axis. So, a simple way to allow the "communication" between both systems is replacing $k_{eq,y}$ and $k_{eq,x}$ to all the original values. As a consequence of this approach, the cycle will change its form. In fact, it was a simultaneous process, namely both equivalent permeability values were calculated at the same time. Due to this improvement, it has become a sequential cycle.

For example, $k^0_{eq,y}$ is normally calculated as shown in equation (6.27) using the original pressure distribution. The next step is to replace k_3 and k_5 with $k^0_{eq,y}$ in equations (6.34) and (6.36) in place of. In this way is possible to calculate a new distribution of pressure for the system whose flow is moving parallel to the x-axis. Then, $k^0_{eq,x}$ can easily be calculated using equation (6.26) but, this time, the pressure distribution is also influenced by $k^0_{eq,y}$.

Now, $k^0_{eq,x}$ and $k^0_{eq,y}$ are placed on the core of both systems instead of all the original permeability values. By using them, it is possible to calculate a new pressure distribution for the system whose flow is parallel to the y-axis using equation (6.29). In this way it is possible to calculate $k^1_{eq,y}$ from equation (6.31). The cycle keeps going and $k^1_{eq,y}$ takes the place of $k^0_{eq,y}$ in the core where the

_____

flow is moving along x-axis. It is useful for the calculation of a new pressure distribution in that system, which will allow to calculate $k^1_{eq,x}$.
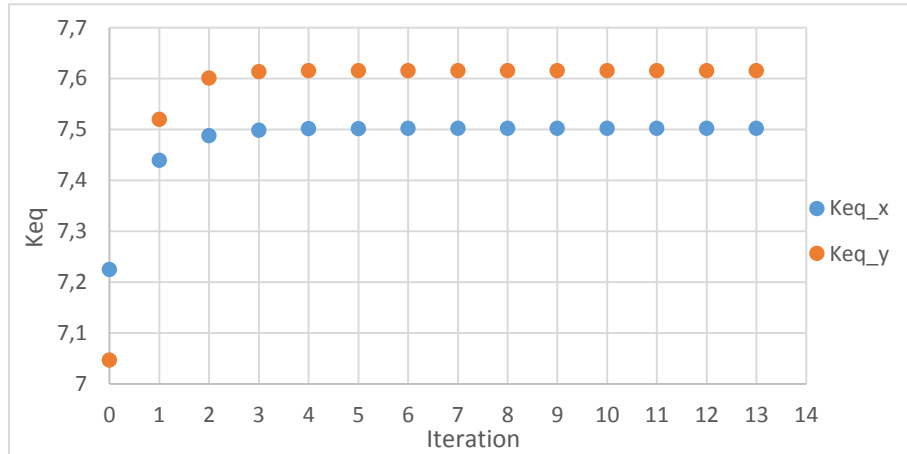
Figure 6.10: Example of convergence using the first version of the method.

So, the process keeps going alternatively substituting $k^n_{eq,y}$ and $k^n_{eq,x}$ on the two systems, till to equation (6.32) is satisfied.

Even if this modification is conceptually an improvement, numerically it is not the solution for convergence problems. It is probably due to the values chosen for the first trials, $k^0_{eq,x}$ and $k^0_{eq,y}$, that may be not always good ones. It's not easy to understand when and why to expect good first trial values. However, it can be useful to see the convergence's trend in order to understand how it is reached. Figure (6.10) shows the convergence path of both equivalent permeability values. It was used part of the two-dimensional SPE's dataset.

It is important to note that after the first iteration $k^0_{eq,y}$ and $k^0_{eq,x}$ "jump" to $k^1_{eq,y}$ and $k^1_{eq,x}$. Afterwards, the iterative values become more stable. In fact, the equivalent permeability value is already close to the final one in the third iteration.

Most of the times, divergence happened if the first trial values were too close or too far from their convergence value. It was noticed that the cycle enters a loop and it oscillates between two boundary values. So, the first trials values can be responsible for divergence problems. However, there is not the absolute certainty about it and a deeper study should be done in order to achieve a full knowledge about these problems.

In order to try solving this problem it has been done another changing.

An important result could be reach the absolute homogenized core. In other words, at the end of the process, this results should be reached:

$$k_{eq,x} = k_{eq,y} = k_{eq,z} \tag{6.37}$$

In this way it should be also easier to represent the scaled model, because just one mesh would be necessary. Even if conceptually it is possible to reach these results, unfortunately the reality is different. Such as the perfect equivalence between fine models and equivalent ones is impossible to reach, also this result is hardly achievable, except for really rare cases.

These exceptional cases may be: symmetric distribution of permeability, cores surrounded by a single or multiple homogeneous "rings", etc.

In a real case, or in geologic models created by numerical probability distributions, these situations are really improbable. However, even if it is impossible to reach the absolute homogenization, this approach could further improve the method.

The iterative process is basically the one explained before, with an exception. Imagining to extend the problem in three dimensions, the permeability values are exchanged at the beginning of the cycle and after the comparisons (equation (6.32)), in this way:

$$k^{n}_{eq,x} = k^{n-1}_{eq,y} \tag{6.38}$$

$$k^{n}_{eq,y} = k^{n-1}_{eq,z} \tag{6.39}$$

$$k^{n}_{eq,z} = k^{n-1}_{eq,x} \tag{6.40}$$

They could be exchanged in a different order but all the tests and simulations were done using this configuration.

This idea was born as a reverse process, namely it was ideated in order to reach a result that was already known. In facts, ideally, at the end of the process it should be indifferent to exchange equivalent permeability values among them.

Another important aspect is relative to the numerical behavior. In fact, if the first trial of one of them is not so good, it will not directly affect its pressure distribution.

_____

This approach had an impact on the convergence that is shown in figure (6.11):
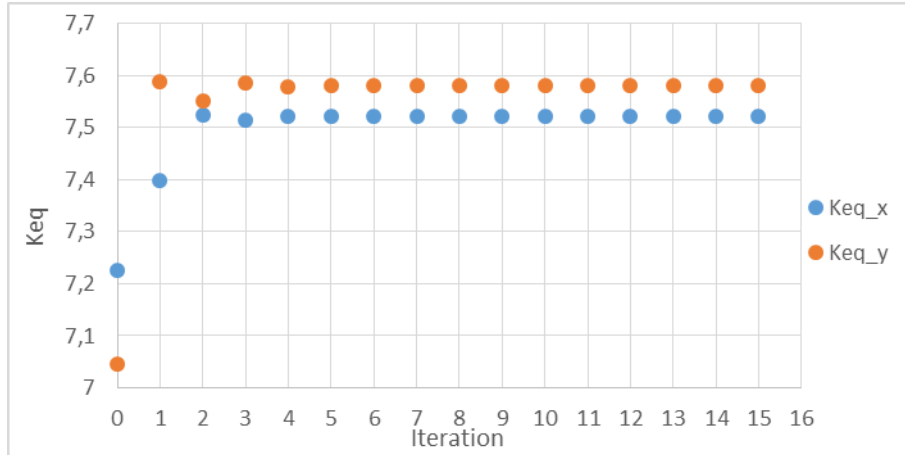
Figure 6.11: Example of convergence using the last version of the method.

The same part of the two-dimensional SPE's model that was used in figure (6.10) to show the convergence's trend, it was used to find out how the new convergence's trend would be. The first attempts, $k^0_{eq,y}$ and $k^0_{eq,x}$, are obviously the same for both figures. Figure (6.10) shows how the two equivalent permeability values are converging in parallel, even if they are affecting each other pressure distribution. Figure (6.11) shows something different, namely $k_{eq,y}$ and $k_{eq,x}$ are trying to reach the same final value. They obviously cannot do it because of numerical limits. However, this is exactly what was expected since the moment that this iterative cycle was ideated.

Figure (6.12) shows the convergence of the three equivalent permeability values for a three-dimensional log-normal permeability distribution:
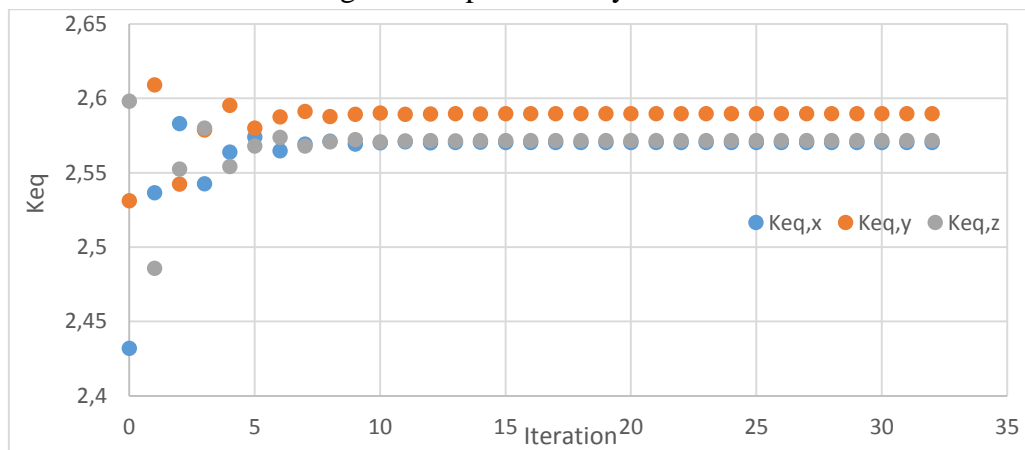
Figure 6.12: Convergence of equivalent permeability values in three dimensions.

The trend is similar to the one shown in figure (6.11). The difference between them, at the end of the process, is quite small.

Another important aspect that deserves to be highlighted here is about the final results. In facts, due to the non-linearity of the problem, the equivalent permeability values are different for the two homogenization processes. However, as for each numerical method, also the one presented in this work is affected by divergence problems and non-positive iterative permeability values. It can happen when an iterative process is used. [3]

In fact, it was seen that, in rare cases, the pressure distribution has generated negative iterative permeability values. In other rare cases, even if the values were positive, they bounced between two values and they could not converge.

It is important to underline that these problems were happened only for the SPEs dataset and never when permeability probability distributions were used.

However, a preventive measure was ideated in order to push the process to the convergence. In particular, if after a great number of iterations the convergence is not reached, the script follows this instruction:

$$k^n_{eq,y} = \frac{k^{n-1}_{eq,y} + k^n_{eq,y}}{2} \tag{6.41}$$

However, non-convergence problems are isolated cases and till now the method has always worked in a satisfactory way. It does not mean that this technique always work, there is not the absolute certainty such as for every single numerical upscaling method.

The next paragraph will show the results obtained by simple simulations on particular permeability distributions.

6.3 Simulation Tests

Simple tests are always useful and necessary to understand if the method is working exactly how is expected or not. One of the doubts that may regards this method is: if the permeability values have exchanged during the homogenization process, how can we be so sure that the final results are exactly the equivalent permeability in x and y?

To clarify what the final results are and what they represent, can be useful to use some particular permeability distributions, whose results are known in advance

_____

because they can be calculated through analytical approaches, such as the ones that were shown in the Chapter 3.

In fact, the results found by combined average techniques were used as references. Some particular matrices were used to understand if the idea is well-founded or not.

In the first test was used a stratified two-dimensional grid was used, whose columns were alternatively filled with 10 and 20 as the figure (6.12) shows. This particular distribution of permeability is useful to understand if the Arithmetic – Harmonic and Harmonic – Arithmetic average techniques and the homogenization process of this work, will give the same results.
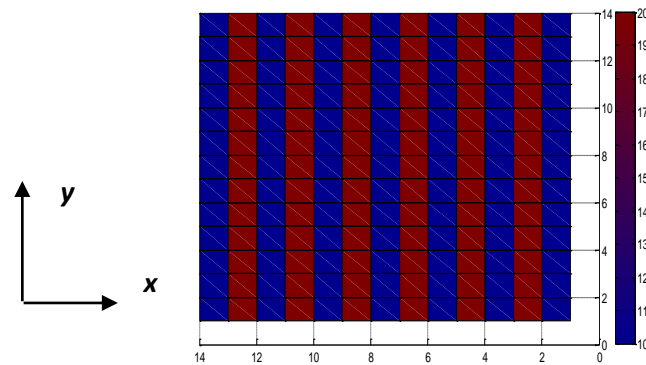
Figure 6.13: Stratified two-dimensional matrix.

When the flow main direction is supposed to be along the *x-axis* then, the direction of permeability main change is parallel to the fluid flow. The Harmonic – Arithmetic average technique can then be applied. It was applied to a square domain that is not influenced by surrounding blocks, because it is a local method.

So, the domain is simply:

$$
\begin{array}{cc}
10 & 20 \\
10 & 20
\end{array}
$$

Figure 6.14: Domain taken into account for the test.

The analytical result given by this technique is:

$$step\ 1 \quad k_H = 2 * \frac{10 * 20}{10 + 20} = 13.3333 \tag{6.42}$$

$$step\ 2 \quad k_A = \frac{13.3333 + 13.3333}{2} = 13.3333 \tag{6.43}$$

When the main direction is *y*, namely the fluid is flowing perpendicularly to the permeability main change, the Arithmetic – Harmonic average technique can be applied and gives the following results:

$$step\ 1 \quad k_A = \frac{10 + 20}{2} = 15 \tag{6.44}$$

$$step\ 2 \quad k_H = 2 * \frac{15 * 15}{15 + 15} = 15 \tag{6.45}$$

So, the expected results are 13.3333, for the equivalent permeability along x, and 15 for the one along y. The method was applied, paying attention to choosing a number of "rings" equal to zero, because it has to be such a local method. The pressure between the entrance and the exit was 1 for both cases and the results are shown graphically in figure (6.14):
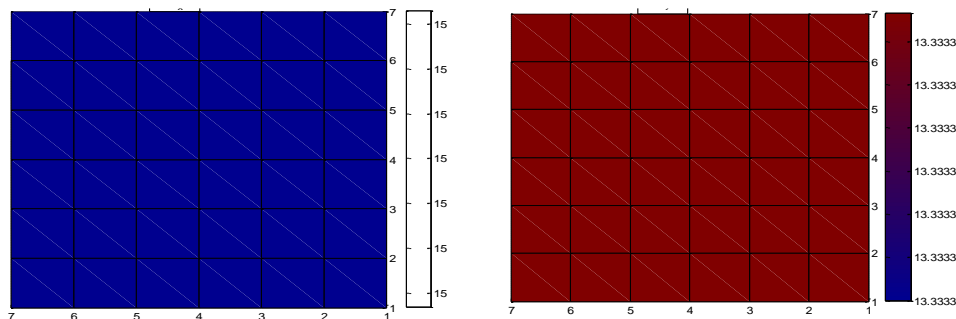
Figure 6.15: Graphical representation of results. On the left, Keq,y; on the right Keq,x.

Exactly the expected results. This is just a simple test in two-dimensions but it proves that the code is well-implemented and even if the permeability are switched, the final results make physically sense. It is important to note that the boundary conditions don't affect the equivalent permeability calculation. It is really important for the results quality.

The last significant test used a sort of "chessboard" matrix, where both lines and columns were alternately filled with 10 and 20. As figure (6.15) shows:
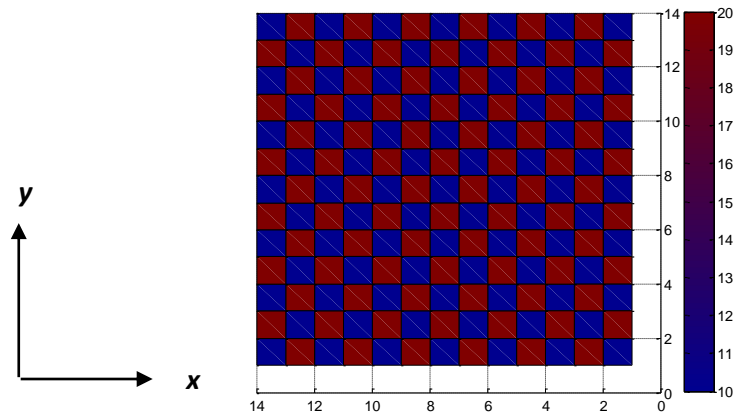
Figure 6.16: Example of chessboard matrix.

In this case, there is not an analytical result that can be taken as reference but, being the permeability field symmetric, the expected result is the same value for both equivalent permeability.

In chapter 3 is explained that the exponent p of equation (3.8) depends on the permeability probability distributions. In this case we don't know what kind of probability distribution can be associated to figure (6.15) and then, it is impossible to calculate the analytical solution.

However, the equivalent permeability, for both systems, is 13.7143, which are the expected results, graphically shown in figure (6.16):
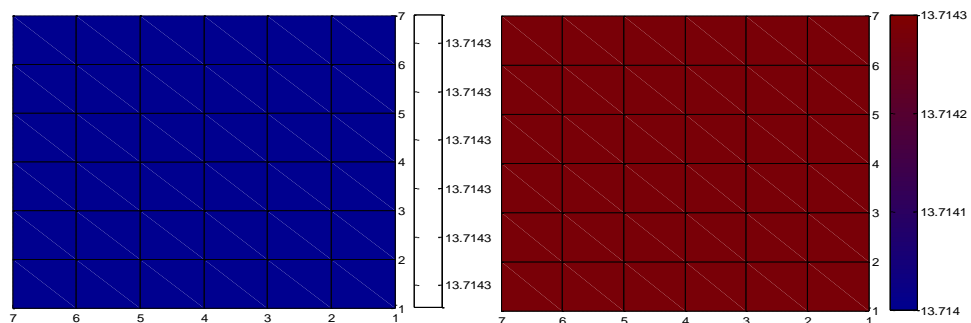
Figure 6.17: Graphical representation of results from the chessboard test.

The same tests were done for a three-dimensional matrix, whose columns were alternatively filled with 10 and 20. The results are in line with the theory. In fact, when the main direction is x, the equivalent permeability is given again by

the harmonic average between 10 and 20. Therefore, when the main direction is y or z, the equivalent permeability is 15.

Even for the "3-D chessboard" matrix, whose columns and lines were alternatively filled with 10 and 20, the results are the expected ones. In fact, the equivalent permeability was the same for the three, and it was equal to 13.8462.

So, the test results gave what was expected but the most important results will be analyzed later.

To conclude, after homogenization the upscaling must be applied. This process involves a change in scale and creating a new coarse field from the homogenized models.

The scaled matrices were used for the simulations and the results will be compared with the ones derived from the fine models. Now, it is necessary to explain how the production well was implemented in two and three dimensions. The approach that was used in this work is the same of Ertekin, Abou – Kassem and King's book and it will be explained in the next chapter.

7 Production Well Implementation

The most important goal of reservoir simulation is to forecast well-flow rates and to estimate pressure and saturation distributions. Production well implementation is always a delicate step because well-blocks treatment presents some difficulties [26]. The well-block is the block where the well is placed. First of all, when a well is placed on a block it is hard to estimate its pressure even if the block dimensions are larger than the well's size [26].

Another critical aspect is due to the difficulty in coupling the complex interaction between the reservoir and the wellbore, especially in case of multi − layer wells. Another complexity is given by the multi − phase flow condition, because it's difficult to allocate the production rate to each phase.

However, the well representation have been adapted accordingly to the purposes of this work. In fact, the goal is a comparison between production rates of both fine and coarse models, and not production estimations using real reservoirs. So, the same simplifications were adopted even when a coarse model was used. It is obviously a basic requirement to ensure that the comparison is valid [26].

The wells are characterized by cylindrical geometries. However, the geological models that were used in this work had prismatic geometries and it is necessary to modify the flow expression. The right way to calculate the well flow is given by the Darcy's law for cylindrical geometries [26]:

$$q = -\frac{2\pi\beta_c k_h H r_w}{\mu}\frac{\partial p}{\partial r} \tag{7.1}$$

The flow is considered negative when it comes out from the well and vice versa, it is positive if the well is injecting fluid (in this case it is called injection well). In equation (7.1), r_w is the well radius, k_h is the horizontal permeability, H is the depth of the well-block. However, the vertical permeability is often negligible, so only the horizontal permeability values were considered [26].

PDEs such as equation (7.1) have no practical uses in this work. Then, separating the variables and integrating equation (7.1) between the wellbore radius (r_w) and an arbitrary radius (r), and between a generic pressure (p) and the sandface pressure (p_{wf}) it is obtained [26]:

$$\int_{r_w}^{r} \frac{1}{r} \partial r = -\frac{2\pi\beta_c k_h h}{\mu} \int_{p_{wf}}^{p} \partial p \tag{7.2}$$

It results in the steady state pressure distribution for an undamaged well expression [26]:

$$p = p_{wf} - \frac{q\mu}{2\pi\beta_c k_h H} \log_e\left(\frac{r}{r_w}\right) \tag{7.3}$$

Equation (7.3) is the mathematical expression of pressure for whatever radius value. Nevertheless, the radius has to stay within the external and the well radius values:

$$r_w \le r \le r_e \tag{7.4}$$

From equation (7.3) it is possible to explicit the flow. It is useful to express it in standard conditions using the FVF. The flow is calculated using the entire well-block space in other words, when the radius is equal to the external radius. When it happens, the generic pressure becomes the external pressure (p_e). Then it is possible to find from equation (7.3) [26]:

$$q_{sc} = -\frac{2\pi\beta_c k_h H}{\mu B \log_e\left(\frac{r_e}{r_w}\right)}(p_e - p_{wf}) \tag{7.5}$$

In reservoir engineering it is common to allow only one well to penetrate a grid – block. Furthermore, it is common to have at least one or two empty grid – blocks between wells, because it is important to avoid pressure interference effects.

The well placement depends on the type of grid. For a block – centered grid, which is the model used in this work, it is really common a well placed on the block center [26].

While, for point-distributed meshes, the well is usually placed on the corners. However, it is not always possible to place the wells on the block centers.

In fact, reservoir engineers have optimize the grid network depending on the reservoir's nature. It means that it could be necessary to place part of the wells in off – center locations in the grid-blocks.

In this work, the production well was collocated on the block center of fine models because of the grid's simple disposition.

_____

Whereas, when the coarse meshes were used, the well has been placed in off –
center, as the figure (7.1) shows:
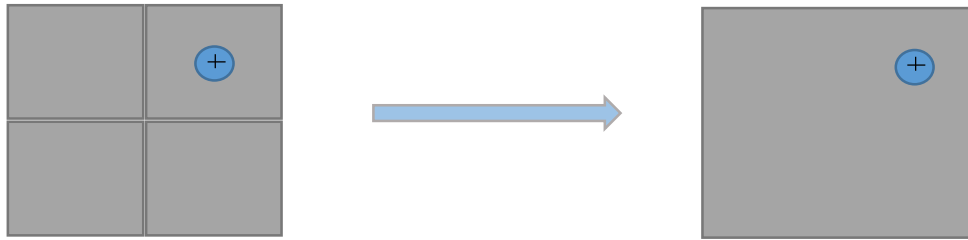
Figure 7.1: Example of centered well-block (on the left) and off-center well-block (on the right).

In fact, it is important to not modify the well position when the coarse model is
used, otherwise the comparison would be not valid.
The next paragraph will discuss about the well implementation in two-
dimensions for a single-phase flow.

7.1   Single Layer Well Model

Single – layer well representation is one of the most used in reservoir
engineering. This approach is used when it is possible to consider the geological
model as two-dimensional. In this model, the well-block is always surrounded
by eight blocks.
Depending on the well placement, the influence of the blocks placed on the
corners can be taken into account or not. For example, if the well is placed on
the well-block center those blocks will not influence the flow. However, this
assumption is useful to simplify the problem. In fact, the corner blocks always
should influence the flow, but in that particular case, their influence is
negligible.
Unlike for a well placed in off-center, whose flow is appreciably influenced
even by corner blocks [26].
In reservoir simulation it is common to implement the single – layer well
choosing one of three most famous methods: the van Poollen et al., Peaceman,
and Abou – Kassem and Aziz's model [26].

The former is one of the earliest attempts of developing a production well simulation model. Nowadays, this model is not used because it is not refined as the other two [26].

Peaceman's model is not applicable for off-center well, so in this work the Abou – Kassem and Aziz's model was used. It is applicable in well-centered and off-centered representations but only if the ratio between Δy/Δx is within the range ½ to 2.

However, the equivalent radius replaces the external radius in equation (7.5) if the grid – block has not a cylindrical geometry. Basically, the difference between the three methods is the equivalent radius definition.

The Abou – Kassem and Aziz's model defines the equivalent radius as [26]:

$$r_{eq} = \left\{ \exp(-2\pi f) \prod_i \left[r_{i,j}{}^{T_i} \prod_j \left(\frac{r_{i,j}}{a_j} \right)^{T_i} \right] \right\}^b \tag{7.6}$$

In equation (7.6) $r_{i,j}$ is the distance between the block i and the well j, T_i is the interface transmissibility for flow between block i and well-block, a_j is the distance from the well to its jth image, f is the fraction of well flow coming from the well-block and it is dimensionless.

This equation can be better understood seeing figure (7.2):
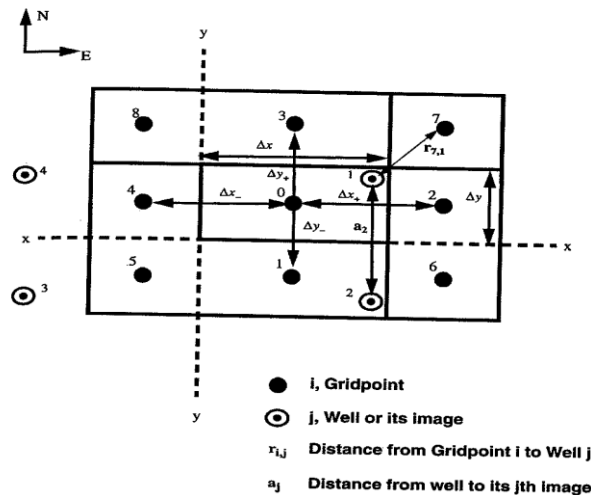
Figure 7.2: Example of off-center well *[26]*

The well is supposed to be placed on the grid-block 0. The well-block can be an interior block if it does not have boundaries in common with reservoir

_____

boundaries. Otherwise it is called boundary well-block. For the purposes of this work, only internal well-block were considered. If the well-block is an interior block and the well is placed on the center, the production rate is affected by blocks number 1 till 4.

However, if one of the reservoir boundaries falls on the southern boundary of the well-block, the production rate is not influenced by grid – blocks 1, 5 and 6. The same consideration is valid when whatever reservoir boundary falls in any well-block's boundary. If the well-block is an interior block and the well is placed in off – center, grid-blocks 5, 6, 7 and 8 influence the flux rate. Due to the fact that they cannot be considered in the finite – difference equations because the contact surface between them and the well-block is zero, it is necessary to adjust the equivalent radius [26]. The term a_j takes into account the image wells, those exist only when the well-block is not an interior block. The number of images depends on the number of well-block boundaries in common with the reservoir boundaries.

However, it doesn't concern this work, which only considers just internal well-blocks. So, the product of the image wells is considered equal to 1. Equation (7.6) can be modified, resulting in [26]:

$$r_{eq} = \left\{ \exp(-2\pi f) \prod_i r_i^{Ti} \right\}^b \qquad (7.7)$$

The factor f is 1 for an interior well-block, ½ for a well-block that has one boundary in common with the reservoir boundary; and ¼ for a well-block that has two boundaries in common. The exponent b is given by [26]:

$$b = 1/\sum_i T_i \qquad (7.8)$$

It includes the sum of all the interface transmissibility factors. They are geometric factors but they are different from the transmissibility that was shown in chapter 4. Interface transmissibility factor depends just on the geometry of surrounding grid – blocks and well-block.

They can be calculated as table (7.3) shows [26]:

$$T1 = \left(\frac{\Delta x}{\Delta y}\right) - (T5 + T6)$$

$$T2 = \left(\frac{\Delta x}{\Delta y}\right) - (T6 + T7)$$

$$T3 = \left(\frac{\Delta x}{\Delta y}\right) - (T7 + T8)$$

$$T4 = \left(\frac{\Delta x}{\Delta y}\right) - (T5 + T8)$$

$$T5 = \frac{1}{3}\left[\frac{(\Delta x)(\Delta y)}{(\Delta x^2) + (\Delta y^2)}\right]$$

$$T6 = \frac{1}{3}\left[\frac{(\Delta x)(\Delta y)}{(\Delta x^2) + (\Delta y^2)}\right]$$

$$T7 = \frac{1}{3}\left[\frac{(\Delta x)(\Delta y)}{(\Delta x^2) + (\Delta y^2)}\right]$$

$$T8 = \frac{1}{3}\left[\frac{(\Delta x)(\Delta y)}{(\Delta x^2) + (\Delta y^2)}\right]$$

Table 7.1: Table of Geometric Transmissibilities factors for rectangular geometries *[26]*

Well implementation steps depend on time. At the beginning there is not fluid flowing through the reservoir boundaries and the pressure distribution is supposed to be constant and uniform over all the reservoir [26]:

$$\nabla p = C \qquad\qquad (7.9)$$

The well implementation can be based on two different approaches: it is possible to keep the production rate constant, or, it is possible to keep the sandface pressure constant. Obviously, only the second option makes sense in order to have a significant comparison between fine and coarse model [26].
The well implementation is also based on mass balance equations, such as the ones that were shown in chapter 5. In particular equation (5.17) was used for the mass balance of the well-block. In equation (5.17) the source term, q_{sc}, has to be replaced by equation (7.5). In this equation the external radius must be replaced by the equivalent, namely equation (7.7). When the block is a simple block, equation (5.17) can be used but the source term doesn't exist. The mass

_____

conservation laws are the same that were shown at the beginning of chapter 6, paying more attention when they have to be applied on the well-block [26].

So, this is what concerns the single – layer model, in other words a well simulation in two dimensions. The implementation in three dimensions should be more complicated but it is possible to simplify it [26].

Vertical, multilayer well models allow to simulate well flow coming from different layers. In other words, the production flow should be the sum of all the flows coming from the perforated layers. However, being this elaborated model unnecessary for the purposes of this work, it was implemented a normal single vertical well [26].

In three dimensions, however, is not possible to neglect the pressure gradient due to the gravity, so:

$$p_{\text{wf}} = p_{\text{wf}_{\text{ref}}} + \int_{H_{\text{ref}}}^{H_{\text{m}}} \gamma_{\text{wb}}\, dH \qquad (7.10)$$

The reference pressure, $p_{\text{wf}_{\text{ref}}}$, is the pressure at the surface. The reference depth is H_{ref} and most of the times is zero. So H_{m} is the well depth. Single-phase hydrostatic wellbore pressure gradient, γ_{wb}, can be defined as [26]:

$$\gamma_{\text{wb}} = \gamma_c\, g\, \frac{\rho_{lsc}}{B_l} \qquad (7.11)$$

Where γ_c is the gravity conversion factor, its value is 10^{-3} for converting the magnitude of the metric unit adjustments.

Basically, the considerations were done for the single – layer well are valid even in this case [26]. In fact, the vertical permeability is often negligible when compared with the horizontal permeability. In other words, the well was modeled such a single-layer. So, it is possible to adopt again the same equivalent radius expression (equation (7.7)) used for the two-dimensional well representation.

Even the interface transmissibility factors can be calculated with the same expressions (table (7.1)), paying attention to only considering grid – blocks oriented along the rights direction [26].

Whereas, the distribution of pressure is obviously influenced by all the grid – blocks, exactly as it was shown in chapter 5 and 6, but in particular way it is influenced by the well. Now, the results will be shown and analyzed in terms of production rates, number of iterations and simulation time [26].

8 Results

In this section all the most significant results will be analyzed, whether they were satisfactory or not. In this work two different SPE's dataset were used, available on the SPE's website. Uniform, normal and log-normal permeability distributions were also numerically generated (by Matlab) and used in order to have a sufficient number of results. The method has been applied to fine models using different changings in scale. It is important to underline that has been used only one "ring", namely one block layer around the core. The role of surrounding blocks is to reduce the influence of the boundary conditions. The simulations showed that using more rings around the core has not a significant impact on the final results. The sandface pressure used for the tests was within a range of 0 to 1.

Production rates, computational time and permeability distributions for both models will be shown here. All the conclusions and comments must be read critically because they have been argued on results obtained from a large number of simulations and there are yet not specific studies have been done on the method.

8.1 Simulation Time comparison

8.1.1 Random Permeability Distribution, Simulation Time

Auto-generated permeability distributions were used in order to have a significant number of results. In this paragraph only results regarding the simulation time will be shown. In fact, it is not correlated with the method, or its quality. In other words, the homogenization process is not responsible for the time decrease but it is important to show how upscaling reduces computational time. The first test has been done for a two dimensional matrix, which size was *80x80.*

The results generated are resumed in table (8.1):

Lognormal Distribution - 2D Model					
Fine Model		Coarse Model			
Dimension	TIME [s]	Dimension	Resolution	TIME [s]	Iterations
80x80	43,64	40x40	2x2	1,27	35977
80x80	46,21	20x20	4x4	0,055	5952
80x80	44,54	10x10	8x8	0,016	1047
80x80	45,97	8x8	10x10	0,016	590

Table 8.1: Results of simulation time and number of iterations for a two-dimensional matrix generated by uniform numerical distribution.

Resolution indicates how the scale has been reduced. For example, if the original matrix was *80x80*, using a resolution of *4x4*, the scaled up one will be *20x20*.

The simulation time regards the time required by the numerical software, which is Matlab, for a single production well simulation. In this work, was used a range of time of one hundred days, subdivided in ten Δt (each one of ten days) in order to not overcharge the computer.

Even if this huge difference is not directly correlate to the technique that was developed here, it is an important result for any upscaling technique. In fact, it varies of magnitude orders.

The number of iterations is referred to the homogenization process, namely the number of steps which are necessary to entirely homogenize the porous medium. Iterations are not correlated with the well simulation.

_____

However, depending on the resolution that is used, iteration vary significantly, as figure (8.1) shows:
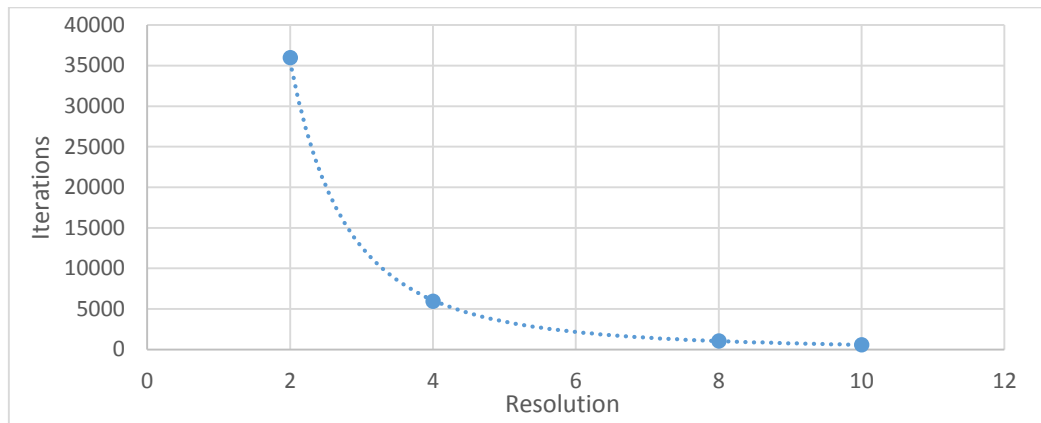
Figure 8.1: Graphic Iteration vs Resolution.

This results are in line with the expectations. The mathematical relationship between iterations and resolutions is clearly exponential and if it was not, probably some important errors would be present in the script.

The simulations for a three-dimensional mesh show us even better results, in terms of computational time, resumed in table (8.2):

Lognormal Distribution - 3D model					
Fine Model		**Coarse Model**			
Dimension	TIME [s]	Dimension	Resolution	TIME [s]	Iterations
20x20x20	82,98	10x10x10	2x2	0,65	20295
20x20x20	82,33	5x5x5	4x4	0,07	1634

Figure 8.2: Results of simulation time and number of iterations, for a three-dimensional matrix, generated by uniform numerical distribution.

The maximum size allowed for whatever three-dimensional mesh, using the best computer in UDESC's department, was *20*x*20*x*20*, namely 8000 elements. In this case the computational time is much larger than whatever two-dimensional grid analyzed and the time reduction is largely convenient.

8.1.2 SPE's Dataset, Simulation Time

The first SPE's dataset used for the test is a two-dimensional model, which purpose is to investigate performance of both upscaling and classical pseudoization approaches. The SPE's website reports that the fine model is a two-phase (oil and gas) model, it is a simple 2D vertical cross-sectional geometry with no dipping or faults. However, in our case a mono-phase model will be used. The dimension of the model are [27]:

- $\Delta x = 7.62\ m$
- $\Delta y = 7.62\ m$
- $\Delta z = 0.762\ m$

The fine scale grid is *100* x *1* x *20* with uniform size for each of the grid blocks. Variables, such as viscosity, density and saturation were not considered because they don't affect the final results. In other words, they are constant and they do not affect the time consumption difference or the error among well flows. Moreover, in the SPE's website it is written that the permeability distribution is a correlated geostatistically generated field with constant porosity of 0.2. [27] In accordance to SPE's description, the fluid is considered to be incompressible and immiscible. Further information about an injection well, the injection rate and the bottom pressure were ignored, because they could be useful just for someone that wants to reach the exercise's purposes. The goals in this section are quite different. So, the time and iterations results are resumed in table (8.2):

SPE dataset 1 - 2D Model					
Fine Model		Coarse Model			
Dimension	TIME [s]	Dimension	Resolution	TIME [s]	Iterations
100x20	2,05	50x10	2x2	0,07	17091
100x20	2,22	25x5	4x4	0,019	8962

Table 8.2: Results of simulation time and iteration number, for a two - dimensional matrix, generated by SPE dataset 1.

The second dataset consists of part of a Brent sequence. The top part of the model is a Tarbert formation, and it is a representation of a prograding near shore environment. It has a simple geometry with no top structure or faults. The fine scale model size is *60* x *220* x *84*. [28] Unfortunately the number of active grid cells is too large for the computer's memory that was used. So, it was

_____

impossible to run a simulation of the entire field. However, only its first layer was taken into account in order to be simulated, giving the following results resumed in table (8.3):

SPE dataset 2 - 2D model					
Fine Model		Coarse Model			
Dimension	TIME [s]	Dimension	Resolution	TIME [s]	Iterations
60x84	24,33	30x42	2x2	0,811	31589
60x84	24,27	15x21	4x4	0,044	5538
60x84	24,27	10x14	6x6	0,018	2026

Table 8.3: Results of simulation time and iteration number, for a two - dimensional matrix, generated by SPE dataset 2.

Therefore, simulation time and iterations are perfectly in line with the expectations.

Computational time is an important parameter that must be kept under control. However, the most important parameter is the error regarding the difference between the production rates, calculated using the original and the scaled geological grids. So, it is possible to conclude this paragraph stating that upscaling reduces consistently the time consumption.

8.2   Production Well Flow Comparison

The errors relative to the well flows depend on several factors, among which the well placement and the heterogeneity level that characterizes the well zone.

Near well regions are always difficulty treatable. In these zones the assumption of constant pressure on the well-bock is not valid [29] and a better discretization in space could be useful to overtake these problems. However, the purpose of upscaling processes is to scale fine models, then it is impossible to avoid this kind of problems. Moreover, the pressure distribution should be really different between the fine and the coarse model. This difference among pressure distributions can be another important factor that negatively influence simulations results. It happens especially when the well-block permeability is low, because the Darcy's velocity is lower [30]. It is not so easy to give a complete and detailed explanation about this phenomena, because this is the first study about this method. For these reasons the results will be showed for

different zones, highlighting what the error trend is in function of the well-block absolute permeability of the fine model.

8.2.1 Numerical permeability distributions, Well Flow

Ten tests will be shown in this paragraph. It is not useful to show all the results that were obtained because all of them follow the same trend of the ones shown here. The first results were obtained by a uniform permeability distribution. The fine model was a two-dimensional matrix of 30x30. It was simulated twice, using two different resolutions. The well-block permeability is indicated in the first column of table (8.4). It is possible to see that highly different well-blocks were chosen in order to simulate a production well in the most different conditions. It is useful to show how the errors get worst when the fine model is excessively scaled up. The equivalent permeability values are also showed to complete the set of information necessary for the reader.
The results are resumed in table (8.4) and (8.5):

Uniform Distribution - 2D Model – Resolution 2x2					
Fine Model		Coarse Model			
K	Well Flow [kg]	Keq,x	Keq,y	Well Flow [kg]	Error
0,07	0,81	0,58	0,52	1,72	112%
0,19	1,40	0,30	0,25	2,34	66%
0,29	1,78	0,64	0,64	2,21	24%
0,40	1,54	0,41	0,42	1,94	26%
0,60	2,32	0,72	0,72	2,46	5%
0,76	2,13	0,64	0,64	2,52	18%
0,97	2,29	0,30	0,31	2,39	4%

Table 8.4: Results of production well flows, using a Rectangular Permeability Distribution.

_____

Uniform Distribution - 2D Model – Resolution 6x6					
Fine Model		Coarse Model			
K	Well Flow [kg]	Keq,x	Keq,y	Well Flow [kg]	Error
0,07	0,81	0,58	0,52	5,26	548%
0,19	1,40	0,30	0,25	5,31	277%
0,29	1,62	0,64	0,64	5,32	227%
0,40	1,66	0,41	0,42	5,61	236%
0,60	2,32	0,72	0,72	5,24	125%
0,74	2,13	0,64	0,64	4,93	130%
0,97	2,29	0,30	0,31	5,62	145%

Table 8.5: Results of production well flows, using a Rectangular Permeability Distribution.

It is important to note that $k_{eq,x}$ and $k_{eq,y}$ are similar even when the resolution is 6. This is a really good result because it is in line with the basic concept behind this method. When the production well is placed on a low permeability region the error increases. In table (8.4) is shown that the higher errors have been registered when the well-block permeability values are low. Whereas, the remaining results, in table (8.4), can be considered good ones.

The error was simply calculated as:

$$error \ = \ \left| \frac{\left| well\ flow, fine\ model\right| - \left| well\ flow, coarse\ model\right|}{\left| well\ flow, fine\ model\right|} \right| \qquad (8.1)$$

It is interesting to note that in those regions, where the absolute permeability and the equivalent permeability values are similar (highlighted in red, in table (8.4)), the error is high. A good explanation may be that the well flow depends also on the difference of pressure and the well-block's size. they are different for the fine and scaled models. In other words, the well-block permeability for both models should be different in order to compensate the pressure and well-block's volume difference. It is important to remember that the block volume influences the pressure distribution (see equation (5.17)).

However, the results in table (8.4) are associated to a low resolution. In other words, the fine model was "slightly" approximated, but the results shown in table (8.5) are really different. In fact, they regard the simulation of the same fine model but it was homogenized using a higher resolution. So, the reader should not be surprised by these results. The most important aspect, which deserves to be highlighted, is the error's trend in function of absolute permeability. It is evident how the error decreases when the well-block

permeability increases. The equivalent permeability values are still similar one to each other. Moreover, $k_{eq,x}$ and $k_{eq,y}$ reported in table (8.5) look similar to the ones reported in table (8.4) but they are different after the forth decimal place.

So, it can be interesting to plot the error as a function of the well-block permeability of the fine model, as figure (8.3) shows:
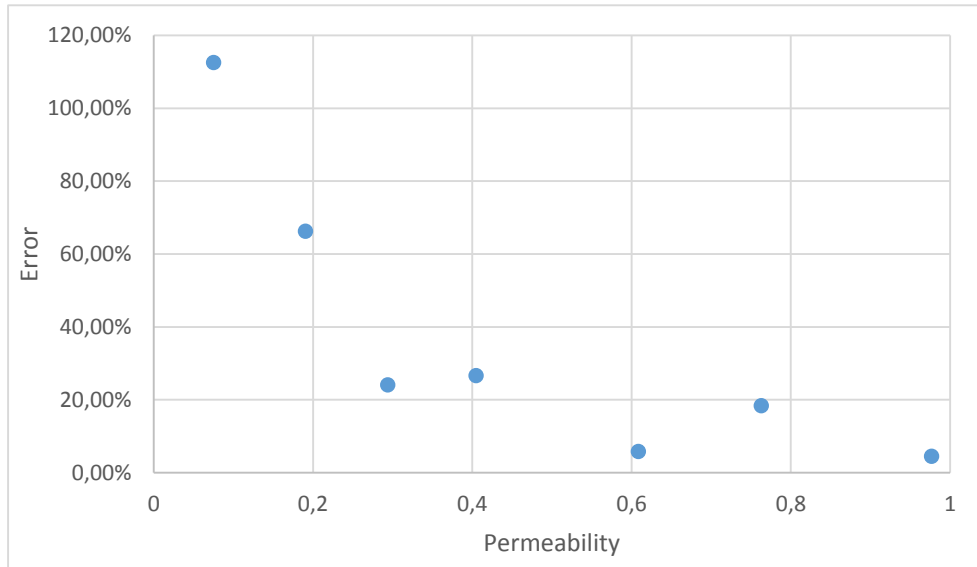
Figure 8.3: Well flow error in function of fine model's absolute permeability

The error may depends on the well-block permeability. In particular, its trend is approximately a negative exponential.

The sandface pressure (or the pressure at the well bottom) must be lower than the well-block pressure. The figure () shows the pressure distributions obtained using a resolution of 2x2:
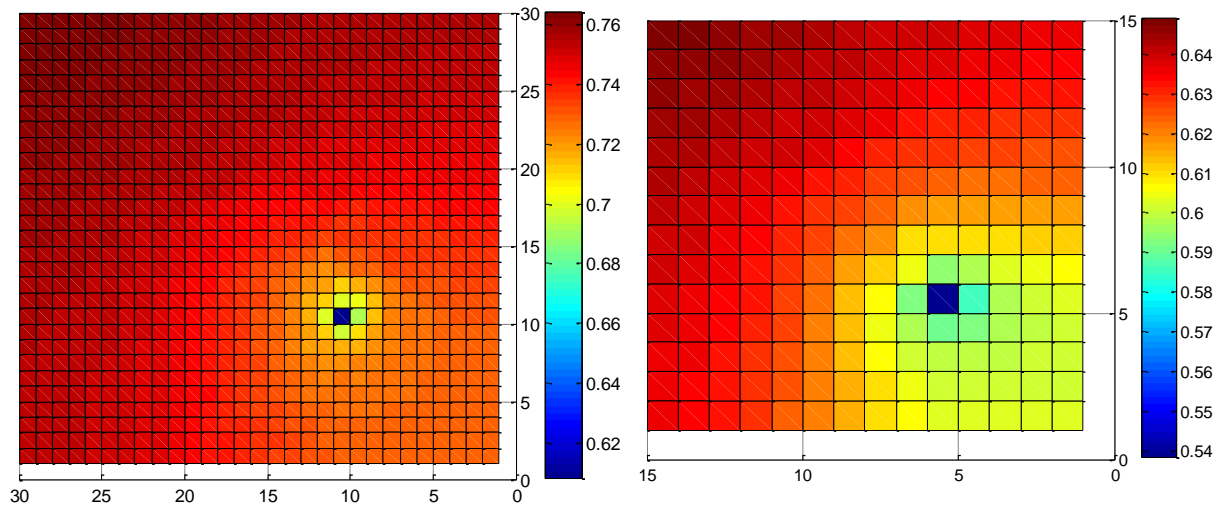
Figure 8.4: Pressure Distributions of Fine and Coarse Model, first test

_____

The sandface pressure had a value of 0.5 and both the systems have a minimum pressure that is higher.

In tables (8.6), (8.7), (8.8) and (8.9) are shown the results generated by a lognormal and normal permeability distributons. The two matrices are two-dimensional but the size was *60x60*. The original matrix size was changed in order to understand if the error is affected by it. Obviously, the matrix size affects the pressure distribution. In fact, a more refined grid will has a "smooth" pressure distribution. Even in this case two different resolutions were adopted. The results are shown in table (8.6) and (8.7):

Lognormal Distribution - 2D Model – Resolution 2x2					
Fine Model		Coarse Model			
K	Well Flow	Keq,x	Keq,y	Well Flow	Error
1,19	3,51	0,57	0,52	3,59	2%
1,42	4,3	0,97	0,96	4,31	0%
0,55	3,13	0,59	0,62	4,01	28%
1,66	3,93	0,61	0,74	3,94	0%
0,81	3,87	0,65	0,92	4,47	15%
1,06	4,07	0,91	0,8	4,44	9%
0,55	3,09	0,79	0,9	4,18	35%

Table 8.6: Results of production well flows, using a Lognormal Permeability Distribution.

Lognormal Distribution - 2D Model – Resolution 4x4					
Fine Model		Coarse Model			
K	Well Flow	Keq,x	Keq,y	Well Flow	Error
1,53	4,8	0,67	0,76	6,07	26%
0,4	2,64	0,66	0,59	6,01	127%
1,28	4,55	0,85	0,94	6,63	45%
0,62	3,33	0,74	0,6	6,57	97%
2,19	4,95	1,05	0,93	6,83	37%
0,53	3,24	0,6	0,42	5,35	64%
1,06	4,77	1,43	1,68	7,14	49%

Table 8.7: Results of production well flows, using a Lognormal Permeability Distribution.

Normal Distribution - 2D Model – Resolution 2x2					
Fine Model		Coarse Model			
K	Well Flow	Keq,x	Keq,y	Well Flow	Error
0,84	2,78	0,87	0,81	3,48	25%
0,65	2,74	0,88	0,89	3,86	40%
0,08	0,93	0,33	0,5	2,39	156%
0,61	2,75	0,91	0,77	3,32	20%
1,21	3,32	0,64	0,67	3,34	0%
3,11	3,89	0,87	1,47	3,51	9%
0,86	2,88	0,36	0,43	2,69	6%

Table 8.8: Results of production well flows, using a Normal Permeability Distribution, resolution 2x2.

Normal Distribution - 2D Model – Resolution 4x4					
Fine Model		Coarse Model			
K	Well Flow	Keq,x	Keq,y	Well Flow	Error
0,55	2,87	0,5	0,83	4,48	55%
0,16	1,53	0,62	0,62	4,01	161%
1,48	3,22	0,5	0,36	4,17	29%
0,22	1,57	0,38	0,34	3,74	137%
2,09	2,42	0,3	0,38	3,22	33%
0,53	2,42	0,37	0,33	3,98	63%
1,75	3,47	0,65	0,46	4,49	29%

Table 8.9: Results of production well flows, using a Normal Permeability Distribution, resolution 4x4.

The results in table (8.6), (8.7), (8.8) and (8.9) follow the same trend as those shown in tables (8.4) and (8.5). In general, the method works better when a log-normal permeability distribution is used. It is in line with all the cases that have been seen in the literature.

_____

To complete this paragraph, the three-dimensional casese must be shown. Obviously, the same permeability distribution must be used in order to have also a comparison with the previous results. The results are shown in table (8.10) (8.11), (8.12) and (8.13):

Rectangular Distribution - 3D Model – Resolution 2x2						
Fine Model		**Coarse Model**				
K	Well Flow	$K_{eq,x}$	$K_{eq,z}$	$K_{eq,y}$	Well Flow	Error
0,03	1,72	0,27	0,23	0,24	12,77	656%
0,11	4,34	0,25	0,56	0,70	11,73	174%
0,31	7,36	0,24	0,28	0,26	12,61	71%
0,41	8,11	0,32	0,23	0,33	14,32	76%
0,52	9,38	0,41	0,37	0,39	14,51	55%
0,77	9,87	0,35	0,34	0,31	12,91	32%
0,97	7,10	0,46	0,07	0,47	15,04	111%

Table 8.10: Results of production well flows for a Rectangular Permeability Distribution, resolution 2x2.

Rectangular Distribution - 3D Model – Resolution 4x4						
Fine Model		**Coarse Model**				
K	Well Flow	Keq,x	Keq,z	Keq,y	Well Flow	Error
0,03	1,72	0,43	0,32	0,43	26,80	1453%
0,11	4,34	0,28	0,41	0,38	25,89	496%
0,31	7,36	0,29	0,31	0,28	26,46	259%
0,41	8,11	0,40	0,40	0,32	27,13	234%
0,52	9,38	0,40	0,40	0,32	27,30	191%
0,77	9,87	0,29	0,31	0,28	26,10	164%
0,97	7,10	0,38	0,38	0,37	28,11	295%

Table 8.11: Results of well flow for a Rectangular Permeability Distribution, resolution 4x4.

Lognormal Distribution - 3D Model – Resolution 2x2						
Fine Model		Coarse Model				
K	Well Flow	Keq,x	Keq,z	Keq,y	Well Flow	Error
0,77	6,93	2,19	2,06	2,32	10,65	53%
1,47	18,48	1,70	1,74	1,75	32,93	78%
1,14	17,36	0,79	0,86	0,75	27,72	59%
2,48	28,04	1,72	2,05	2,10	36,17	28%
1,12	23,37	2,79	2,60	2,76	38,05	62%
0,61	15,80	1,76	1,82	1,47	33,78	113%
1,09	20,54	1,18	1,12	1,20	33,92	65%

Table 8.12: Results of well flows for a Log-normal Permeability Distribution, resolution 2x2.

Normal Distribution - 3D Model – Resolution 2x2						
Fine Model		Coarse Model				
K	Well Flow	Keq,x	Keq,z	Keq,y	Well Flow	Error
0,66	10,47	0,63	0,63	0,59	19,88	89%
1,18	14,52	0,75	0,88	0,89	20,68	42%
0,12	5,35	0,54	0,57	0,54	18,59	247%
0,77	10,34	0,24	0,36	0,38	14,94	44%
1,12	23,37	2,79	2,60	2,76	38,05	62%
0,72	11,56	0,54	0,18	0,96	18,30	58%
1,72	13,69	0,54	0,50	0,86	17,66	28%

Table 8.13: Results of well flows for a Normal Permeability Distribution, resolution 2x2.

The results show clearly the same trend of the two-dimensional models. The error always increases when the resolution is higher. Again, it also decreases passing from low to high well-block permeability values.

Due to the small original grid size, the results in table (8.11) are obviously unsatisfactory. It can be explained thinking about the pressure distribution. In fact, when the grid is small (such as a 5x5x5) a really rough pressure distribution characterizes the model. It's almost obvious that in these conditions is not possible obtain realistic and satisfactory results. For three-dimensional models is

_____

possible to represent the pressure distributions by three-dimensional grids, but will be difficult for the reader to clearly understand them.

The error's trend as a function of the well-block permeability is plotted in figure (8.5), using the table (8.10):
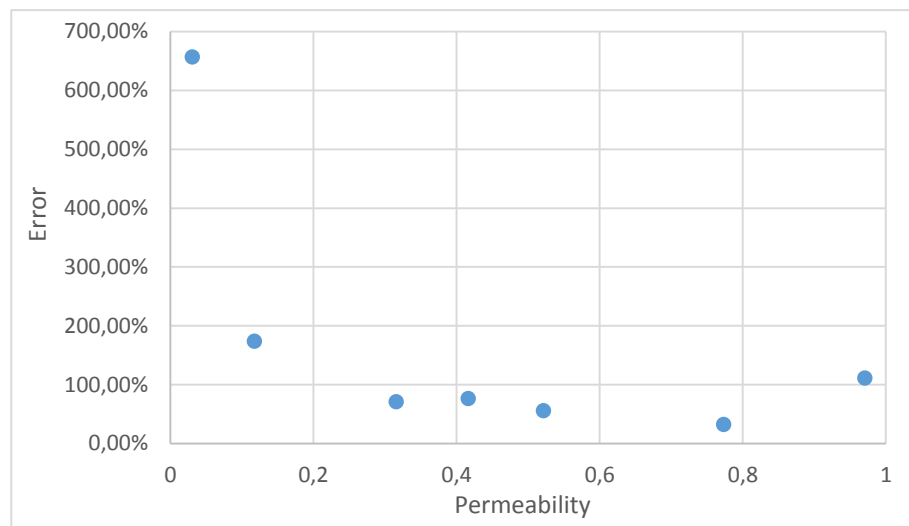
Figure 8.5: Error of well flows in function of well-block permeability

8.2.2 SPE's Datasets – Well flow

SPE's datasets have been simulated collocating a single well in several different regions, such as the auto-generated permeability fields of the previous paragraph.. The results are summarized in the following tables:

SPE dataset 1 - 2D Model – Resolution 2x2					
Fine Model		**Coarse Model**			
K	Well Flow	Keq,x	Keq,y	Well Flow	Error
4,01	9,51	13,80	264,49	16,63	74%
78,45	14,62	66,90	67,47	14,85	1%
7,69	9,91	1,46	2,93	7,52	24%
321,87	11,06	20,67	20,12	11,74	6%
0,11	1,41	3,18	17,61	10,33	630%
11,12	12,11	89,17	112,96	15,61	28%
20,34	13,27	38,86	39,26	15,00	12%

Table 8.14: Results of production well flows, using the SPE's dataset number 1.

SPE dataset 2 - 2D Model – Resolution 2x2					
Fine Model		**Coarse Model**			
K	Well Flow	Keq,x	Keq,y	Well Flow	Error
0,79	3,82	2,45	2,40	5,97	56%
23,73	10,24	24,84	24,03	10,88	6%
0,09	0,53	0,10	0,09	0,68	27%
157,86	24,20	127,71	129,90	20,28	0%
50,83	21,02	57,61	58,80	22,14	5%
10,55	16,73	17,47	17,13	20,65	23%
323,22	25,00	215,55	214,29	25,14	0%

Table 8.15: Results of production well flows, using the SPE's dataset number 2.

_____

SPE dataset 2 - 2D Model – Resolution 6x6					
Fine Model		**Coarse Model**			
K	Well Flow	Keq,x	Keq,y	Well Flow	Error
0,18	1,09	0,09	0,11	1,41	29%
0,06	0,42	0,12	0,13	0,85	103%
47,37	12,54	84,45	83,93	13,56	8%
18,32	10,12	1,84	3,83	8,03	20%
145,06	23,55	43,81	32,89	22,93	2%
530,03	26,61	176,67	193,70	26,43	0%
7,47	13,17	2,99	5,49	16,89	28%

Table 8.16: Results of production well flows, using the SPE's dataset number 2.

Table (8.14) contains the errors that regard dataset number 1. It is a two-dimensional model and it has been simulated using a single resolution value because of its original size. The results are considerably different from one another. In fact, when the well-block permeability is really low, the error is incredibly high and again, to higher well-block permeability values are associated lower errors.

The second dataset contains a great number of elements. In order to simulate it in two dimensions only its top layer was taken into account. So, the fine model's size was *60x84* and two different resolutions have been used to understand how and if the error gets worse when the scale decreases too much. The results are shown on tables (8.15) and (8.16). They can be considered satisfactory results for both resolutions. The dataset number 2 is less heterogeneous than the dataset number 1.
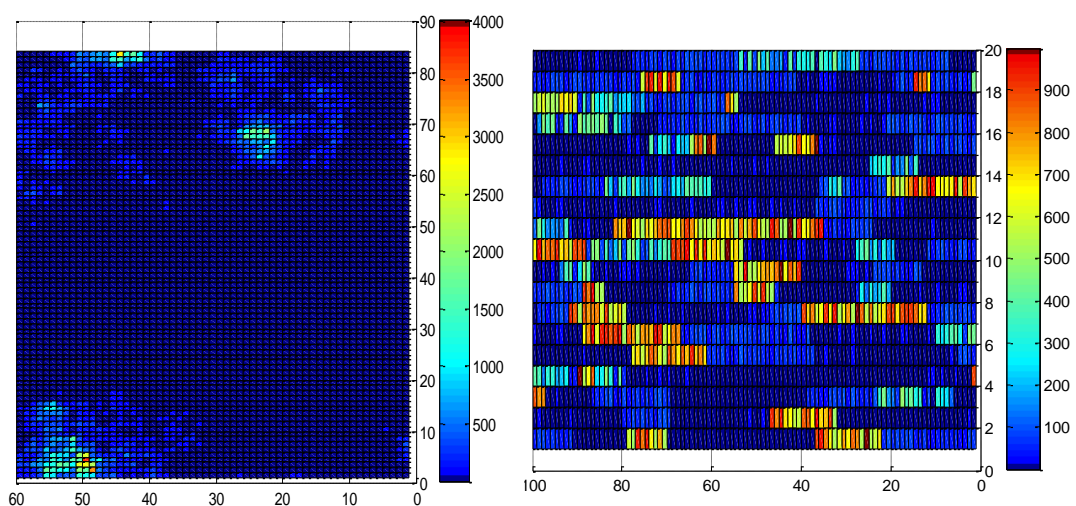
Figure 8.6: Representation of SPE dataset 1 (on the right) and SPE dataset 2 (on the left)

It may mean that this new technique is particularly sensitive when the permeability field is extremely heterogeneous. This aspect must be improved because this method was born in order to be also applicable on heterogeneous reservoirs. Being this work a preliminary study of this method, future improvements are surely possible and some of them will be suggested in the next chapter.

To conclude this paragraph, it is important to show the results obtained by the SPE dataset 2 in three dimensions. Unfortunately, due to technological limits it was not possible to simulate the entire grid. So, the maximum size allowed was *20*x*20*x*20* and its results are shown in table (8.17).

SPE dataset 2 - 3D Model – Resolution 2x2						
Fine Model		**Coarse Model**				
K	Well Flow	Keq,x	Keq,z	Keq,y	Well Flow	Error
0,13	3,83	2,15	0,10	2,99	36,51	852%
36,90	70,10	38,77	58,36	44,98	92,45	31%
261,40	96,54	51,75	28,07	48,50	101,45	5%
3,47	36,85	1,50	0,05	5,47	36,41	1%
2487,8	104,23	295,75	5,08	12,61	105,78	1%
17,43	72,31	63,95	0,13	35,49	92,38	27%
119,16	89,14	38,77	58,36	44,98	92,61	3%

Table 8.17: Well flow results obtained by SPE's dataset 2 in three dimensions.

Except for the lowest well-block's permeability, whose error is really large, the other results are brilliant. This is probably due to the weak heterogeneity that characterizes this dataset and it favors the homogenization process.

Even in this case, a higher resolution was not used because of the pressure distribution.

Several conclusions can be drawn from this brief analysis. Most of the times, the simulation generates an important error when the production well is collocated in a low well-block permeability. However, the reader has to take into account some particular cases, such as the one reported in table (8.17) and highlighted in green. Even if the well-block's permeability is low (when it is compared with the other cases) the error is really small.

Another important aspect is relative to the fine model. Strongly heterogeneous models could generate bad results, independently of the resolution or the well-block permeability. It could explain why the second SPE's dataset generates good results using both resolutions.

_____

Self-similarity is one of parameters that should be used in order to evaluate the quality of an upscaling method. So, in the next paragraph a self-similarity analysis of this method will be carried out.

8.3 Self-Similarity

It could be interesting to investigate about the nature of the method. Upscaling methods are particularly appreciated when they conserve the cumulative probability distribution function. Criteria such as self – consistency characterizes numerical techniques. Then, a comparison between cumulative probability distributions of both fine and coarse model can be used to determine if the method is characterized by self-similarity. So, for example the Matlab function *"rand"* generates a uniform probability distribution, as figure (8.7) shows.

The cumulative function associated to a uniform probability distribution is a straight line. If the method was characterized by self – similarity, the cumulative distribution function of both the coarse models should be a line that lies over the green one shown in figure (8.8).
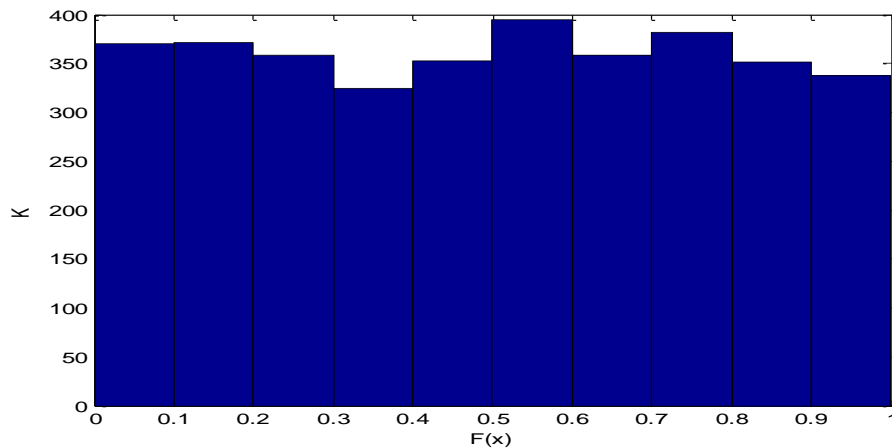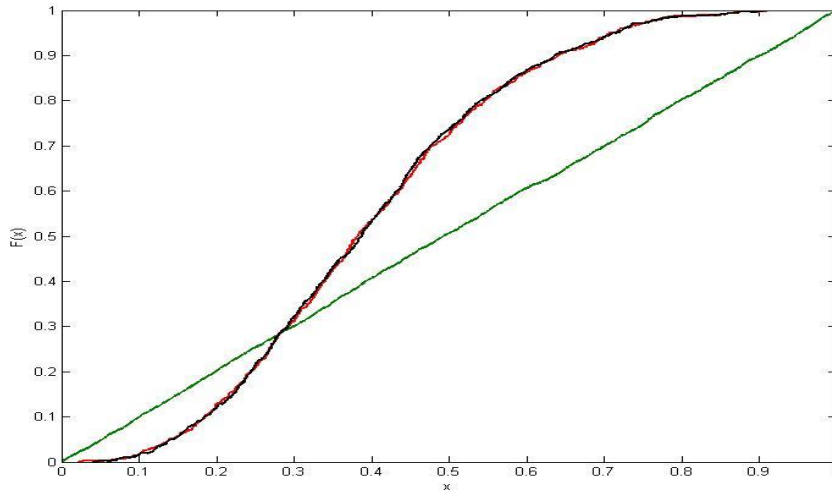

Figure 8.7: Example of square distribution function

Figure 8.8: Example of cumulative distribution functions. The green line regards the fine model, while the red and the black ones regard the coarse matrices.

The curves in red and black represent the cumulative distribution functions for the scaled up matrices. While the green one is the cumulative function that belongs to the original matrix. It is evident that the coarse cumulative distributions are absolutely different from the original one. In fact, the probability function of both scaled matrices is plotted in figure (8.7). So, it clearly shows how the original distribution was not kept and they turn in log-normal distributions.
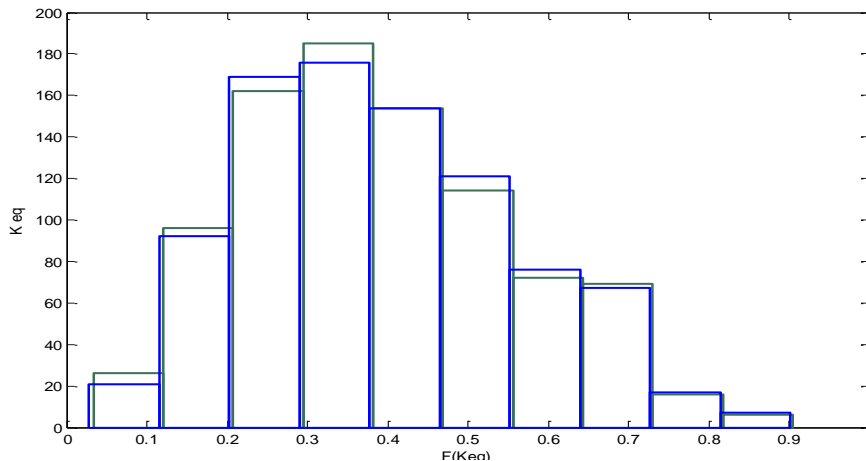
Figure 8.9: Coarse model's permeability probability distribution functions.

_____

So, it is possible to affirm that this numerical technique is not characterized by self − similarity.

However, it could be interesting to verify if the scaled distribution functions are kept when the upscaling process is applied on them. In other words, if the the log − normal distribution is the definitive distribution one or not. So, in figure (8.8) is possible to see that scaling three times the original model, the distribution function turns in a Dirac's Delta probability function.
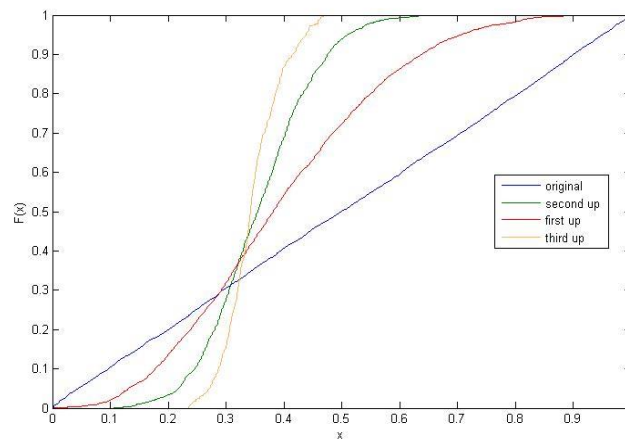
Figure 8.10: Cumulative distribution functions, turning into a Dirac's Delta distribution.

The self similarity is not respected, but it is not a problem, just a clarification. In practical terms, it is not so probable that a coarse model, which was already subjected to upscaling, it will be scaled up again. So, the most important concept of this chapter is always the error between well flows.

9 Conclusions and Future Directions

The simulation time is obviously decreased because of the size models reduction. The results in terms of production flow can be considered satisfactory, especially for the problems in two-dimensions (see tables (8.4), (8.6) and (8.8)). The error among well flows is often within the range $0 - 25\%$, which it is normally considered as an excellent result. One of the most interesting aspect is that the error does not strongly depends on the original permeability distribution. So, low errors were registered using uniform, log-normal, normal and SPE permeability distribution but, most of the times, the lower errors occurred when a log-normal distribution was used.

However, it must be considered all the approximations that were done, especially close to the well. In fact, in the near-well region the steady state pressure varies as log r, where r is the well radius [5], and not linearly. The approximation of equivalent radius (see equation (7.7)) affects the flow calculation for both models. This aspect is more accentuated when the well-block permeability is low, which affects the pressure distribution calculation, and the error increases. It was plotted in function of the well-block permeability of the fine model (see figure (8.5) and (8.1)), giving a trend that is approximately the same for the two and three dimensional case.

However, the grade of heterogeneity apparently influences the production well simulation. It is highlighted in table (8.15), (8.16) and (8.17) when the second SPE dataset, which is less heterogeneous than the number 1, was used. The results can be considered good for both cases, in two dimensions and three dimensions.

However, this method is not characterized by self-similarity. It is an expected result due to the fact that it generates equivalent permeability values that are obviously within the maximum and minimum permeability values of the core. So, it means that when the upscaling is applied, the range of permeability becomes narrower. As a consequence, the probability function changes and it turns in a Dirac's Delta probability function.

So, this numerical technique can be improved and extended to more general cases. For example, it is possible to implement it for multi-phase flows. This extension is a computational challenge but conceptually nothing varies. Script improvements are necessary in order to make the method more efficient. For

example, it is possible to give to the user the freedom of choosing the "resolution" along each dimension. In fact, till now, the method considers only square (or cubic) cores but, depending on the fine model, it could be better considers rectangular (or prismatic) cores.

However, the actual method give to the user the possibility to choose how many "rings" around the core have to be taken into account. In other words, if the rings number is zero, the method can be considered as local. It was shown in chapter 6 when two particular permeability distribution were used in order to test the method and the results were equal the analytical ones. When one or more rings are taken into account the method becomes no-local. The flow through the entire block is kept constant but just the core is homogenized. If the flow was kept constant only in the core, independently of the number of rings around it, the method would become absolutely local. Unfortunately, this new conceptual form can be reached only considering all the elements of the local permeability tensor. In other words, the method should turn in a full-tensor method.

To conclude, a different numerical method was developed in this work and the results obtained till now were satisfactory enough.

It is also going to be presented to the National Brazilian Congress "CILAMCE 2015", November 2015 in Rio de Janeiro.

Appendix

A.1 2D Matlab Main Script

```
%%% SPE dataset %%%
%pc=fopen('spe_perm.dat');k=fscanf(pc,'%f',[60 84]);
%por=fopen('spe_phi.dat');
%phi=fscanf(por,'%f',[60 84]);
%pc=fopen('perm_case1.dat');k=fscanf(pc, '%f', [100 20]);
%phi=0.2*ones(100,20);
%k=rand(80,80); % rectangular permeability distribution%

%%% Lognormal permeability distribution %%%%
m = 1;
v = 0.5;
nu = log((m^2)/sqrt(v+m^2));
sigma = sqrt(log(v/(m^2)+1));
X = lognrnd(nu,sigma,1,3600);
P=zeros(1,3600);
P(1,1:2:3599)=X(1,3600:-2:2);
P(1,2:2:3600)=X(1,1:2:3599);
k=zeros(60,60);phi=rand(60,60);
a=1;
for i=1:60
    for j=1:60
        k(i,j)=P(1,a);
        a=a+1;
    end
end

%% Parameters %%%
n=size(k,1);
m=size(k,2);
res=2;
rn=1;
k2=k';
Pa=1;
Pb=0;
Dx=1;
Dy=1;
Dz=1;
Dy_up=res*Dy;Dx_up=res*Dx;Dz_up=res*Dz;
mu=1;
beta=1;
B=1;
H=1;
A1=(Dx*Dz)/(mu*Dy); A2=(Dy*Dz/(mu*Dx));
P_1_log=0.5;
```

Appendix

```
P_2_log=0;

%%&& original matrices pressure distribution %%%%
[coef,sol]=fun_coef_GS(Dy,Dz,Dx,n,m,mu,k,k2,Pa,Pb);
pres = coef\sol;
[coef2,sol2]=fun_coef_GS(Dy,Dz,Dx,m,n,mu,k2,k,Pa,Pb);
pres2 = coef2\sol2;

 %%%% Homogenization process %%%%
[k_hom_a,k_hom2_a,step_a]=gs_hom_a(n,m,res,rn,k,Dy,Dz,Dx,mu,Pa,P
_2_log,A2,A1,P_1_log,Pb);

[k_hom_c,k_hom2_c,step_c]=gs_hom_c(n,m,res,rn,k,Dy,Dz,Dx,mu,P_1_
log,P_2_log,A2,A1);

[k_hom_s,k_hom2_s,step_s]=gs_hom_s(n,m,res,rn,k,Dy,Dz,Dx,mu,Pa,P
_2_log,P_1_log,A2,A1,Pb);

iteractions = step_a+step_c+step_s;
k_hom_x=k_hom_a+k_hom_c+k_hom_s;
k_hom_y=k_hom2_a+k_hom2_c+k_hom2_s;

[coef,sol]=fun_coef_GS(Dy,Dz,Dx,n,m,mu,k_hom_x,k_hom_y,Pa,Pb);
pres_hom_x = coef\sol;
[coef2,sol2]=fun_coef_GS(Dy,Dz,Dx,m,n,mu,k_hom_y,k_hom_x,Pa,Pb);
pres_hom_y = coef2\sol2;
err_x=zeros(m*n,1);
err_y=zeros(m*n,1);
for i=1:n
    for j=1:m
        el_x=m*(i-1)+j;
        err_x(el_x,1)=(pres(el_x,1)-pres_hom_x(el_x,1))^2;
        el_y=n*(j-1)+i;
        err_y(el_y,1)=(pres2(el_y,1)-pres_hom_y(el_y,1))^2;
    end
end
Err_x=sum(err_x);
Err_y=sum(err_y);
[k_up_x,k_up_y]=fun_up(n,res,m,k_hom_x,k_hom_y);

n_up=size(k_up_x,1);
m_up=size(k_up_x,2);

[pres_x,pres_y,Q_in_x,Q_out_x,Q_in_y,Q_out_y]=gs_pres(Dy,Dz,Dx,n
,m,k,mu,Pa,Pb);

[pres_x_up,pres_y_up,Q_up_in_x,Q_up_out_x,Q_up_in_y,Q_up_out_y]=
gs_pres_up(m_up,n_up,k_up_x,k_up_y,Dy_up,Dz,Dx_up,mu,Pa,Pb);

error_x = abs(abs(Q_in_x)-abs(Q_up_in_x))/abs(Q_in_x)*100;
```

_____

```matlab
error_y= abs((abs(Q_in_y)-abs(Q_up_in_y)))/abs(Q_in_y)*100;
error_abs=abs((abs(Q_in_x+Q_in_y)-
abs(Q_up_in_x+Q_up_in_y)))/abs(Q_in_x+Q_in_y)*100;

%%%% Well parameters %%%%
p_wf=0.5;
r_w=0.8;
x_w=10; %lungo le colonne
y_w=10; %lungo le righe
x_up=ceil(x_w/res) ;
y_up=ceil(y_w/res);

%%%%% Production well simulation %%%%%
[pres_well,coef_well,q_sc,matr_pres]=fun_w(Dy,Dz,Dx,Pa,n,m,beta,
k,y_w,x_w,h,mu,B,r_w,phi,p_wf);
[phi_up,pres_well_up,coef_well_up,q_sc_up,matr_pres_up]=fun_up_w
(res,Dy,Dz,Dx,Pa,n_up,m_up,x_up,y_up,x_w,y_w,k_up_x,k_up_y,beta,
h,mu,B,r_w,n,m,phi,p_wf);
%[pres_well_up,coef_well_up,q_sc_up,matr_pres_up]=fun_up_w(res,D
y,Dz,Dx,Pa,n_up,m_up,x_up,y_up,x_w,y_w,k_up_x,k_up_y,beta,h,mu,B
,r_w,phi,p_wf);
flux_fine=sum(q_sc)
flux_up=sum(q_sc_up)
error_well= abs((abs(flux_fine)-
abs(flux_up))/abs(flux_fine))*100

%%% Cumulative distribution function plot %%%%%
[o]=fun_norm_dens(n,m,k);
[o_x]=fun_norm_dens(n_up,m_up,k_up_x);
[o_y]=fun_norm_dens(m_up,n_up,k_up_y);
v_up=zeros(n_up*m_up*2,1);
v_up(1:n_up*m_up,1)=o_x(:,1);
v_up(n_up*m_up+1:n_up*m_up*2,1)=o_y(:,1);
o_up=sort(v_up);
el_w=m*(y_w-1)+x_w;
el_up=m_up*(y_up-1)+x_up;
k_up_y=k_up_y';
k(y_w,x_w)
k_up_x(y_up,x_up)
k_up_y(y_up,x_up)
```

A.2 3D Matlab Main Script

```matlab
clear all
close all

%%% 3D Model Size %%%
l=20;
c=20;
```

```
f=20;

%%% SPE dataset %%%
%pc=fopen('spe_perm.dat');vec_perm=fscanf(pc,'%f',[l*c*f]);
%por=fopen('spe_phi.dat');vec_phi=fscanf(por,'%f',[l*c*f]);

%%% Lognormal permeability distribution %%%%
%load k.mat;%vec_perm=fscanf(pc,'%f',[l*c*f]);
phi=0.3*ones(l,c,f);
%k(1:2:l-1,:,:)=100*k(1:2:l-1,:,:);
%k(:,1:2:c-1,:)=10*k(:,1:2:c-1,:);
%k(:,:,1:2:f-1)=k(:,:,1:2:f-1);
%k=10000*rand(l,c,f);
%pc=fopen('bo.dat');vec_perm=fscanf(pc,'%f',[l*c*f]);
k=zeros(l,c,f);
for i=1:l
    for j=1:c
        for z=1:f
         X = abs(random('logn',0.5,1));
         k(i,j,z)=X;
        end
    end
end


%% Parameters %%%
n=size(k,1);
m=size(k,2);
p=size(k,3);
res=2;
rn=1;
Pa=1;
Pb=0;
Dx=1;
Dy=1;
Dz=1;
Dx_up=res*Dx;
Dy_up=res*Dy;
Dz_up=res*Dz;
mu=1;
beta=1;
B=1;

%%%% Well parameters %%%%
p_wf=0.4;
r_w=0.5;
x_w=10; %lungo le colonne
y_w=10; %lungo le righe
z_w=10;
x_up=ceil(x_w/res);
y_up=ceil(y_w/res);
```

```
z_up=ceil(z_w/res);
n_up=n/res;
m_up=m/res;
p_up=p/res;
H=Dy_up*y_up;

%%%% original matrices pressure distribution %%%%%
[pres_x,pres_y,pres_z,Q_in_x,Q_out_x,Q_in_y,Q_out_y,Q_in_z,Q_out
_z]=fun_pres_3D(Dy,Dz,Dx,m,n,p,k,mu,Pa,Pb);
A1=(Dx*Dz); A2=Dy*Dz; A3=Dx*Dy;
P_1_log=1;
P_2_log=0;

 %%%% Homogenization process %%%%
[k_hom_d,k_hom2_d,k_hom3_d,it_d]=gs_d_3d(n,m,p,res,rn,k,Dy,Dz,Dx
,mu,Pa,P_2_log,A2,A3,A1);
[k_hom_a,k_hom2_a,k_hom3_a,it_a]=gs_a_3d(n,m,p,res,rn,k,Dy,Dz,Dx
,mu,Pa,P_2_log,A2,A1,A3);
[k_hom_s,k_hom2_s,k_hom3_s,it_s]=gs_s_3d(n,m,p,res,rn,k,Dy,Dz,Dx
,mu,Pa,P_2_log,A2,A3,A1);
[k_hom_c,k_hom2_c,k_hom3_c,it_c]=gs_c_3d(n,m,p,res,rn,k,Dy,Dz,Dx
,mu,Pa,P_2_log,A1,A3,A2);
[k_hom_f,k_hom2_f,k_hom3_f,it_f]=gs_f_3d(n,m,p,res,rn,k,Dy,Dz,Dx
,mu,A1,A3,A2);
iterations=it_d+it_a+it_s+it_c+it_f;
k_hom=(k_hom_a+k_hom_c+k_hom_s+k_hom_f+k_hom_d);
k_hom2=(k_hom2_a+k_hom2_c+k_hom2_s+k_hom2_d+k_hom2_f);
k_hom3=(k_hom3_a+k_hom3_c+k_hom3_s+k_hom3_d+k_hom3_f);
[k_up_x,k_up_y,k_up_z]=fun_up_3D(n_up,m_up,p_up,res,n,m,p,k_hom,
k_hom2,k_hom3);

[pres_up_x,pres_up_y,pres_up_z,Q_up_in_x,Q_up_out_x,Q_up_in_y,Q_
up_out_y,Q_up_in_z,Q_up_out_z]=fun_pres_up_3D(Dy_up,Dz_up,Dx_up,
n_up,m_up,p_up,mu,k_up_x,Pa,Pb,k_up_y,k_up_z);
error_x = abs(Q_in_x-Q_up_in_x)/abs(Q_in_x)*100;
error_y= abs(Q_in_y-Q_up_in_y)/abs(Q_in_y)*100;
error_z= (abs(Q_in_z-Q_up_in_z)/Q_in_z)*100;
error_abs=abs(((Q_in_x+Q_in_y+Q_in_z)-
(Q_up_in_x+Q_up_in_y+Q_up_in_z)))/abs((Q_in_x+Q_in_y+Q_in_z))*10
0;

%%%%% Production well simulation %%%%%
[coef_well,pres_well,q_sc,Flux_well]=fun_w_3D(Dy,Dz,Dx,Pa,n,m,p,
beta,k,y_w,x_w,z_w,H,mu,B,r_w,phi,p_wf);
[coef_well_up,pres_well_up,q_sc_up,Flux_well_up,phi_up]=fun_w_up
_3D(Dy_up,Dz_up,Dx_up,Pa,n_up,m_up,p_up,x_up,res,z_up,x_w,z_w,k_
up_x,y_up,k_up_y,beta,H,mu,B,r_w,phi,k_up_z,p_wf);
error_well= abs((abs(Flux_well)-
abs(Flux_well_up))/abs(Flux_well))*100
Flux_well
Flux_well_up
```

```
k(y_w,x_w,z_w)
k_up_x(y_up,x_up,z_up)
k_up_z(y_up,x_up,z_up)
k_up_y(y_up,x_up,z_up)
```

A.3 3D Example of Homogenization Function

```
function
[k_hom_c,k_hom2_c,k_hom3_c,it]=gs_c_3d(n,m,p,res,rn,k,Dy,Dz,Dx,m
u,Pa,P_2_log,A1,A3,A2)


k_hom_c=zeros(n,m,p);
k_hom2_c=zeros(n,m,p);
k_hom3_c=zeros(n,m,p);
it=0;

 for f=res+1:res:p-2*res+1
  for c=res+1:res:m-2*res+1    % a indicates how many times I
have to move through the Columns.
    for l=res+1:res:n-2*res+1 %b is the same of a, but it is
moving through the Lines.

e=res+2*rn;
p_core=zeros(res^2,1);p_core2=zeros(res^2,1);p_core3=zeros(res^2
,1);
q_core=zeros(res^2,1);q_core2=zeros(res^2,1);q_core3=zeros(res^2
,1);
q_area=zeros(e^2,1);q_area2=zeros(e^2,1);q_area3=zeros(e^2,1);
q_mid=zeros(e^2,1);q_mid2=zeros(e^2,1);q_mid3=zeros(e^2,1);
Keq_x_it=inf; Keq_y_it=inf; Keq_z_it=inf;

k_it_x=k(l-rn:l+res-1+rn,c-rn:c+res-1+rn,f-rn:f+res-1+rn);
k_it_y=zeros(e,e,e);
k_it_z=zeros(e,e,e);

for i=1:e
   k_it_y(:,:,i)=k_it_x(:,:,i)';
   k_it_z(:,i,:)=k_it_x(:,:,i);
end

[pres_it_x]=gs_coef_3d(Dy,Dz,Dx,e,e,e,mu,k_it_x,k_it_y,k_it_z,Pa
,P_2_log) ;
[pres_it_y]=gs_coef_3dy(Dy,Dz,Dx,e,e,e,mu,k_it_y,k_it_x,k_it_z,P
a,P_2_log) ;
[pres_it_z]=gs_coef_3dz(Dy,Dz,Dx,e,e,e,mu,k_it_z,k_it_y,k_it_x,P
a,P_2_log) ;

ind=1;
```

_____

```
for z=1:e
 for i=1:e
     j=round(e/2);
     el=e*e*(z-1)+e*(i-1)+j;

q_mid(ind,1)=(A2/(mu*Dx))*((2*(k_it_x(i,j,z)*k_it_x(i,j+1,z)))/(
k_it_x(i,j,z)+k_it_x(i,j+1,z))*(pres_it_x(el,1)-
pres_it_x(el+1,1)));

q_mid2(ind,1)=(A1/(mu*Dy))*((2*(k_it_y(i,j,z)*k_it_y(i,j+1,z)))/
(k_it_y(i,j,z)+k_it_y(i,j+1,z))*(pres_it_y(el,1)-
pres_it_y(el+1,1)));

q_mid3(ind,1)=(A3/(mu*Dz))*((2*(k_it_z(i,j,z)*k_it_z(i,j+1,z)))/
(k_it_z(i,j,z)+k_it_z(i,j+1,z))*(pres_it_z(el,1)-
pres_it_z(el+1,1)));
     ind=ind+1;
 end
end

             Q_mid=sum(q_mid);
             Q_mid2=sum(q_mid2);
             Q_mid3=sum(q_mid3);

ind=1;
for z=rn+1:e-rn
for i=rn+1:e-rn
   j=round(e/2);
   el=e*e*(z-1)+e*(i-1)+j;

q_core(ind,1)=(A2/(mu*Dx))*((2*(k_it_x(i,j,z)*k_it_x(i,j+1,z)))/
(k_it_x(i,j,z)+k_it_x(i,j+1,z))*(pres_it_x(el,1)-
pres_it_x(el+1,1)));
   p_core(ind,1)=A2/(mu*Dx)*(pres_it_x(el,1)-pres_it_x(el+1,1));
   ind=ind+1;
end
end

Keq_x=(sum(q_core))/(sum(p_core))
k_it_x(rn+1:e-rn,rn+1:e-rn,rn+1:e-rn)=Keq_x;
[pres_it_y]=gs_coef_3dy(Dy,Dz,Dx,e,e,e,mu,k_it_y,k_it_x,k_it_z,P
a,P_2_log) ;

ind=1;
for z=rn+1:e-rn
   for i=rn+1:e-rn
   j=round(e/2);
   el=e*e*(z-1)+e*(i-1)+j;

q_core2(ind,1)=(A1/(mu*Dy))*((2*(k_it_y(i,j,z)*k_it_y(i,j+1,z)))
```

```
/(k_it_y(i,j,z)+k_it_y(i,j+1,z))*(pres_it_y(el,1)-
pres_it_y(el+1,1)));
    p_core2(ind,1)=A1/(mu*Dy)*(pres_it_y(el,1)-
pres_it_y(el+1,1));
    ind=ind+1;
    end
end

Keq_y=(sum(q_core2))/(sum(p_core2))
k_it_y(rn+1:e-rn,rn+1:e-rn,rn+1:e-rn)=Keq_y ;
[pres_it_z]=gs_coef_3dz(Dy,Dz,Dx,e,e,e,mu,k_it_z,k_it_y,k_it_x,P
a,P_2_log) ;

ind=1;
for z=rn+1:e-rn
    for i=rn+1:e-rn
    j=round(e/2);
    el=e*e*(z-1)+e*(i-1)+j;

q_core3(ind,1)=(A3/(mu*Dz))*((2*(k_it_z(i,j,z)*k_it_z(i,j+1,z)))
/(k_it_z(i,j,z)+k_it_z(i,j+1,z))*(pres_it_z(el,1)-
pres_it_z(el+1,1)));
    p_core3(ind,1)=A3/(mu*Dz)*(pres_it_z(el,1)-
pres_it_z(el+1,1));
    ind=ind+1;
    end
end

Keq_z=(sum(q_core3))/(sum(p_core3));
k_it_z(rn+1:e-rn,rn+1:e-rn,rn+1:e-rn)=Keq_z;
step=0

while abs(Keq_x_it/Keq_x - 1)>10^-8 || abs(Keq_y_it/Keq_y -
1)>10^-8 || abs(Keq_z_it/Keq_z - 1)>10^-8

Keq_x_it=Keq_x;
Keq_y_it=Keq_y;
Keq_z_it=Keq_z;
Keq_x=Keq_y_it;
Keq_y=Keq_z_it;
Keq_z=Keq_x_it;
k_it_x(rn+1:e-rn,rn+1:e-rn,rn+1:e-rn)=Keq_x;
k_it_y(rn+1:e-rn,rn+1:e-rn,rn+1:e-rn)=Keq_y;
k_it_z(rn+1:e-rn,rn+1:e-rn,rn+1:e-rn)=Keq_z;
[pres_it_x]=gs_coef_3d(Dy,Dz,Dx,e,e,e,mu,k_it_x,k_it_y,k_it_z,Pa
,P_2_log) ;

ind=1;
for z=1:e
 for i=1:e
```

_____

```
    j=round(e/2);
    el=e*e*(z-1)+e*(i-1)+j;

q_area(ind,1)=(A2/(mu*Dx))*((2*(k_it_x(i,j,z)*k_it_x(i,j+1,z)))/
(k_it_x(i,j,z)+k_it_x(i,j+1,z))*(pres_it_x(el,1)-
pres_it_x(el+1,1)));
    ind=ind+1;
 end
end


ind=1;
for z=rn+1:e-rn
for i=rn+1:e-rn
   j=round(e/2);
   el=e*e*(z-1)+e*(i-1)+j;

q_core(ind,1)=(A2/(mu*Dx))*((2*(k_it_x(i,j,z)*k_it_x(i,j+1,z)))/
(k_it_x(i,j,z)+k_it_x(i,j+1,z))*(pres_it_x(el,1)-
pres_it_x(el+1,1)));
   p_core(ind,1)=A2/(mu*Dx)*(pres_it_x(el,1)-pres_it_x(el+1,1));
   ind=ind+1;
end
end

Keq_x=(Q_mid-sum(q_area)+sum(q_core))/(sum(p_core));
if Keq_x<0
Keq_x=abs(Keq_x);
end
k_it_x(rn+1:e-rn,rn+1:e-rn,rn+1:e-rn)=Keq_x;
[pres_it_y]=gs_coef_3dy(Dy,Dz,Dx,e,e,e,mu,k_it_y,k_it_x,k_it_z,P
a,P_2_log) ;

ind=1;
for z=1:e
for i=1:e
    j=round(e/2);
    el=e*e*(z-1)+e*(i-1)+j;

q_area2(ind,1)=(A1/(mu*Dy))*((2*(k_it_y(i,j,z)*k_it_y(i,j+1,z)))
/(k_it_y(i,j,z)+k_it_y(i,j+1,z))*(pres_it_y(el,1)-
pres_it_y(el+1,1)));
    ind=ind+1;
end
end

ind=1;
for z=rn+1:e-rn
for i=rn+1:e-rn
   j=round(e/2);
   el=e*e*(z-1)+e*(i-1)+j;
```

```
q_core2(ind,1)=(A1/(mu*Dy))*((2*(k_it_y(i,j,z)*k_it_y(i,j+1,z)))
/(k_it_y(i,j,z)+k_it_y(i,j+1,z))*(pres_it_y(el,1)-
pres_it_y(el+1,1)));
    p_core2(ind,1)=A1/(mu*Dy)*(pres_it_y(el,1)-
pres_it_y(el+1,1));
    ind=ind+1;
end
end

Keq_y=(Q_mid2-sum(q_area2)+sum(q_core2))/(sum(p_core2));
if Keq_y<0
   Keq_y=abs(Keq_y);
end
k_it_y(rn+1:e-rn,rn+1:e-rn,rn+1:e-rn)=Keq_y;
[pres_it_z]=gs_coef_3dz(Dy,Dz,Dx,e,e,e,mu,k_it_z,k_it_y,k_it_x,P
a,P_2_log);

ind=1;
for z=1:e
for i=1:e
 j=round(e/2);
 el=e*e*(z-1)+e*(i-1)+j;

q_area3(ind,1)=(A3/(mu*Dz))*((2*(k_it_z(i,j,z)*k_it_z(i,j+1,z)))
/(k_it_z(i,j,z)+k_it_z(i,j+1,z))*(pres_it_z(el,1)-
pres_it_z(el+1,1)));
 ind=ind+1;
end
end

ind=1;
for z=rn+1:e-rn
for i=rn+1:e-rn
   j=round(e/2);
   el=e*e*(z-1)+e*(i-1)+j;

q_core3(ind,1)=(A3/(mu*Dz))*((2*(k_it_z(i,j,z)*k_it_z(i,j+1,z)))
/(k_it_z(i,j,z)+k_it_z(i,j+1,z))*(pres_it_z(el,1)-
pres_it_z(el+1,1)));
    p_core3(ind,1)=A3/(mu*Dz)*(pres_it_z(el,1)-
pres_it_z(el+1,1));
    ind=ind+1;
end
end

Keq_z=(Q_mid3-sum(q_area3)+sum(q_core3))/(sum(p_core3));
if Keq_z<0
   Keq_z=abs(Keq_z);
end
it=it+1;
```

```
step=step+1;

if step>1000
  Keq_x=(Keq_x+Keq_x_it)/2;
  Keq_y=(Keq_y+Keq_y_it)/2;
  Keq_z=(Keq_z+Keq_z_it)/2;
end
k_it_z(rn+1:e-rn,rn+1:e-rn,rn+1:e-rn)=Keq_z;

    end

        k_hom_c((l):(l+res-1),(c):(c+res-1),f:f+res-1)=Keq_x;
        k_hom2_c((l):(l+res-1),(c):(c+res-1),f:f+res-1)=Keq_y;
        k_hom3_c((l):(l+res-1),(c):(c+res-1),f:f+res-1)=Keq_z;

    end
  end
 end
end
```

Bibliography

[1]   E. Skripkin, A. Kantzas e S. Kryuchkov, "Upscaling of reservoir properties," GeoConvention focus 2014, 2014.

[2]   M. A. Christie , "Upscaling for Reservoir Simulation," SPE, BP Exploration, 1996.

[3]   T. Chen, "New methods for accurate upscaling with full-tensor effects," Standford University, March 2009.

[4]   L. V. Odsæter, "Chapter 3: Upscaling of Permeability and Relative Permeability," em *Numerical Aspects of Flow Based Local Upscaling* , Trondheim, NTNU - Trondheim, January 2013 , pp. 19-20.

[5]   L. J. Durlofsky, "Upscaling and Gridding of fine scale geological models for flow simulation," em *International Forum of Reservoir Simulation Iles Borromees*, Stresa, Italy, 2005.

[6]   M. A. Abunaja, "Chapter 3: Conclusions," em *Comparison of flow models at different scales using the 10th SPE comparative solution project*, Loeben, MONTANUNIVERSITÄT LEOBEN, AUSTRIA, Natural resources and petroleum engineering department, October 2007, pp. 72-74.

[7]   M. A. Abunaja, "Chapter 2: Results and Observation," em *Comparison of Flow Models at Different Scales Using the 10th Comparative Solution Project*, Loeben, Austria, MONTANUNIVERSITÄT, October 2007, pp. 28-30.

[8]   L. V. Odsæter, "Chapter 2: Reservoir Simulation," em *Numerical Aspects of Flow Based Local Upscaling*, Trondheim, Norwegian University of Science and Technology, January 2013, pp. 12-13.

[9]   R. Casnedi, "Caratteristiche geologiche dei giacimenti di idrocarburi," em *Enciclopedia degli idrocarburi*, Pavia, pp. 85-86.

[10] P. Macini e E. Mesini, "Caratteristiche dei giacimenti e relativi studi," em *Enciclopedia degli idrocarburi*, Bologna, pp. 455-470.

[11] T. Ertekin , J. H. Abou-Kassem e G. R. King, "Basic Reservoir Engineering Concepts and Reservoir-Fluids and Rock-Properties," em *Basic Applied Reservoir Simulation*, Richardson, Texas, Henry L. Doerty Memorial Fund of AIME, Society of Petroleum Engineers, 2001, pp. 14-15.

Bibliography

[12] M. A. Abunaja, "Chapter 1: Technical Description of the Upscaling problems," em *Comparison of Flow Models at Different Scales Using the 10th SPE Comparative Solution Project* , Loeben, Austria , MONTANUNIVERSITÄT, October 2007, pp. 24-25.

[13] T. Ertekin , J. H. Abou-Kassem e G. R. King, "Basic Reservoir - Engineering Concepts and Reservoir - Fluid and -Rock Properties," em *Basic Apllied Reservoir Simulation*, Richardson, Texas, Henry L. Doerty Memorial Fund of AIME, Society of Petroleum Engineers, 2001, pp. 27 - 30.

[14] P. Renard e G. de Marsily, "Calculating equivalent permeability: a review," *Advances in Water Resources,* vol. 20, pp. 253 - 278, 1997.

[15] L. J. Durlofsky, "Numerical Calculation of Equivalent Grid Block Permeability Tensor for Heterogeneous Porous Media," Chevron Oil Field Research Company , La Habra, California, 1991.

[16] X.-H. Wen e J. Gomez-Hernandez, "Upscaling Hydraulic conductivities in heterogeneous media: An overview," *Journal of Hydrogeology,* vol. 183, pp. 9-32, 1996.

[17] Society of Petroleum Engineers, "Upscaling of grid properties in reservoir simulation," Society of Petroleum Engineers, 12 June 2015. [Online]. Available: http://petrowiki.org/Upscaling_of_grid_properties_in_reservoir_simulation. [Acesso em 29 June 2015].

[18] M. A. Abunaja, "Appendix A: Derivation of Some Existing Algorithms," em *Comparison of Flow Models at Different Scales Using the 10th SPE Comparative Solution Project*, Loeben, Austria, MONTANUNIVERSITÄT, October 2007, pp. 79-82.

[19] T. Ertekin, G. R. King e J. H. Abou-Kassem, "Formulation of Basic Equation for Single-Phase Flow," em *Basic Applied Reservoir Simulation* , Richardson, Texas, Henry L. Doerty Memorial Fund of AIME, Society of Petroleum Engineers, 2001, pp. 57 - 74.

[20] EPFL, "VICAIRE-Module 3-Chapter 5.4," [Online]. Available: http://echo2.epfl.ch/VICAIRE/mod_3/chapt_5/main.htm. [Acesso em 23 June 2015].

[21] C. R. Fitts, "3.4.2 Laminar and Turbulent Flow," em *Groundwater Science*, London, Academic press. An impriming of Elsevier Science LTD, 2002, pp. 46-49.

_____

[22] R. McKibbin, "Groundwater Pollutant Transport: Transforming Layered Models To Dynamical Systems," An. St. Univ. Ovidius Constanta, October 2009.

[23] U. D. o. Energy, "Introduction," em *DOE Fundamentals Handbook*, Washington, D.C. , U.S. Department of Energy, June 1992, pp. 1-5.

[24] T. Ertekin , J. H. Abou-Kassem and G. R. King, "Finite-Difference Approximation to Linear-Flow Equations," in *Basic Applied Reservoir Simulation*, Richardson, Texas, Henry L. Doherty Memorial Fund of AIME, Society of Petroleum Engineers., 2001, pp. 75-91.

[25] L. F. Konikow, "Numerical Models of Groundwater Flow and Transport," em *US Geological Survey* , Reston, Virginia, USA.

[26] T. Ertekin, J. H. Abou-Kassem and G. R. King, "Well Representation," in *Basic Applied Reservoir Simulation*, Richardson, Texas, Henry L. Doerty Memorial Fund of AIME, Society of Petroleum Engineers., 2001, pp. 105-119.

[27] S. o. P. Engineers, "SPE comparative solution project," SPE, 27 March 2000. [Online]. Available: http://www.spe.org/web/csp/datasets/set01.htm. [Acesso em 20 February 2015].

[28] S. o. P. Engineers, "SPE comparative solution project," SPE, 16 May 2000. [Online]. Available: http://www.spe.org/web/csp/datasets/set02.htm. [Accessed 20 February 2015].

[29] E. L. Ligero, B. A. Sanjombi e D. J. Schiozer , "ABSOLUTE PERMEABILITY UPSCALING NEAR WELLS IN FINE GRIDS REPRESENTING PETROLEUM RESERVOIRS," em *17th International Congress of Mechanical Engineering* , Sao Paolo, Brasil, November 2003 .

[30] L. Holden e F. B. Nielsen, "GLOBAL UPSCALING OF PERMEABILITY," Norwegian Computing Center, Oslo, Norway.

[31] R. L. P. W. T. Cardwell, "Average Permeability of Heterogeneous Oil Sands," Junio Member A.I.M.E., Los Angeles Meeting, October, 1944.

[32] P. Zhang, G. E. Pickup e M. A. Christie , "A New Method for Accurate and Practical Upscaling In Highly Heterogeneous Reservoir Models," November 2006.

Bibliography

[33] M. Prevost, "Accurate coarse reservoir modeling using unstructured grids, flow based upscaling and streamline simulation," Standford University, December 2003.

[34] B. Noetinger e A. Haas, "Permeability Averaging for Well Tests in 3D Stochastic Reservoir Models," em *Annual Technical Conference and Exhibition* , Denver, Colorado, October 1996.